THE USE OF PERFLUOROCARBONS IN ENCAPSULATED CELL SYSTEMS: THEIR EFFECT ON CELL VIABILITY AND FUNCTION AND THEIR USE IN NONINVASIVELY MONITORING THE CELLULAR MICROENVIRONMENT

A Dissertation
Presented to
The Academic Faculty

by

Fernie Goh

In Partial Fulfillment
Of the Requirements for the Degree
Doctor of Philosophy in
Chemical and Biomolecular Engineering

Georgia Institute of Technology

May, 2011

The Use of Perfluorocarbons in Encapsulated Cell Systems: Their Effect on Cell Viability and Function and their Use in Noninvasively Monitoring the Cellular Microenvironment

Approved by:

Dr. Athanassios Sambanis, Advisor
School of Chemical and Biomolecular Engineering
Georgia Institute of Technology

Dr. Hang Lu
School of Chemical and Biomolecular Engineering
Georgia Institute of Technology

Dr. Lakeshia Taite
School of Chemical and Biomolecular Engineering
Georgia Institute of Technology

Dr. Robert Long, Jr
School of Medicine, Department of Radiology
Emory University

Dr. Susan Safley
School of Medicine, Department of Surgery and Ophthalmology
Emory University

Dr. Nicholas Simpson
Department of Medicine, Division of Endocrinology
University of Florida

Date Approved: 11th March 2011

ACKNOWLEDGEMENTS

I would like to express my deepest gratitude to my advisor, Dr. Athanassios Sambanis for all the support and guidance he has shown me throughout the years. He has been an incredible advisor and I will always be grateful for the impact he has made on my professional development. I would also like to thank Dr. Robert Long for his very useful NMR teachings and for assistance with the animal studies. It was definitely a pleasure working with him. My gratitude also goes to Dr. Nicholas Simpson for showing me such wonderful hospitality when I was working at the University of Florida, and also for helping me with my projects. I would like to thank Dr. Susan Safley for her *in vivo* expertise and for all of her encouragement. In addition, I would like to thank Drs. Hang Lu and Lakeshia Taite for their critical and constructive feedback on my work.

I am very thankful for all the Sambanis lab members; previous members - Heather Bara, Neil Mukherjee, Angie Gulino, and especially Jeffrey Gross for mentoring me. Current lab members – Hajira Ahmad, Alison Lawson, Saif Al-Mamari, Stephanie Duncanson, Aubrey Tiernan, Priya Jayachandran, and Sudhakar Muthlaya for all the many useful discussions and support, especially when experiments do not work.

I would like to thank everyone at the University of Florida, especially Jim Rocca, an NMR specialist at the Brian McKnight Institute, for his tremendous help with my NMR studies, for staying there with me day and night, and for being such a great host when I make my visits. And to Mark Beveridge who was so kind to provide all the laboratory assistance I needed.

I would also like to express my gratitude to Johannes Leisen, an NMR specialist at Georgia Tech, who has helped me with my *in vivo* NMR studies and has been extremely patient with me. I would like to thank Dr. O'Farrell for her expertise in animal work and for teaching me all the techniques I need to know regarding animal handling and surgical procedures.

And finally, I would like to greatly acknowledge my friends and family for their unwavering support, especially my mom and dad for always listening to my complaints and for their constant encouragement.

This work was supported by grants from the National Institutes of Health (DK76801, DK47858, DK73991) and by a GAANN Fellowship from the U.S. Department of Education through the Center for Drug Discovery, Development and Delivery (CD4). This financial support is gratefully acknowledged. Additionally, the *in vitro* NMR work was supported by the National High Magnetic Field Laboratory (NHMFL).

TABLE OF CONTENTS

LIST OF TABLES

LIST OF FIGURES

LIST OF ABBREVIATIONS

AGE	Advanced glycated end products
AIDO	Average intrabead dissolved oxygen
ANOVA	Analysis of variance
APA	Alginate/PLL/alginate
CSII	Continuous subcutaneous insulin infusion
DO	Dissolved oxygen concentration
ΔDO	Difference in DO concentration
DMEM	Dulbecco's Modified Eagle's Medium
GCR	Glucose consumption rate
IDDM	Insulin dependent diabetes mellitus
ISR	Insulin secretion rate
NMR	Nuclear Magnetic Resonance
PFC	Perfluorocarbon
PFCE	Perfluoro-15-crown-5-ether
PFTBA	Perfluorotributylamine
PLL	Poly-L-lysine
RIU	Relative intensity units
STZ	Streptozotocin
TEPC	Tissue engineered pancreatic construct
TLM	Two layer method
UW	University of Wisconsin

SUMMARY

Oxygen is a key parameter in maintaining cell viability and functionality. This is especially true in encapsulated cell systems, as the cells within the constructs rely solely on diffusion for the transport of dissolved oxygen. Furthermore, many poorly known *in vivo* factors influencing construct oxygenation strongly affect the implant's therapeutic function. However, construct function is only assessed based on end physiologic effects or post-explantation studies at which an animal is euthanized. In order to develop a long-term functional implant, finding a means to enhance and monitor construct oxygenation *in vivo* is crucial. In this regard, perfluorocarbons (PFCs) can be utilized as an oxygen carrier, due to its high capacity for dissolving oxygen, to potentially improve the survival and function of encapsulated cells. Besides that, PFCs also serve as oxygen concentration markers for ^{19}F Nuclear Magnetic Resonance (NMR), whereby this method can be used to noninvasively track the oxygenation state of cells in a construct *in vitro* and *in vivo*.

The addition of a PFC emulsion improves the overall construct oxygenation by increasing the effective diffusivity of dissolved oxygen into the constructs. Whether this enhancement is sufficient to significantly improve cell viability and function is still a subject of debate, as there have been conflicting reports in literature regarding the beneficial effects of PFCs. The work in this thesis investigated this question as it relates to encapsulated cell systems. Perfluorotributylamine (PFTBA) emulsion was co-encapsulated at 10 vol% with βTC-tet cells in alginate beads and the cell/PFC constructs were cultured under normoxic and severely hypoxic conditions in the long- and short-

term. The alginate-PFC-cell system was also modeled mathematically, and simulations tracked dissolved oxygen concentration (DO) and the number of viable cells within the constructs over time under the same conditions used experimentally. Experimental results showed no significant improvement in cell metabolic activity, viability, and insulin secretory function with the addition of PFTBA. This finding was consistent with the results of mathematical simulations that noted only a small, likely experimentally undetectable, increase in cell density in PFC-containing beads. Simulations also indicated an increased positive effect of PFC on cells with a higher oxygen consumption and growth rates, but this was also modest in magnitude.

Besides having a high solubility of oxygen, the high fluorine content of PFCs makes them good oxygen concentration markers for ^{19}F NMR. As the relaxation rates ($R_1 = 1/T_1$) of excited fluorine nuclei increase in the presence of oxygen, DO within an implant can be measured through ^{19}F NMR when PFCs are incorporated. The ability to noninvasively monitor DO allows for an assessment of the metabolic activity of the cells within the construct, and for important correlations to be established between these *in vivo* measurements and construct function. The work in the second part of this thesis involved the development of a dual PFC noninvasive method of monitoring DO in a tissue engineered pancreatic construct using ^{19}F NMR. The dual PFC method consists of the incorporation of each of two different PFCs with proximal chemical shifts, either in the experimental tissue implant (βTC-tet cells encapsulated in alginate beads) or in cell-free alginate beads; the cell-free beads are used to monitor DO in the surrounding medium or implantation milieu, as equilibration of the intrabead and external DO is assumed to be rapid.

The feasibility of this method was tested *in vitro* where the encapsulated cells were cultured under perfused and static conditions in an NMR-compatible bioreactor. T_1 relaxation measurements were acquired over time at different encapsulated cell densities. Using this method, T_1 relaxations within the cell-containing beads and cell-free beads can be obtained simultaneously; therefore DO within the constructs containing metabolically active cells can be measured relative to the surrounding medium. Steady-state DO measurements acquired under medium perfusion showed minimal DO difference between the cell-containing beads and the surrounding medium; a considerable difference was only detected at a high encapsulated cell density of 7×10^7 cells/ml. Under static conditions, however, significantly lower DO levels were measured within the cell-containing beads when compared to the surrounding medium, which demonstrated the capability of the method to track the oxygenation state of beads containing metabolically active cells. The DO profiles obtained under static conditions were also supported by mathematical simulations of the system, indicating that the observed trends were not measurement artifacts.

The dual PFC method of monitoring was implemented *in vivo* using murine models. The βTC-tet cell-containing alginate beads were implanted in the peritoneal cavity of normal and streptozotocin-induced diabetic mice. Cell-free alginate beads were co-implanted to track the DO in the implantation milieu. T_1 measurements were acquired from the two bead populations over time, and construct physiology and therapeutic function were assessed through post-explantation studies and blood glucose measurements, respectively. Through ^{19}F NMR, the capability of acquiring real-time *in vivo* DO measurements using the dual PFC method was demonstrated. In both normal

and diabetic mice, measurements showed the peritoneal environment to be hypoxic and variable. DO within cell-containing beads decreased over time and correlated with relative changes in the number of viable encapsulated cells and/or the extent of host cell attachment. The presence of the viable cell implant also caused a significant decrease in the surrounding peritoneal DO. Diabetic mice receiving βTC-tet cell constructs remained normoglycemic for the duration of the experiment; the reduction in construct DO due to the metabolic activity of the encapsulated cells was observed to be compatible with the implant therapeutic function.

In conclusion, the work in this thesis demonstrated the limited beneficial effect of PFC in encapsulated cell systems. A noninvasive ^{19}F NMR method of monitoring the functional state of a tissue engineered pancreatic construct was also developed. The established method allowed for the evaluation of the oxygen environment in the animals, and of the effect of construct implantation on animal physiology.

CHAPTER 1

INTRODUCTION

In the United States alone, approximately 1.8 million people are diagnosed with type 1 diabetes [1]. The majority of diabetic patients currently rely on exogenous insulin, delivered through daily injections or pumps, to normalize their blood glucose. However, even with vigorous insulin therapy, a tight regulation of blood glucose cannot be achieved, therefore leading to long-term complications of the disease [2]. Cell-based therapies such as pancreas and islet cell transplantation emerged to be promising treatment alternatives as the physiological secretion of insulin by the cells provides for a better glucose regulation. While a reduction in glycemic fluctuations and improvement in the quality of life have been observed, there still exist challenges preventing the success of these treatments. Transplant recipients are required to take immunosuppressive drugs for the rest of their lives to avoid organ or cell rejection, and transplantation is limited by the scarcity of human donors [3].

Many studies have been and are currently focused on developing tissue engineered pancreatic constructs (TEPCs) to alleviate the issues associated with these therapies. The use of alternative cell sources such as xenogeneic islet cells and genetically-engineered β or non- β cells are being investigated [4-6]. These cells are entrapped in a 3-dimensional, biocompatible material for protection from the host immune system. Such a construct is an insulin reservoir of infinite capacity and is capable of regulating insulin delivery continuously as long as the cells remain viable. A significant concern, however, is the delivery of oxygen into the construct, as oxygen is

usually the limiting nutrient in maintaining cell viability and function. The encapsulated cells might be subjected to transient hypoxia, as a result of construct handling, or to constant hypoxia, due to the hypoxic *in vivo* environment and the absence of vascularization around the constructs [7, 8]. Furthermore, many other poorly known factors that affect construct oxygenation, thus cell function *in vivo* often lead to implant failure, and can be detected only based on end physiologic effects [9]. An understanding of the mechanisms of implant failure and early detection will aid the development of an optimum construct design and increase safety if implanted in patients. Therefore, finding a way to enhance oxygen delivery and to noninvasively monitor the functional state of a TEPC would be invaluable.

Perfluorocarbons (PFCs) are unique nontoxic compounds that have a high capacity for dissolving oxygen [10] and have been used for many years as oxygen carriers [11, 12]. As it has also been shown that the ^{19}F Nuclear Magnetic Resonance (NMR) spin-lattice relaxation rates of PFCs are highly sensitive to oxygen, there has been developing interest in using these compounds to probe tissue physiology [13, 14]. The **overall goal** of this thesis was to investigate the use of PFCs in improving cell viability and function in a TEPC, and to develop a method to noninvasively monitor the functional state of a TEPC *in vitro* and *in vivo*, through ^{19}F NMR. For the latter, the objective was to establish a method to measure the dissolved oxygen concentration (DO) that the cells experience in the constructs, and to draw correlations between construct oxygenation and cell viability and function. This goal was achieved by completing the following specific aims:

Specific Aim 1: Investigate the effects of PFCs on the viability and function of encapsulated cells under normoxic and hypoxic conditions.

Specific Aim 2: Establish and validate the feasibility of a dual PFC method of monitoring DO within a TEPC *in vitro* through ^{19}F NMR.

Specific Aim 3: Implement the dual PFC method to monitor DO within a TEPC *in vivo* through ^{19}F NMR.

In this thesis work, the TEPC employed for both *in vitro* and *in vivo* studies consisted of murine βTC-tet insulinomas encapsulated in alginate beads (Figure 1.1).

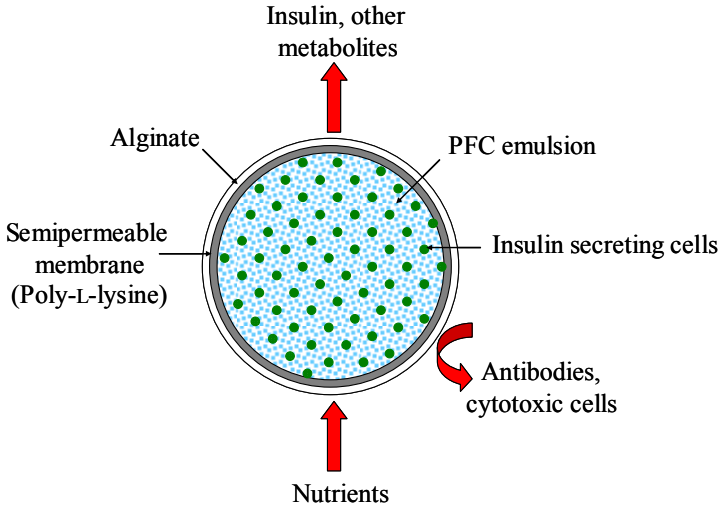

Figure 1.1 Configuration of the TEPC used.

PFCs were incorporated in the form of an emulsion, with the droplets immobilized and homogeneously dispersed throughout the alginate matrix. The cells were only present in the aqueous phase of the construct. Oxygen does not bind chemically to the PFC, but it dissolves and equilibrates between the PFC and aqueous phase with a partition coefficient favoring the PFC phase. Two types of beads were studied; calcium alginate-poly-L-lysine-alginate (APA) beads and barium alginate beads (without poly-L-lysine).

CHAPTER 2 of this thesis provides the details of the TEPC, and the background of the different applications of PFCs in such constructs and in other biological systems.

As oxygen availability affects cell function and limits the number of cells that can be supported by a construct, researchers are constantly investigating methods to enhance construct oxygenation. The use of PFCs is an appealing approach as these compounds have the ability to dissolve approximately 10 to 20 times more oxygen than water [10]. In tissue constructs where the PFC is not convectively transported, the PFC phase can act as an oxygen carrier by improving the overall construct oxygenation through the increase in the oxygen effective diffusivity, or as a transient oxygen reservoir by releasing oxygen to the aqueous phase under hypoxic conditions. The incorporation of PFCs, whether in the form of pure liquid or an emulsion, has been shown to increase oxygenation and hence improve cell viability and function in different tissues [15-17]. Despite encouraging results however, there are studies that show the contrary [18-20]. The benefits are still unclear as the significance of the PFC effect is likely dependent on each system, such as the cell type used, the concentration of PFC incorporated, and the external oxygen conditions. In CHAPTER 3 of this thesis, we investigated this question specifically to applications with encapsulated insulin-secreting cells. We studied experimentally the effect of a PFC emulsion, perfluorotributylamine (PFTBA), on the metabolic activity, viability, and insulin secretory function of βTC-tet insulinoma cells encapsulated in calcium alginate beads under normoxic and hypoxic conditions. A mathematical model of the alginate-PFC-cell system was also constructed under both of these conditions and simulation results were compared to those obtained experimentally.

Besides enhancing oxygen delivery, PFCs have been used as oxygen concentration markers for ^{19}F NMR to probe tissue oxygenation. DO within a tissue engineered construct is a significant parameter to be measured due to the high dependence of cell survival and function on oxygen. The presence of oxygen, which is paramagnetic, causes the spins of excited fluorine nuclei from the PFCs to relax faster. A linear relationship exists between the inverse spin-lattice relaxation time ($1/T_1$) of the fluorine resonances and oxygen, enabling the determination of DO when PFCs are incorporated into the constructs. The advantage of the ^{19}F nucleus is its absence in most biological tissues, thus eliminating the problem of interfering background signals. Furthermore, its high sensitivity enables T_1 acquisitions even at low concentrations of PFCs. We developed a dual PFC method (Figure 1.2) capable of tracking DO within a tissue implant and in its surroundings. The latter measurement is important as the *in vivo* oxygen environment can vary significantly over time and among animals.

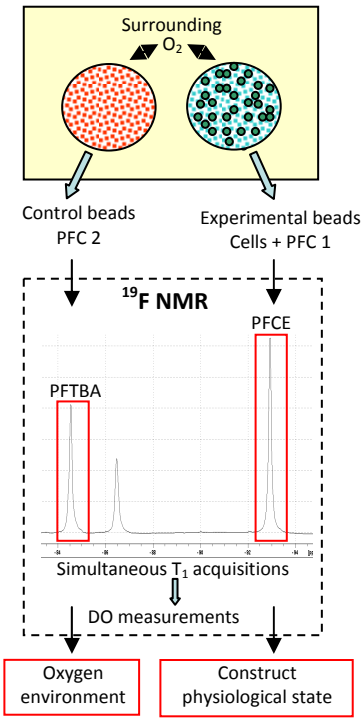

Figure 1.2 The dual PFC method

The dual PFC method consists of the incorporation of each of two different PFCs with proximal chemical shifts, either in the experimental tissue implant (βTC-tet cells encapsulated in alginate beads) or in cell-free alginate beads. The cell-free beads are used to monitor DO in the surrounding medium or implantation milieu, as equilibration of the intrabead and external DO is assumed to be rapid. In this work, the two PFCs used, perfluorotributylamine (PFTBA) and perfluoro-15-crown-5-ether (PFCE), have chemical shifts 9 ppm apart, close enough to allow for simultaneous T_1 acquisitions. Our approach in this ^{19}F NMR monitoring method is to acquire a single DO from the entire construct representing a volume average measurement of oxygen concentrations within the volume of interest.

The feasibility of the monitoring method was tested *in vitro* by culturing the dual PFC bead population in an NMR-compatible bioreactor. The work, as reported in CHAPTER 4 of this thesis, was done to demonstrate that (1) DO measurements in the two groups of beads can be simultaneously obtained through ^{19}F NMR, and (2) the DO level in beads with encapsulated cells can be distinguished from the DO level in beads without cells, where the latter is equal to the DO in the surrounding medium. DO differences between these two groups of beads were assessed under perfused and static culturing conditions. The DO profiles under static culturing conditions were also simulated using a mathematical model of the system and compared to the experimental results.

Following *in vitro* feasibility studies, the dual PFC method was implemented *in vivo* using murine models. The function of an implanted TEPC is influenced by many poorly known *in vivo* factors; however, the assessment of construct function is solely

based on the observed end physiologic effects. The development of the dual FPC method of monitoring will aid in the understanding of implant function through correlations established between *in vivo* DO measurements and both the construct physiology and therapeutic function, assessed through post-explantation studies and blood glucose measurements, respectively. CHAPTER 5 of this thesis reports on the implementation of the dual PFC method *in vivo*, in normal mice (Part I) and in diabetic mice (Part II). In Part I of chapter 5, we investigated the feasibility of acquiring *in vivo* DO measurements in the dual PFC bead population using ^{19}F NMR, and established correlations between the measured construct DO with cell growth and host cell attachment examined post-explantation. In Part II of this chapter, in addition to examining construct physiology, construct therapeutic function was assessed through blood glucose measurements and correlated to the measured construct DO. Real-time DO measurements were obtained in functional and non-functional constructs implanted in both normal and streptozotocin-induced diabetic mice. The usefulness of the information provided by these studies on the *in vivo* functionality of the cell implants, and on the effect of such implants on host animal physiology, is discussed.

Finally, the conclusions drawn from these studies are summarized in CHAPTER 6 of this thesis. The potential and research directions of the dual PFC method are also discussed.

CHAPTER 2

BACKGROUND

2.1 Diabetes

There is an increasing prevalence of diabetes worldwide. According to the Centers for Disease Control and Prevention, a total of 23.6 million people in the United States alone suffer from this disease, with medical costs totaling to approximately $174 billion in 2007 [1]. Type 1 diabetes, formerly known as insulin-dependent diabetes mellitus, accounts for 5% to 10% of all diagnosed cases of diabetes [1]. This disease develops when the body's immune system destroys the β cells of the pancreatic islets, the only cells in the body that produce insulin to regulate blood glucose. Thus type I diabetic patients depend upon exogenous insulin therapy for life [3]. On the other hand, type 2 diabetes, formerly known as non-insulin-dependent diabetes mellitus, accounts for 90% to 95% of all diagnosed cases of diabetes [1]. It is a milder form of diabetes which occurs when the pancreas loses its ability to produce insulin or when the body is resistant to the action of insulin produced. While oral medication, exercise, and diet are usually sufficient to temporarily stabilize blood glucose levels, type 2 diabetes usually develops into insulin-dependence [3, 21].

Insulin deficiency or resistance results in an increase in blood glucose levels; diabetes is diagnosed when the fasting or non-fasting plasma glucose is $\geq$ 7.0 mmol/l (126 mg/dl) and $\geq$11.1 mmol/l (200 mg/dl), respectively [22]. It is associated with unusual thirst, frequent urination, weight loss, extreme fatigue and can sometimes lead to coma. Diabetics have an increased susceptibility to infections and are prone to develop

vascular complications such as stroke, heart attack, blindness, renal failure, and peripheral nerve damage. One proposed mechanism which has been postulated to play a central role in vascular complications is the process of advanced glycation. This process involves the generation of advanced glycated end products (AGEs) as a result of glucose interacting with the amine residues on proteins, lipids, and nucleic acids. The cross-linking of AGE with type I collagen and elastin leads to increased stiffness of blood vessels, which eventually causes tissue and organ damage [23, 24]. Diabetes therapy aims to normalize glucose control without introducing severe hypoglycemic episodes [2] as low blood glucose levels result in dizziness, weakness, heart palpitation, anxiousness, and tremor among others. If blood glucose levels continue to fall, neurologic manifestations can occur, which cause loss of consciousness, convulsion, and deep coma. Prolonged severe hypoglycemia may even lead to brain damage [24].

2.1 Current Type 1 Diabetes Treatment Methods

The discussion focuses on the treatment methods for type 1 diabetics; however, most of these considerations apply to insulin-dependent type 2 diabetics as well. Type 1 diabetes is treated with insulin replacement therapy where exogenous insulin is delivered subcutaneously by injections or an insulin pump. Insulin injections continue to be the treatment choice for many because of its simplicity and low cost. Patients receiving this type of treatment inject themselves with insulin multiple times a day, with the frequency of injections dependent on their lifestyle and the insulin formulation (short, intermediate, or long-lasting) used. Nevertheless, multiple daily injections are inconvenient and hypoglycemic occurrences are still common. An alternative insulin replacement therapy

is through the use of external pumps for continuous subcutaneous insulin infusion (CSII). It is estimated that 20-25% of type 1 diabetic patients are using insulin pumps [25]. Evidence suggests that CSII improves blood glucose control and significantly reduces hypoglycemic episodes [25, 26]. As current pumps are based on an open-loop system where insulin delivery is not automatically adjusted, failure of this treatment can still happen due to the need to continually adapt insulin infusion according to blood glucose oscillations [25]. Many investigators are currently working towards designing a closed-loop system, where there is real-time communication between an infusion pump and a glucose sensor. This technology requires a glucose-sensing device capable of modulating insulin infusion at all times. At present, most glucose sensors are lacking in reliability and sustained stability, and are still being evaluated in clinical trials. Intensive insulin therapy through injection or pump delivery can delay the onset and reduce the progression of chronic diabetes complications, but it also significantly increases the occurrences and severity of hypoglycemic episodes [27, 28]. Despite considerable improvement in this therapy through the development of novel insulin formulations and infusion pumps, tight glycemic control remains difficult to attain.

Whole pancreas transplantation was the first biological substitute of the β cell function. This treatment approach offers the benefits of the avoidance of insulin administration and reduction of hypoglycemic episodes. A successful pancreas transplantation restores glucose homeostasis in a patient and is shown to be more effective than intensive insulin treatment [29]. Since the first pancreas transplantation in 1966 [30], this treatment has progressed significantly, with improved graft and patient survival rates [31]. Nevertheless, there are still a high rate of technical failures and risks

of post-transplant complications, with thrombosis accounting for more than 70% of all the failures that invariably lead to graft loss [32]. Another major downside of this procedure is the need for immunosuppression for the rest of the patient's life; but even with immunosuppression, acute rejection of the transplanted pancreas can still occur.

Alongside pancreas transplantation, islet cell transplantation was progressively introduced as a potentially less invasive therapeutic technique. Islets are usually infused into the liver through the portal vein, through the use of ultrasound and radiography. Initial trials to implement islet cell transplantation had limited success, with almost all failing mainly due to rejection. However, after the publication of the use of a steroid-free protocol in 2000, also known as the Edmonton protocol which established insulin independence in 7 diabetic patients [33], islet cell transplantation regained interest among many researchers. Since then, major islet transplant centers have been established and refined new procedures, involving the use of low-dose immunosuppressive therapy without glucocorticoid drugs, and improved islet preparation have been developed [27, 34]. Recent data indicate that insulin secretion by the transplant is associated with an improvement in the quality of life, with a reduction in hypoglycemic episodes and potentially with a reduction in long-term diabetic complications [35-37]. Despite major progress in islet cell transplantation, however, its widespread application is limited by the need for immunosuppression and shortage of human donors [28, 34]. Even though current immunosuppressive therapies are safer than those used in the past, there are still increased risks of infection and malignancy due to the toxicity of the drugs. Furthermore, these drugs have diabetogenic properties that may be responsible for the continuous loss of β cells [3, 7, 38]. In order to achieve insulin independence, two or more donor

pancreata (~10,000 to 14,000 islet equivalents per kilogram of recipient's body weight) are usually needed [28]. Currently, only 0.1% of the type 1 diabetic population could be transplanted with the limited supply of donor organs [7]. These difficulties have prompted the search for alternative cell sources and the development of encapsulated devices to prevent the need for immunosuppressive drug regimes.

2.3 Tissue Engineered Pancreatic Constructs (TEPCs)

Pancreas and islet transplantation are now the only means of achieving physiologic insulin regulation. There is ongoing research to developing tissue engineered pancreatic constructs (TEPCs) to address the problems of immune rejection and donor tissue scarcity [39]. TEPCs generally contain living cells within a biocompatible matrix which separates the transplanted cells from the host immune system. The matrix is usually surrounded by a semipermeable membrane that allows the passage of nutrients and metabolites, including dissolved oxygen, glucose, and insulin, but excludes high molecular weight antibodies and cytotoxic cells of the host. The protection from the host immune system also makes possible the use of alternative cell sources, thereby alleviating the problem of human donor shortages; alternative cell sources that have been investigated include xenogeneic islet cells, β cells genetically engineered to proliferate in culture, and non- β cells genetically engineered to secrete insulin in a glucose-responsive manner [3]. When designing TEPCs, properties that are desirable include biocompatibility of the material, good diffusional properties through the membrane, easy implantation and retrievability, and the ability to keep the cells properly nourished and thus alive and functional.

2.3.1 Insulinoma-derived Cell Lines

A number of different methods have been applied to generate continuous, insulin-secreting cell lines. A major advantage of adopting the use of cell lines is that they provide an abundant and reproducible source. Transformed human β cell lines are more compatible with the human physiological environment and induce less severe immune rejection [40], but the complications in generating allogeneic cell sources have led researchers to investigate the use of xenogeneic cell sources instead. Although xenotransplantation is far from becoming a reality due to safety concerns and immunological problems, the development of these cell sources are useful for β cell research and as a model for the engineering of human islet β cells [40, 41].

The laboratory of Shimon Efrat has established successful functional β cell (βTC) lines [42-44]. These cells were developed from insulinomas induced in transgenic mice expressing the SV40 T-antigen (Tag) under the control of the insulin promoter. One of the earlier variant of these cell lines, βTC3, displays good growth and retention of insulin secretion in culture; these cells, however, exhibit glucose-responsiveness within subphysiological ranges and uncontrolled proliferation. To regulate βTC replication, the expression of the Tag oncogene was placed under a conditional, bacterial tetracycline operon regulatory system [44]. This newer stable cell line, βTC-tet, has shown more physiologic responsiveness to glucose and maintains a low hexokinase activity for > 60 passages [43-45]. When implanted in a syngeneic diabetic mouse model, tetracycline-induced inhibition of the Tag expression controlled cell proliferation, but cells remained viable and capable of glucose sensing and insulin secretion, which led to the correction of hyperglycemia [5]. These cells expressed regulated insulin secretion by increasing their

insulin release up to 13-fold when a high concentration of glucose was infused in the mice. Encapsulated βTC-tet cells were also successful in restoring normoglycemia for 8 weeks in an allogeneic NOD mouse model [46].

2.3.2 Construct Technology

Microencapsulation devices are extensively used in the development of TEPC due to the simplicity of construction, flexibility of modifying the key components, good transport properties, and ease of handling and implantation [3, 47]. In such devices, cells are typically encapsulated in microspheres (beads) of alginate or agarose gel, and sometimes coated with a semipermeable membrane. Alginate, which exists in varying composition and sequence of linear copolymers of 1-4-linked β-D-mannuronic acid (M) and α-L-guluronic acid (G), is widely used for reasons including biocompatibility, polymerization under physiological conditions, easy gelling kinetics, porosity, and the good environment it provides for the encapsulated cells [48-50]. Lim and Sun were the first to introduce what is now one of the most common techniques of islet and cell encapsulation [51]. Using this method, the cells are suspended in sodium alginate solution and the cell suspension is extruded into a calcium chloride solution to form beads. Gelling occurs when the α-L-guluronate alginate residues crosslink with the divalent Ca^{2+} [49]. To add a semipermeable membrane, the beads were incubated in poly-L-lysine (PLL) solution, where the incubation time determines the membrane pore size. However, because poly-L-lysine is inflammatory, beads are generally coated with a final layer of alginate, forming calcium alginate-PLL-alginate (APA) beads [52]. Restoration of normoglycemia through implanted islets encapsulated in APA beads has

been demonstrated in diabetic murine models and larger animals, including monkeys and dogs [51, 53-57]. Although normoglycemia was achieved with these implanted constructs, reduced and delayed insulin secretion was still observed in certain cases [58]. As alginate encapsulation introduces minimal resistance to mass transfer, the observation was largely attributed to the occurrence of fibrotic overgrowth. The intensity of fibrotic response can vary significantly, even within the same species, and significantly hinders the diffusion of nutrients and metabolites into and out of the constructs. While differences in the tissue donor and recipients strongly influence the extent of the overgrowth, incomplete covering of the PLL coating also results in inflammatory reactions, usually observed within 1 week post-implantation [6].

More recently, many researchers have also investigated the use of non-coated barium alginate as an immunoisolation material. One concern often raised about barium alginate beads is the toxic effect it may have on the animals due to the release of barium ions [59], although this can be avoided with sufficient cross-linking time and multiple washes of the beads before implantation [60]. The cross-linking of alginate with barium ions produces a much more mechanically stable matrix than with calcium ions and could potentially exclude the entry of antibodies, but this has yet to be investigated [59, 61]. Implantation of islets encapsulated in barium alginate has shown to be successful in restoring normoglycemia in diabetic rodents [62-64]. In fact, when compared to APA beads, barium beads were proven to be more biocompatible and capable of prolonging the survival of encapsulated adult porcine islets in NOD mice [65]. Even though the reasons why barium beads perform so well are not clearly understood, researchers offered a few explanations for these observations: the higher biocompatibility due to the absence

of PLL, the strong affinity of barium for alginate, and the prevention of communication between the encapsulated islets and the splenocytes [3, 62, 65].

2.3.3 *In vivo* Construct Integration

Understanding the *in vivo* environment and how it affects the efficacy of a TEPC is crucial in designing the optimal construct for post-implant survival. Upon implantation, the recipient reacts against both the construct material and the islets or cells within the constructs [66]. Inflammatory reaction due to a lack of biocompatibility of the construct is one of the main reasons for implant failure. This is dependent on the composition and purity of the alginate used, and the integrity of the construct, as characterized by its stability and physical perfection [7]. However, even if inflammatory reaction against the biomaterial is eliminated and the membrane is able to protect the transplanted cells from host antibodies, the recipient may still react against proteins released or secreted by the cells. In this context, host antibodies can combine with shed donor antigens, forming complexes which bind to the Fc receptor of macrophages. This elicits the release of cytokines, nitric oxide, and oxygen radicals, all which are small enough to enter the constructs and destroy the cells [63, 67].

Another challenging issue *in vivo* is ensuring good mass transfer of nutrients and metabolites into and out of the constructs. Both the construct design and the distance between the implantation site and the bloodstream affect the rapidness of response by the cells towards changes in blood glucose levels [7, 68]. The transport of oxygen, in particular, is especially crucial as its availability strongly influences implant survival and function. As normal pancreatic islets are highly vascularized and thus well oxygenated,

encapsulated islets usually suffer from hypoxic stress since revascularization cannot occur around the implant and the supply of oxygen is through passive diffusion only [7]. Furthermore, any inflammatory reaction towards the implant may result in a further decrease in construct oxygenation. Oxygen limitation compromises insulin secretory responses and leads to graft failure [7, 69, 70]. While intact islets have their secretory function compromised at oxygen tensions below 60 mmHg, studies have shown that βTC3 are more tolerant to hypoxic conditions and therefore may function better than islets in implanted constructs [68, 71].

Another issue to be considered during the development of a TEPC is the ability to monitor implant function *in vivo* as constructs are usually highly dynamic post-implantation. In this regard, Nuclear Magnetic Resonance (NMR) spectroscopy and imaging are very useful modalities that can be used to noninvasively track the changes occurring to the constructs [52]. Correlations drawn between *in vivo* measurements and end physiological effects, as usually determined through blood glucose measurements, can assist in understanding construct function and mechanisms that lead to construct failure.

2.4 Perfluorocarbons (PFCs)

Perfluorocarbons (PFCs) are highly fluorinated compounds wherein all or most of the hydrogen atoms in the molecule are replaced with fluorine atoms [72]. These compounds are chemically and biologically inert, and are both hydrophobic and lipophobic [14, 72] Due to low intermolecular interactions, PFCs have a capacity for dissolving large amounts of respiratory and other nonpolar gases. The solubility of

oxygen in PFC is approximately 10 to 20 times that in water [10]. This unique property has been exploited for use by many biotechnologists and clinicians in various biological applications. As PFCs are not miscible with water, they are usually used in the form of an emulsion. They are prepared through homogenization or sonication of the liquid PFC and an emulsifier such as Pluronic-68, egg yolk phospholipids, and triglycerides, forming typical droplet sizes of approximately 1 – 2 μm (Figure 2.1)

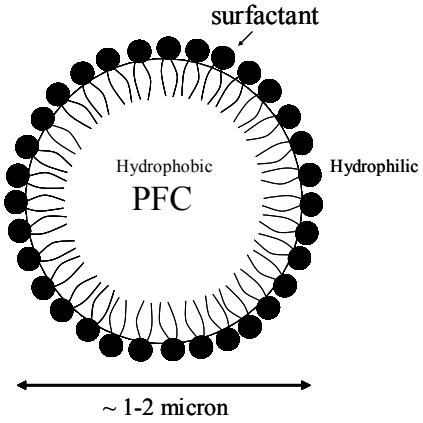

Figure 2.1 PFC emulsion

PFC emulsions are generally stable, although stability does decrease over time through two proposed mechanisms, coalescence and molecular diffusion [73]. After *in vivo* administration, PFCs are not metabolized by the tissues but are cleared by circulation and excreted through exhalation [14].

2.4.1 PFCs as Oxygen Carriers

Due to the high solubility of oxygen in PFCs, these compounds have been utilized as oxygen carriers in many biological applications including blood substitutes, organ preservation, and tissue engineered devices. In the development of artificial blood, Fluosol-DA (20 % wt/vol coemulsion of perfluorodecalin and perfluorotripropylamine

with egg yolk phospholipid and Pluronic-68, Green Cross Corp., Osaka, Japan) was the first PFC emulsion commercially made for use as a blood substitute where its safety and efficacy was tested in patients with acute anemia. Although no serious adverse reactions were noted in this clinical study, no appreciable beneficial effects of Fluosol-DA were seen either [74]. The PFC emulsion did not meet the metabolic oxygen demand as the emulsion contained a very low concentration of pure PFC [75]. Since then, many other second-generation PFC emulsions with a higher PFC content have been developed including Oxyfluor (HemaGen/PFC, St. Louis, MO), Oxycyte (Oxygen Biotherapeutics, Inc., Costa Mesa, CA), and Perftoran (Perftorwn, St. Petersburg, Russia) [11, 75]. Oxygent (60% wt/vol perfluorooctyl bromide with phospholipid, Alliance Corp., San Diego, California) in particular, had a high emulsion stability despite its high PFC content, and was assessed in a variety of hemodilution studies [76]. In a model of anesthesized hemodiluted dogs, administration of Oxygent was effective in maintaining tissue oxygenation [77]. Other studies with dogs demonstrated positive findings of improved oxygen content and saturation [78] and myocardial contractility properties [79]. The use of PFCs as blood substitutes has also been tested in humans. In patients undergoing major noncardiac surgery, hemodilution and Oxygent administration was shown to reduce the need for blood transfusion [80]. Additionally, when blood transfusion is needed, the use of Oxygent was shown to treat such transfusion triggers more effectively than autologous blood in orthopedic surgery [81] and prevent gastrointestinal tract ischemia in cardiac surgery patients [82]. Despite all the successful outcomes, however, the use of Oxygent was eventually suspended due to adverse neurological effects. Even though many PFC emulsions offer attractive characteristics as

a blood substitute, there is currently no PFC approved for clinical use in the United States due to the secondary effects of the surfactants employed [74]. Further work is being done to obtain a safe PFC emulsion; this includes improving the emulsion stability, prolonging intravascular persistence of the emulsion, and establishing the appropriate formulations with the adequate properties for each application [11].

In the area of pancreas preservation, PFC was first used as a component of the two-layer method (TLM) developed by Dr. Kuroda in 1988 at Kobe University [83]. In this method, the pancreas is suspended between pre- or continuously-oxygenated PFC and a standard organ preservation solution, typically University of Wisconsin (UW) solution [84]. This cold storage method has been shown to be an effective way of preserving the pancreas before islet isolation or transplantation in animal models and also clinically. The TLM reduced ischemic injury and resuscitated the pancreas that experienced ischemic injury during preservation, prolonged the preservation period before islet isolation, and improved the quality of the pancreas, resulting in a high yield of islets during isolation [12, 84-87]. These positive findings were reported for both non-human and human pancreata [85-89]. One proposed explanation for the observed success is the continuous supply of sufficient oxygen from the PFC to the pancreas, thereby increasing the synthesis of adenosine triphosphate which maintains cellular integrity and controls cell swelling [90]. However, other groups have also observed contrary results whereby the TLM does not improve islet isolation or transplantation [18, 19]. For example, other studies indicate that there was no significant increase in the yield, purity, or function of islets isolated from TLM-preserved pancreas when compared to the UW-

preserved pancreas. Furthermore, no significant difference was observed in islet post-transplant function [18, 19].

In cell culture and the development of tissue engineered constructs, PFCs are being incorporated either in the culture medium or within the tissue constructs to enhance oxygenation. In studies where the PFC phase is convectively transported by medium perfusion through the tissue constructs, positive effects of PFC have been observed. For example, in a study by Kinasiewicz et al., medium supplemented with a PFC emulsion, Perftoran, was used for the culture of human hepatoma cells seeded on mineral fibers coated with collagen type I. Cells perfused with PFC-containing medium showed significant increase in protein synthesis, including albumin, the main protein produced by hepatocytes in the liver [15]. Similarly, in the study of Radisic et al., the addition of a PFC emulsion, Oxygent, to medium perfusing a parallel plate cardiac bioreactor increased the DO throughout the bioreactor and consequently supported a greater density of cardiomyocytes. Further studies with the same system showed improved properties of cardiac constructs cultured in PFC-supplemented medium. Tan et al. also reported on increased tissue engineered trachea epithelial oxygenation when the perfused culture medium was supplemented with the Oxygent, which subsequently improved epithelial metabolism [16].

On the other hand, in systems where PFC is incorporated to a static culture medium, mixed results on the effects of PFC have been obtained. When PFC-supplemented medium was used to culture rat islets, Zekorn et al. observed a marked increase in insulin secretory function in comparison to medium without PFC supplementation [91]. Similarly, Takahashi et al. also reported the use of oxygenated

PFC with culture medium to result in better insulin release [92]. While it was suggested that the elevated metabolic potency was due to the increased oxygenation, Bergert et al. did not observe similar results [20]. The viability and function of PFC-cultured rat islets were not significantly better than the control groups without PFC. In fact, in certain cases, there were trends of islet deterioration after PFC treatment [20]. Supporting this observation was Terai et al. who demonstrated that the addition of oxygenated PFC to UW solution lowered islet quality and was not beneficial in improving the cure rate of diabetic rats [93]. In a different system, where a PFC emulsion was encapsulated along with human HepG2 hepatomas in calcium alginate hydrogels, cellular growth and metabolic activity were shown to increase under both atmospheric and reduced oxygen conditions [17, 94]. The contradictory results reported in literature on the effects of PFC on organ preservation and on cell or islet viability and function in static systems necessitate further investigation.

2.4.2 PFCs as Oxygen Concentration Markers

PFCs have been increasingly used as physiological markers of tissue oxygenation in ^{19}F NMR spectroscopy and imaging [95-99]. The linear relationship between the spin lattice relaxation rate ($R_1 = 1/T_1$) of the PFC fluorine resonances and oxygen is used as a calibration curve (as observed in Figure 2.2 below) to derive oxygen concentration values following *in vivo* measurement of T_1 [100-102].

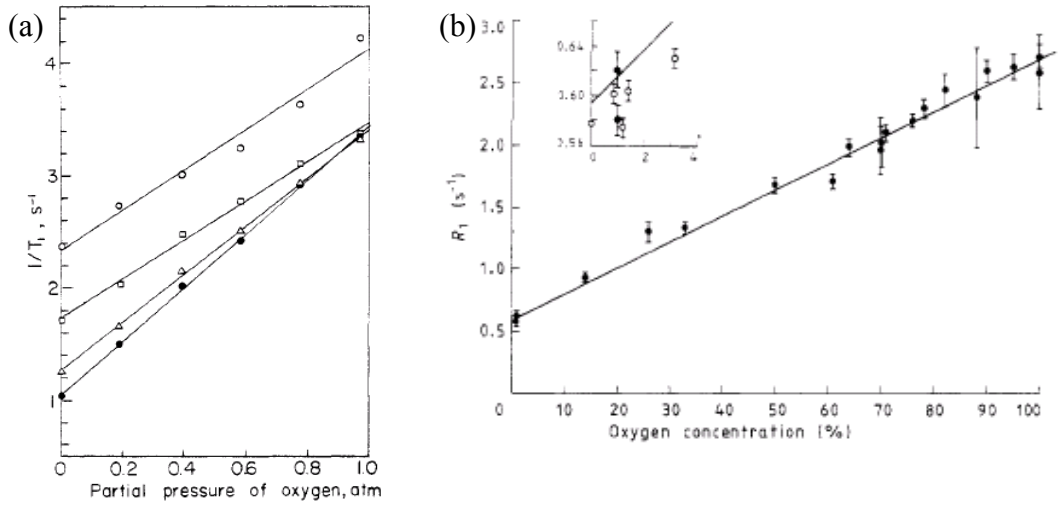

Figure 2.2 Linear calibration curves of $1/T_1$ versus oxygen for (a) perfluorotributylamine and (b) Fluosol-DA (perfluorodecalin + perfluorotripropylamine). Figure adapted from Parhami et al. [102] and Reid et al.[100] .

Due to their high oxygen solubility and hydrophobicity, PFCs display excellent sensitivity to oxygen and insensitivity to variations in ionic constituents compared to the surrounding tissue water [103]. The ^{19}F isotope presents several advantages including a 100% natural abundance, a relative sensitivity of 83% that of ^{1}H, which is the second most sensitive nucleus, and an absence of naturally occurring fluorine in biological tissues; this enables signal acquisition of very small amounts of exogenous fluorine [14, 100].

Oxygen is crucial in maintaining cellular homeostasis and preserving tissue physiological function. The ability to monitor *in vivo* oxygen aids in understanding mechanisms of tissue function and progression of disease, as well as in clinical prognosis. Previous studies have shown the feasibility of using ^{19}F NMR to noninvasively monitor oxygen levels in the liver, spleen, lung, heart, and brain through the distribution of PFC emulsion in these organs and tissues administered intraveneously or intraperitoneally

[104-107]. Noth et al. and Zimmermann et al. have also performed quantitative oxygen measurements in PFC-loaded alginate beads implanted in the peritoneal cavity, under the kidney capsule, and in the muscles of rats to identify the optimal implantation sites for cell survival. They reported low, variable oxygen levels in all the implantation sites [108, 109].

Similar monitoring methods have been used in studies of *in vivo* tumor oxygenation. It is widely recognized that the efficacy of many therapeutic approaches to tumor treatment is influenced by oxygen tension [110-113]. Studies have shown that chronic hypoxia that develops as large tumors outgrow their blood supply causes tumor aggressiveness, metastasis, and resistance to radiotherapy and chemotherapy [110, 114]. Furthermore, there is a widespread variation in tumor oxygenation where distinct heterogeneity exists among tumors independent of type, size, or stage [115, 116]. Oxygen measurements through ^{19}F NMR have been used to investigate the dynamic changes in tumor oxygenation in rats and mice [111, 113, 116, 117]. Also, given the resistance of hypoxic tumors to treatment, this method is used to guide oxygen tension modulation in tumor tissue through carbogen breathing, a technique used to enhance radiosensitization [111, 112, 118].

In partial liquid ventilation (PLV), gas is delivered into a lung which has been filled with PFC to improve gas exchange in patients with acute respiratory distress syndrome. Since PFCs already contain the ^{19}F isotope, they are simultaneously adapted as oxygen monitors to quantify oxygen partial pressure in the lungs, to understand the mechanisms of action of PLV and to improve treatment efficacy [119]. In studies by Laukemper-Ostendorf et al. and Heussel et al., this method was used to qualitatively and

quantitatively assess the regional distribution of the oxygen partial pressure in a porcine lung during PLV [95, 120].

PFCs can also be incorporated in tissue engineered constructs to noninvasively monitor construct oxygenation. Measuring DO within a construct helps determine the physiological status of the cells as there is a high dependence of cell function on oxygen, and an almost linear correlation between cell oxygen consumption and the number of viable cells [71, 121-123]. For encapsulated cell systems in particular, this method has been proven successful in tracking the metabolic state of cells *in vitro* [9]. The experimentally measured DO levels in the constructs were shown to correlate well with the encapsulated cell metabolic activity and also to the DO values predicted by a mathematical model [9, 124].

2.5 Noninvasive Monitoring of Tissue Engineered Pancreatic Constructs (TEPCs) by Nuclear Magnetic Resonance (NMR) Spectroscopy and Imaging

TEPCs are highly dynamic post-implantation. The extent of cell growth and remodeling, host-construct interaction, diffusion limitation of nutrients and metabolites, and the integrity and mechanical stability of the constructs all influence their functional outcome [9, 125]. In this context, NMR is a very useful noninvasive modality that can be used to probe the structure and function of a TEPC via imaging and spectroscopy, respectively [126-128]. The ability to noninvasively monitor the physiological state of a construct through NMR enables us to better understand construct function and therefore optimize their design. Dynamic changes occurring to the construct can be evaluated directly, therefore reducing the number of animals that needs to be euthanized.

Furthermore, it offers an early diagnosis of construct function post-implantation and also assists in understanding the underlying mechanisms that lead to implant failure [129].

Before implantation, *in vitro* studies under well controlled conditions are essential in understanding cell behavior in an encapsulation environment and in developing optimized NMR measurement methods. Commonly used nuclei to study cellular metabolism are ^{31}P and ^{1}H due to their relatively high sensitivity and natural abundance. Metabolites detectable by ^{31}P include nucleotide triphosphates (NTPs), whose primary component is attributable to adenosine triphosphate (ATP), inorganic phosphate (P_i), phosphocreatine (PCr), and other intermediates in phospholipids metabolism [129, 130]. Quantitative analysis of the biochemistry of recombinant, insulin-secreting mouse pituitary AtT-20 cells encapsulated as spheroids in alginate was initially performed by Constantinidis and Sambanis. The bioenergetics of cells cultured in a fixed bed bioreactor were measured using ^{31}P NMR spectroscopy for a period of 70 days. Results showed that the observed changes in high energy phosphates, PCr and NTP, were in agreement with changes in the metabolic activity of the cells [131]. Using similar methods, Papas et al. studied the effects of repetitive exposure to low or high glucose on the bioenergetic status of alginate-encapsulated βTC3 mouse insulinomas [132]. It was observed that for βTC3 cells, step changes in extracellular glucose concentration did not affect intracellular ATP, and that a correlation between ATP and insulin secretion rate existed only under certain culturing conditions [130, 132]. Further studies showed that ATP levels were reduced under short- and long-term hypoxia [8, 71]. Similar correlations between β-NTP and oxygen levels were also observed with βTC-tet cells [9]. These studies are useful in identifying key metabolic features of β cells and

elucidating mechanisms associated with glucose-stimulated insulin secretion. Unfortunately for tissue engineered constructs, ^{31}P sensitivity is still too low for detection of metabolites *in vivo*; therefore, in order to obtain sufficient signal, a high implanted cell number is required.

The ^{1}H nucleus appears to be a good alternative as it has a higher sensitivity when compared to ^{31}P. Nevertheless, a major issue with ^{1}H is the presence of the large water signal in biological tissues that masks the detection of intracellular metabolites [133]. To circumvent this problem, Long et al. developed solvent-suppression adiabatic pulse sequences to minimize the intensity of the water resonance, making it possible to monitor ^{1}H metabolites, specifically the total choline signal, from alginate-encapsulated βTC3 cells by NMR. Initial *in vitro* studies conducted in a packed-bed bioreactor showed that the total choline resonance can be used to track the net cell growth in the system, and is sensitive to changes in oxygen concentration [133]. Stabler et al. employed this method in a slightly different system where βTC3 cells were encapsulated in agarose disk-shaped constructs, and reported a strong linear correlation between total choline and the viable cell number and insulin secretion rate [134]. When implanted in the peritoneal cavity of mice, total choline measurements acquired noninvasively by localized ^{1}H NMR were used to quantify and monitor changes in the number of viable cells over time [125]. ^{1}H MR imaging techniques have also been developed to visualize both alginate and agarose constructs containing βTC3 cells *in vitro* and *in vivo* [125, 127, 128, 134]. This method was capable of detecting structural changes and host response effects on implanted agarose constructs [125]. Barnett et al. tried a different imaging approach by using PFCs as ^{19}F MR contrast agents. ^{19}F images of PFC-containing encapsulated islets implanted

in the peritoneal cavity were overlaid over anatomic ^{1}H MR images. Using this approach, the constructs were easily distinguishable from the surrounding tissues [135]. With the development of higher magnetic field strengths and better coil designs, *in vivo* NMR measurement sensitivity has been significantly improved, and spectroscopy and imaging methods are becoming more feasible [136].

CHAPTER 3

LIMITED BENEFICIAL EFFECTS OF PERFLUOROCARBON EMULSIONS ON ENCAPSULATED CELLS IN CULTURE: EXPERIMENTAL AND MODELING STUDIES*

3.1 Abstract

Due to the high solubility of oxygen in perfluorocarbons (PFCs), these compounds have been explored for improved cell and tissue oxygenation. The goal of this study is to investigate the effects of a PFC emulsion on cellular growth and function in a tissue engineered construct. A perfluorotributylamine (PFTBA) emulsion was co-encapsulated at 10 vol% with mouse βTC-tet insulinoma cells in calcium alginate beads and cultured under normoxic and severely hypoxic conditions. The number of metabolically active cells and the induced insulin secretion rate were measured over time for up to 16 days. Results showed no significant effect of PFTBA relative to the PFTBA-free control. The alginate-PFC-cell system was also modeled mathematically, and simulations tracked the number of viable cells over time under the same conditions used experimentally. Simulations revealed only a small, likely experimentally undetectable difference in cell density between the PFC-containing and PFC-free control beads. It is concluded that PFTBA up to 10 vol% has no significant effect on the growth and function of encapsulated βTC-tet cells under normoxic and hypoxic conditions.

* Modification of a paper published in the **Journal of Biotechnology**, 2010 Oct 15; 150(2):232-9

3.2 Introduction

A major challenge in developing and implementing tissue engineered substitutes is ensuring sufficient oxygenation of cells within constructs, as oxygen is a significant parameter affecting cell viability and function [8, 9, 71]. This is especially true for substitutes which rely on diffusion for the transport of dissolved oxygen. Therefore, a means of enhancing oxygen delivery by increasing the solubility and/or diffusivity of dissolved oxygen within a construct might prove beneficial and desirable.

The high solubility of oxygen in perfluorocarbons (PFCs) has led investigators to explore their use in the form of a non-aqueous phase or an emulsion, as a blood substitute, in organ preservation, and in tissue engineered devices. It is reasonable to expect a positive effect in systems where the PFC phase is convectively transported between an oxygenator and a culture or tissue where oxygen is delivered and used. This has been confirmed experimentally, as in the study of Radisic et al. who demonstrated that adding the PFC emulsion, Oxygent, to medium perfusing a parallel plate cardiac bioreactor increased the dissolved oxygen concentration (DO) throughout the bioreactor and consequently supported a greater density of cardiomyocytes [137]. In their system, the DO in the medium entering the bioreactor was kept constant at 160 Torr using a gas exchanger, thereby replenishing the PFC emulsion with oxygen after each bioreactor pass. Further studies with the same system showed improved properties of cardiac constructs cultured in PFC-supplemented medium [138].

In systems where PFCs are not convectively transported, enhanced oxygenation can be achieved by the delivery of oxygen from the PFC to an aqueous phase in contact, and/or by the increased effective diffusivity realized when PFCs are dispersed as an

emulsion in an aqueous phase. An example of the former is the two-layer method (TLM) of pancreas preservation, in which the organ is suspended between University of Wisconsin (UW) solution and oxygenated PFC. The PFC layer serves as an oxygen reservoir, while the UW solution provides other nutrients, including adenosine to promote ATP synthesis in the tissue [84]. With non-human pancreata, there exist reports of significantly improved islet yield and *in vitro* function when islets were isolated from organs preserved in the TLM relative to organs preserved in UW solution alone [85, 89]. Improved islet yields for pancreata preserved by the TLM versus the UW solution alone have also been reported for human tissues [86-88]. Other groups have observed contrary results, however, in which the TLM did not improve islet isolation or transplantation outcomes. For example, Caballero-Corbalan et al. compared the outcome of 200 human islet isolations performed after storage in either the UW solution only or by the TLM over short (<6 hours) or prolonged (up to 18 hours) cold ischemic time. They observed no significant improvement in the islet yield, purity, or function with the TLM [139]. Similarly, Kin et al. reported no beneficial effects of the TLM on human islet isolation and transplantation [18]. Papas et al. offered a mechanistic explanation of these outcomes, in that PFCs do indeed improve oxygenation but only in a thin peripheral layer of tissue, while oxygen is not delivered to inner tissue domains [140]. For this, convective oxygen transport through the native organ vasculature may be necessary.

PFC addition to culture media has also produced mixed results. With rat islets in culture, Zekorn et al. observed a marked improvement in islet insulin secretory function when the culture medium was supplemented with PFCs [91]. On the other hand, Bergert et al. [20] did not observe similar results. In the latter study, the effects of PFCs on islet

viability and function were characterized by measuring cell death, apoptosis, mRNA levels of insulin, insulin content, and stimulated insulin secretion. These extensive measurements indicated that the incorporation of PFC failed to provide any advantage over conventional protocols for islet culturing [20].

In tissue engineering, there is a gaining interest to incorporate PFCs in hydrogels to improve the oxygenation of encapsulated cells. Khattak et al. reported that encapsulating a PFC emulsion along with human HepG2 hepatomas in calcium alginate hydrogels increased cellular growth and metabolic activity over a 10-day period [17, 94]. With islets, mathematical simulations indicated that cell oxygenation was improved when a PFC emulsion was incorporated at a 70% PFC concentration in the encapsulating material, or when islets were dispersed into smaller aggregates, in both spherical microcapsules and planar slabs [141]. It is generally accepted that in these systems PFCs increase oxygenation by enhancing dissolved oxygen effective diffusivity through the matrix, not by serving as an oxygen reservoir, as the PFCs have only limited capacity to supply oxygen and they do not become reoxygenated. However, it remains unclear whether the increase in effective diffusivity is sufficient to produce consistent, statistically significant, and experimentally measurable positive effects, especially in applications with encapsulated insulin-secreting cells, which constitute a commonly used architecture for a pancreatic tissue substitute. Furthermore, in the design of such systems, it would be important for the PFC to be incorporated at a concentration that does not compromise the mechanical integrity and immunoprotective properties of the encapsulating matrix.

In this study, we addressed this question by investigating experimentally the effect of a PFC emulsion, perfluorotributylamine (PFTBA), on the viability, metabolic activity, and insulin secretory function of mouse βTC-tet insulinoma cells encapsulated in calcium alginate beads and cultured under normoxic and hypoxic conditions. We limited the PFTBA concentration to 10 vol% to ensure that the bead properties would not be compromised, as the alginate/PFC beads were unstable when prepared with higher PFC concentrations. Furthermore, we constructed a mathematical model of the alginate-PFC-cell system and compared simulations with the experimental results. The implications of our findings in the development of pancreatic substitutes based on encapsulated cells are discussed.

3.3 Materials and Methods

3.3.1 Cell culture and Cell Encapsulation

Murine insulinoma βTC-tet cells [142] were obtained from the laboratory of Shimon Efrat, Albert Einstein College of Medicine, Bronx, NY. Cells were cultured as monolayers in T-175 flasks, in a 37^{o}C, 5% CO_2 humidified incubator. Culture medium consisted of Dulbecco's Modified Eagle's Medium (DMEM, Sigma Chemical Co., St. Louis MO) with 25 mM glucose, supplemented with 10% fetal bovine serum, 1% penicillin-streptomycin, and L-glutamine to a final concentration of 6 mM, and it was changed every 2-3 days. Cell monolayers that reached 80% to 90% confluency were split by treatment with 0.25% trypsin-EDTA (Sigma); passage number increased by one at each splitting. Cells of passage number 36-48 were used in this study.

For encapsulation, cells were harvested by trypsin-EDTA and encapsulated at a density of 3.5×10^7 cells/ml in 2% w/v low viscosity, high mannuronic content alginate (product LVM, NovaMatrix, Drammen, Norway) containing the appropriate concentration of PFTBA emulsion (0 or 10 vol%). Using an electrostatic droplet generator (Nisco Engineering Inc., Zurich, Switzerland), cells were encapsulated according to the procedure of Stabler et al. [143]. Certain alginate bead preparations were coated with poly-L-lysine (PLL) (MW = 19,200; Sigma, St. Louis, MO) and a final alginate layer to form alginate/PLL/alginate (APA) beads. The coating protocol was as described by Papas et al. [144], which was based on a protocol by Lim and Sun [145]. Studies were performed with two bead sizes, 500 ± 150 μm and 1000 ± 200 μm in diameter.

The PFTBA emulsion was prepared following a protocol adapted from Joseph et al. [146]. An amount of 600 μl of Tyrode's salt solution (Sigma) was added to 95 mg of egg yolk lecithin (~99% purity, Sigma) and sonicated twice for 15 seconds at 300 W, with a one minute interval between each sonication. An amount of 400 μl of PFTBA (Sigma) was then added to the mixture and sonicated the same way for ten times The emulsion was filtered through a 0.8 μm membrane filter (Millipore, Billerica MA) and added to alginate at a 1:10 ratio. For one of the control groups, 1000 μl of Tyrode's salt solution was added to 95 mg of egg yolk lecithin and sonicated twelve times. This solution was added to alginate, also at a 1:10 ratio.

3.3.2 Culturing of Encapsulated Cells

Alginate-encapsulated βTC-tet cells were cultured in a 37°C, 5% CO_2 incubator for 1 day before experimentation to allow for recovery from the encapsulation procedure. The coating procedure was carried out a day after encapsulation. For normoxic experiments, encapsulated cells were placed into T-75 flasks and cultured on a rocking platform in a 37°C, 5% CO_2 incubator for 16 days. Number of metabolically active cells and insulin secretory function were assessed on Days 1, 2, 4, 8, 12, and 16. For hypoxic experiments, T-flasks or multiwell plates were placed in a Plexiglas chamber with inlet and outlet ports, which was placed on a rocking platform in a 37^{o}C incubator. A gas mixture of 5% CO_2 balanced with N_2 was continuously supplied through the chamber, lowering the oxygen to a severely hypoxic level of approximately 2% air saturation, as measured by an oxygen polarographic sensor (Ingold Messtechnik, Urdorf, Switzerland). For experiments under long-term hypoxia, encapsulated cells in T-75 flasks were cultured in the chamber for 13 days. Number of metabolically active cells and cell viability were assessed on Days 1, 4, 7, 10, and 13. For short-term hypoxic experiments, encapsulated cells were transferred to a 6-well plate and cultured in the chamber for 3 hours. Insulin secretion tests were then carried out, also in the chamber. In all studies, cells were fed by completely replacing the medium with fresh every 2-3 days.

To measure the rates of glucose consumption of encapsulated cells under normoxia, 0.5 ml of beads were cultured in 2.5 ml of fully supplemented medium in T-12.5 flasks for 7 days. Medium samples of 1.0 ml volume were collected daily and replaced with fresh medium. Rates of glucose consumption were evaluated by measuring the concentrations in samples.

3.3.3 Insulin Secretion Measurements

A bead volume of 0.1 ml was removed from the main culture and loaded in a well of a 6-well plate, which was placed on a rocking platform in a 37°C, 5% CO_2 incubator, or, for hypoxia studies, in the chamber. The beads were exposed to 5.0 ml of basal medium (glucose-free, non-supplemented DMEM) for 60 min, then switched to 3.2 ml of stimulating medium (16 mM glucose, fully supplemented DMEM) for 30 min. Medium samples withdrawn at the start and end of each stimulation period were stored at -80^{o}C for later assay of insulin by radioimmunoassay. The beads used in these insulin secretion experiments were not returned to the main culture. The 30 min secretion period was sufficient to capture the stimulated secretory response [147]. Secretion rates were calculated in pmol insulin per hour per 10^8 cells.

3.3.4 Assays

Numbers of metabolically active encapsulated cells were measured using the metabolic indicator alamarBlue^{TM} (Invitrogen Corp, Carlsbad, CA). A bead volume of 0.1 ml was placed in a well of a 12-well plate and mixed with 1.0 ml of medium and 0.1 ml of alamarBlue^{TM} reagent. Plates were positioned on a rocking platform in a 37°C, 5% CO_2 incubator. After 1.5 hours (3 hours for hypoxia experiments), 0.1 ml medium sample was withdrawn from each well, and its absorbance measured using a Spectra Max Gemini Plate Reader (Molecular Devices, Sunnyvale, CA) with an excitation wavelength of 544 nm and an emission wavelength of 590 nm. Relative intensity units (RIUs) were normalized to the RIUs of the Day 1 samples measured under the same conditions. Cell viability was determined using Trypan Blue assay (Sigma), where 0.1 ml of alginate

beads were dissolved in 0.2 ml of 2% sodium citrate solution (Sigma). A volume of 0.1 ml of the resulting suspension was added to 0.2 ml of Trypan Blue reagent and loaded on a hemocytometer for cell counting.

Insulin concentration in collected samples was assayed by rat insulin radioimmunoassay (Linco Research, St Charles, MI), using a CobraTM II Series Auto-Gamma Counter (Packard Instruments). Glucose concentrations were determined by the Glucose Trinder Assay (Diagnostic Inc., Oxford, CT), with absorbance measured at 505 nm wavelength using a SpectraMax Plus Plate Reader (Molecular Devices, Sunnyvale, CA).

3.3.5 Statistical Analysis

Statistical significance of differences between experimental groups and days were evaluated using General Linear Model, ANOVA. Statistical significance was defined as $p<0.05$.

3.3.6 Mathematical Simulations

The mathematical model used to simulate the system of encapsulated cells with a perfluorocarbon emulsion was an extension of the previously published model of Gross et al [148]. The assumptions incorporated in the model are listed below.

1. Dissolved oxygen is the only nutrient that limits cell proliferation (i.e., all other essential nutrients are in excess throughout the construct).
2. Spatial constraint is the only other factor besides DO that limits the rate and extent of cell proliferation within the construct.

3. As cells cannot adhere to the alginate matrix, cells do not migrate within the matrix; hence any remodeling in cell distribution is due entirely to cellular growth and death at each locale.
4. The PFC emulsion is homogeneously distributed throughout the contiguous alginate matrix.
5. Equilibration of dissolved oxygen between the aqueous and PFC phases at each locale is instantaneous.
6. The values of the model parameters, including the effective diffusivity of oxygen through the encapsulated system, remain constant over the time period of the simulations.
7. The concentration gradient within the aqueous phase is the only driving force for oxygen diffusion.
8. There is no external boundary layer effect when modeling the beads placed in well mixed medium, as in this study.

Figure 3.1 is a schematic of the configuration that is considered. Volume elements along a bead radius each consist of an aqueous and a PFC phase, with cells present in the aqueous phase only and dissolved oxygen in both phases. Diffusion of oxygen occurs between compartments, and the aqueous and PFC phases in each compartment are always in equilibrium (assumption 5 above).

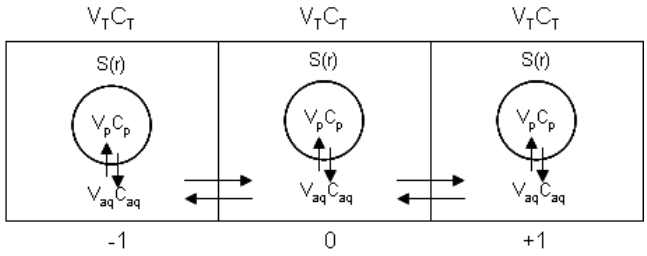

Figure 3.1 Configuration considered to solve for the DO profile. In solving for the total DO (C_T, amount of oxygen in aqueous plus PFC phases divided by the compartment volume) at compartment '0', diffusional transport occurs by the DO differences in the aqueous phase (C_{aq}) between compartment '0' and the neighboring compartments ('-1' & '+1'). Additionally, the DO in the PFC and aqueous phases, C_P and C_{aq}, respectively, are always in equilibrium based on the partition coefficient. Parameter *S(r)* is the oxygen consumption rate by the cells per unit volume of aqueous phase, as described in Equation (3).

The model equations describing oxygen diffusion for spherical geometry are as follows

$$\frac{\partial\left(V_T C_T(r,t)\right)}{\partial t} = V_{aq} D_{eff}\left(\frac{\partial^2 C_{aq}(r,t)}{\partial r^2} + \frac{2}{r}\frac{\partial C_{aq}(r,t)}{\partial r}\right) - V_{aq} S(r) \tag{1}$$

$$V_T \cdot C_T(r,t) = V_{aq} \cdot C_{aq}(r,t) + V_p \cdot C_p(r,t) \tag{2}$$

$$S(r,t) = X(r,t) \cdot \frac{\nu_{\max} C_{aq}(r,t)}{K_m + C_{aq}(r,t)} \tag{3}$$

where, t is time and r is radial position in the construct; $C_T(r,t)$, $C_{aq}(r,t)$, and $C_p(r,t)$ are the DO in the total volume (V_T), the volume of the aqueous phase (V_{aq}), and the volume of the PFC phase (V_p), respectively, as functions of radial position and time; D_{eff} is the effective oxygen diffusivity through the alginate/PFC matrix; V_T, V_{aq}, and V_p are the total, aqueous, and PFC volumes; $S(r,t)$ is the rate of oxygen consumption per unit volume of aqueous phase as a function of radial position and time, which is based on a Monod model with kinetic parameters ν_{max} (maximum oxygen consumption rate) and K_m (Monod model parameter); and $X(r,t)$ is the cell density as a function of radial position and time.

The effective diffusivity was calculated using the equation given by Radisic et al. [137], describing D_{eff} in a two phase system.

$$D_{eff} = D_{aq}\left[1+3\left(\frac{\gamma-1}{\gamma+2}\right)\phi\right] \tag{4}$$

$$\gamma = \frac{K \cdot D_p}{D_{aq}} \tag{5}$$

$$K = \frac{C_p(r,t)}{C_{aq}(r,t)} \tag{6}$$

In the above equations, D_{aq} and D_p are the diffusivities of oxygen through the aqueous calcium alginate phase and the PFC phase, respectively; K is the partition coefficient of oxygen in PFC vs. the aqueous phase; and ϕ is the volume fraction of the PFC emulsion (V_p/V_T).

The equations used for determining the growth and death of cells radially through the alginate matrix over time are the same as reported in Gross et al [148] and are listed below.

$$\frac{dX_{aq}(r,t)}{dt} = X_{aq}(r,t)\left(\mu_g - \mu_d\right) \tag{7}$$

$$\mu_g = \frac{\mu_{g,\max} C_{aq}(r,t)}{K_g + C_{aq}(r,t)}\left(1-\frac{X_{aq}(r,t)}{X_{\max}}\right) \tag{8}$$

(Monod's model for the specific growth rate μ_g with kinetic parameters $\mu_{g,max}$ and K_g, accounting for spatial constraints)

$$\mu_d = \mu_{d,\max} - \left(\mu_{d,\max} - \mu_{d,\min}\right)\frac{C_{aq}(r,t)}{K_d + C_{aq}(r,t)} \tag{9}$$

(modified Monod's model for the specific death rate μ_d maximizing the cell death rate at C_{aq}=0 and minimizing it at C_{aq}>>K_d)

In the above equations, μ_g and μ_d are the specific cell growth and death rates, respectively; $\mu_{g,max}$ and $\mu_{d,max}$ are the maximum specific growth and death rates, respectively; $\mu_{d,min}$ is the minimum death rate, which prevails under an abundance of oxygen; K_g and K_d are Monod model parameters; and X_{max} in the maximum cell density that can be accommodated in the construct. The ratio X/X_{max} is thus the fractional maximum occupancy at a particular locale in the construct.

Initial and boundary conditions

Equations (1)-(8) were solved with the following initial and boundary conditions.

$$C_{aq}(r,t=0)=C_o \tag{10}$$

(the initial concentration of oxygen throughout the spherical construct is constant and known)

$$X_{aq}(r,t=0)=X_o \tag{11}$$

(the cells are initially distributed homogeneously throughout the construct at a known density)

$$\frac{\partial C_{aq}}{\partial r}(r=0,t)=0 \tag{12}$$

(symmetry condition for oxygen concentration at the center of the sphere)

To simulate encapsulated cells in an infinite volume of medium, Equation 13 was used:

$$C_{aq}(r = R, t) = C_b \tag{13}$$

(DO at the surface of the bead is equal to the DO in the surrounding medium, C_b, which is known and assumed constant). This approximates beads cultured in T-flasks, in a large volume of medium on a rocking platform.

The appropriate initial and boundary conditions, and baseline parameter values listed in Table 3.1 were used.

Table 3.1 Baseline parameter values used in simulating the temporal profiles of cell density and DO in the system of βTC-tet cells encapsulated in spherical calcium alginate beads with and without a perfluorocarbon emulsion.

Parameter		Value	Reference
Diffusivity of oxygen in cell-containing alginate	D_{aq}	1.4 cm^2/day	[152]
Diffusivity of oxygen in PFTBA	D_p	4.85 cm^2/day	[199]
Partition coefficient of oxygen between PFTBA and water	K	16	[153]
Maximum oxygen consumption	v_{max}	2.88 mmole/(day x 10^9 cells)	[152]
Monod parameter - oxygen	K_m	0.01 mM	[152]
Maximum specific growth rate	$\mu_{g,max}$	0.04 day^{-1}	Sensitivity analysis
Maximum specific death rate	$\mu_{d,max}$	1.4 day^{-1}	[200]
Minimum specific death rate	$\mu_{d,min}$	0.00273 day^{-1}	[152]
Monod parameter - growth	K_g	0.01 mM	[152]
Monod parameter - death	K_d	0.001 mM	[152]
Maximum cell density	X_{max}	9 x 10^8 cells/ml	Calculated based on a
		8.1 x 10^8 cells/ml (With PFC)	10 μm diameter cell

The ratio of the diffusion coefficient of oxygen in the PFC vs. the aqueous phase is 3.46. With this value and the partition coefficient being equal to 16, the effective diffusivity in the composite alginate/10% PFC material was calculated from equations (4), (5) and (6) to be 1.8 cm^2/day, compared to 1.4 cm^2/day for the alginate-only material. Model equations were solved using finite differences. From $C_{aq}(r,t)$, the average aqueous intrabead DO, or AIDO, was calculated as follows:

$$\mathrm{AIDO}(t) = \frac{\int_0^R 4\pi r^2 C_{aq}(r,t)\,dr}{\frac{4}{3}\pi R^3} \tag{14}$$

3.4 Results and Discussion

3.4.1 PFTBA Effects on Encapsulated βTC-tet Cells under Normoxic Conditions

Cell metabolic activity in APA beads with no PFTBA (Control 1), 10 vol% lecithin solution (Control 2), and 10 vol% PFTBA emulsion (Experimental) was assessed over a period of 16 days. The second control group was included to ensure that lecithin, the emulsifier used to make the PFTBA emulsion, did not have an effect on cells by itself, and that any changes observed in the PFC group were solely due to the presence of PFTBA. The droplet size of the PFTBA emulsion in the alginate beads was measured microscopically and remained at 1-2 μm throughout the experimental period, indicating that the emulsion was stable. The integrity of APA beads was also maintained throughout this period as the PLL layer reduced the diffusion of calcium ions out of the alginate matrix and has an overall stabilizing effect on the beads [50, 149]. All data were normalized to the measurement on Day 1, which was set equal to 1. Results with 1000 μm APA beads are shown in Figure 3.2.

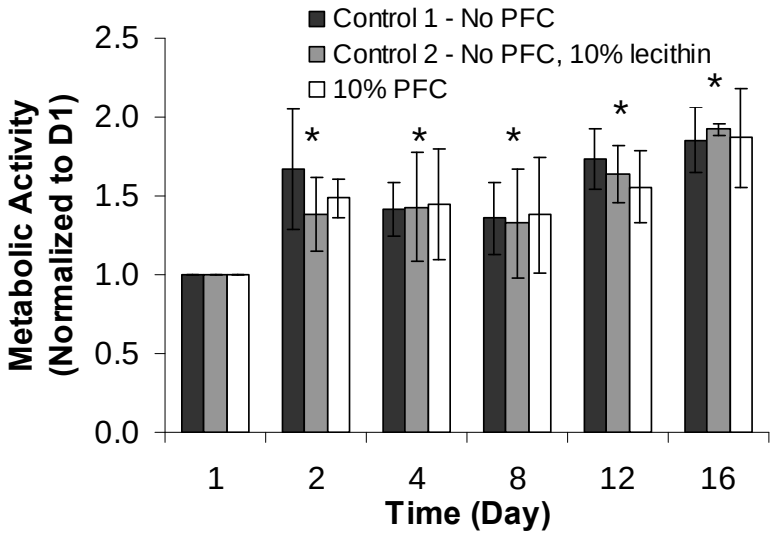

Figure 3.2 Metabolic activity of encapsulated βTC-tet cells under normoxic conditions. The number of metabolically active cells was measured as a function of time by alamarBlue™ and normalized to Day 1. Measurements were performed with calcium alginate/ poly-L-lysine/ alginate (APA) beads of 1000 μm average diameter with no PFTBA, APA beads with 10 vol% lecithin, and APA beads with 10 vol% PFTBA (n = 3 each). The initial density of the encapsulated cells was 3.5×10^7 cells/ml. * $p<0.05$ when compared to Day 1.

There was a gradual increase in the number of metabolically active cells over time for all groups. This trend is compatible with earlier findings with βTC insulinomas encapsulated in high mannuronic alginate beads [143]. At any particular time point, there were no statistical differences in metabolic activity among the different groups of beads.

Data on the insulin secretion rates (ISR) measured under 16 mM glucose stimulation are shown in Figure 3.3.

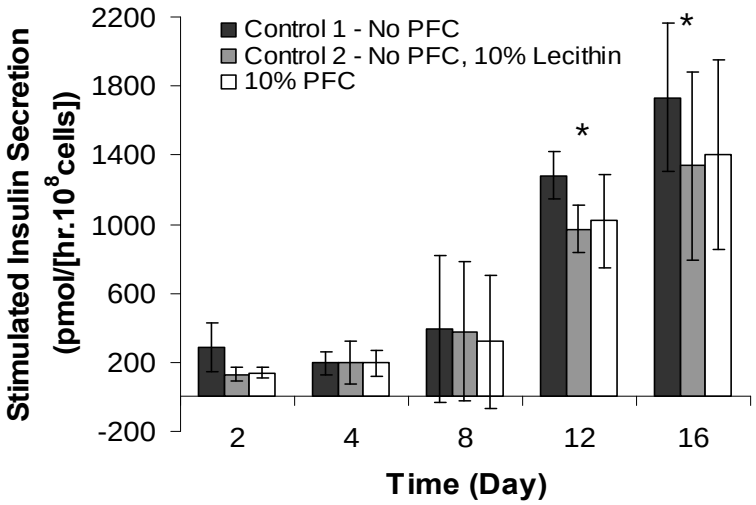

Figure 3.3 Stimulated insulin secretion rate (ISR) of βTC-tet cells under normoxic conditions. ISR was measured over 30 min of stimulation by 16 mM glucose, normalized to the initial number of encapsulated βTC-tet cells, and expressed on a per unit time basis. Measurements were carried out with 1000 μm average diameter APA beads with no PFTBA, APA beads with 10 vol% lecithin, and APA beads with 10 vol% PFTBA (n = 3 each). Each glucose stimulation episode followed 1 hour of exposure to basal, 0 mM glucose, medium. * $p<0.05$ when compared to Day 1.

There was a general increase in ISR with time up to Day 16 for all groups. As with the alamarBlue™ measurements, there were no statistical differences in ISR among the different bead groups at any time point. However, the temporal increase in insulin secretion was higher than the increase in metabolic activity shown in Figure 3.2, suggesting an increase in the insulin secretion rate per cell over time. Although the precise reason for this is unclear, it is possible that it was caused by an increasing hypoxic environment within the bead due to cell growth, which resulted in higher lactate production and locally more acidic conditions over time; an acidic pH has been shown to cause elevated insulin release from βTC3 cells, an earlier variant of the βTC-tet insulinoma line [150].

It should be noted that similar results were obtained with βTC-tet cells encapsulated in calcium alginate beads without PLL coating of both 500 and 1000 μm beads (n = 4, results shown in Figure A2.a in Appendix II). In these experiments, too, there were no differences in metabolic activity or insulin secretion rates between PFTBA-containing beads and PFTBA-free controls at all time points (n = 4, results shown in Figure A2.b in Appendix II). However, the integrity of these beads started to become compromised towards the end of the 16-day experiment due to the absence of the stabilizing PLL layer.

The effects of PFTBA on the glucose consumption rate (GCR) were also studied with βTC-tet cells encapsulated in 1000 μm average diameter calcium alginate beads with no PFTBA (control 1) and 10 vol% PFTBA emulsion. The GCR in both bead groups increased by approximately 60% over seven days of culture due to cell growth. However, the presence of PFTBA had no significant effect on the GCR of the cells over that time period (n = 4, results shown in Figure A2.c in Appendix II).

3.4.2 PFTBA Effects on Encapsulated βTC-tet Cells under Hypoxic Conditions

Figure 3.4(a) shows the temporal profile of the cell metabolic activity, measured by alamarBlue^{TM} and normalized to Day 1, for βTC-tet cells in 500 μm alginate-only beads with no PFTBA (Control) and 10 vol% PFTBA emulsion, under severely hypoxic conditions (~2% air saturation, or 0.004 mM). The percent viability of the cells in the beads was also measured by Trypan Blue and is reported in Figure 3.4(b). A smaller bead size was chosen for this hypoxic study to ensure that the only oxygen-limiting factor was the external condition, not diffusion limitation within the beads.

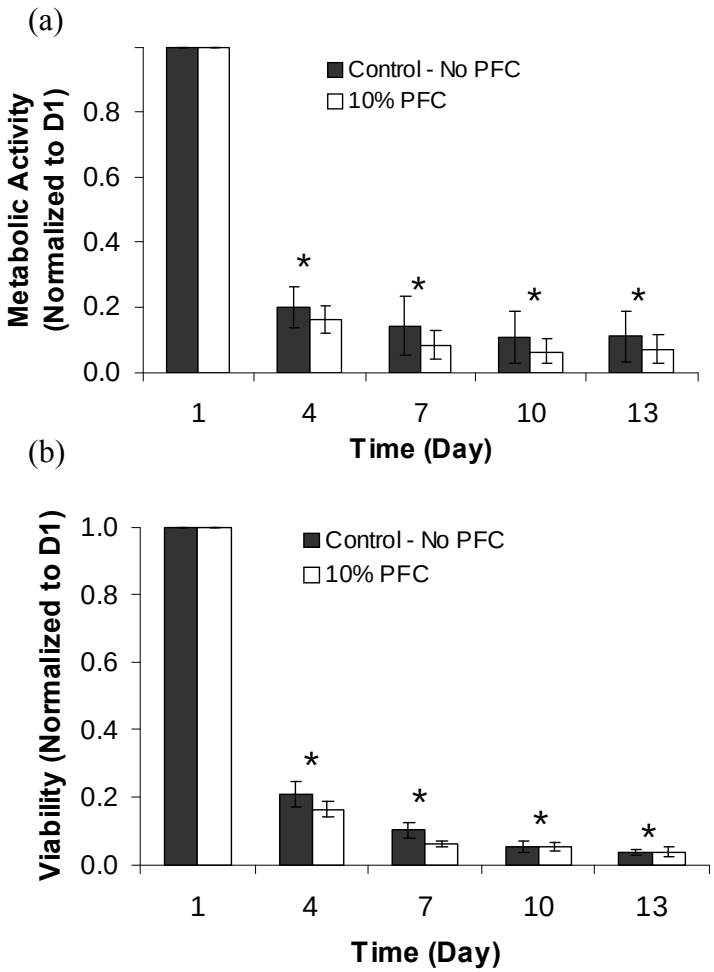

Figure 3.4 Metabolic activity and % viability of encapsulated βTC-tet cells under severely hypoxic conditions (2% air saturation, or 0.004 mM). (a) The number of metabolically active cells and (b) % viability were measured by alamarBlue™ and Trypan Blue respectively, as a function of time and normalized to Day 1. Measurements were performed with calcium alginate beads of 500 μm average diameter with no PFTBA and 10 vol% PFTBA (n = 5 each). * $p<0.05$ when compared to Day 1.

Results showed that both the metabolic activity and the cell viability for the two groups of beads declined significantly from Day 1 to Day 4, to a lesser extent from Day 4 to Day 7, and stayed at a very low level until the end of the experiment on Day 13. As with the normoxic experiment, there were no statistical differences in cell metabolic activity and viability between the two bead groups at any time point. Due to the significant cell death, ISR measurements were not performed with these hypoxic cultures.

Experiments were also carried out under short-term hypoxia to investigate whether the PFTBA phase had a significant effect on the encapsulated cells under these conditions. For this, cells in 500 μm alginate-only beads with no PFTBA (control) and 10 vol% PFTBA emulsion were cultured under hypoxia for 3 hours, then subjected to an insulin secretion test, also under hypoxia. Results on ISR measured over 30 min under 16 mM glucose stimulation are shown in Figure 3.5

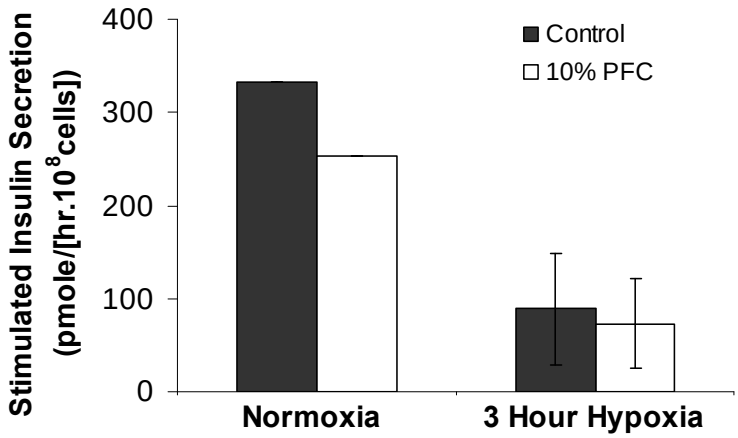

Figure 3.5 Stimulated insulin secretion rate (ISR) of βTC-tet cells under severely hypoxic conditions. The encapsulated cells were cultured for 3 hours under hypoxic conditions, then subjected to a secretion test. The secretion episode consisted of cells exposed for 1 hour to basal, 0 mM glucose medium, followed by a 30 min of stimulation in 16 mM glucose medium, all under hypoxia. The ISR over the stimulation period was measured and is reported in the figure (n = 5 each). The ISR under normoxic conditions is included for reference (n = 1 each). Beads were of 500 μm average diameter.

The insulin secretory function of the encapsulated cells was compromised under the hypoxic conditions implemented; however, the presence of 10% PFTBA did not have an effect on the induced insulin secretion relative to the control.

3.4.3 Simulations under Normoxic Conditions

The model equations were solved to calculate the concentration of oxygen, C_{aq} and cell density in the aqueous phase, X_{aq} as functions of radial position and time for beads of 1000 μm in diameter. Figures 3.6(a) and (b) show the time profiles of the cell density, normalized to Day 1, along with experimental data on cell metabolic activity from Figure 3.2, and AIDO with no PFC (Control) and 10% PFC over 16 days in culture.

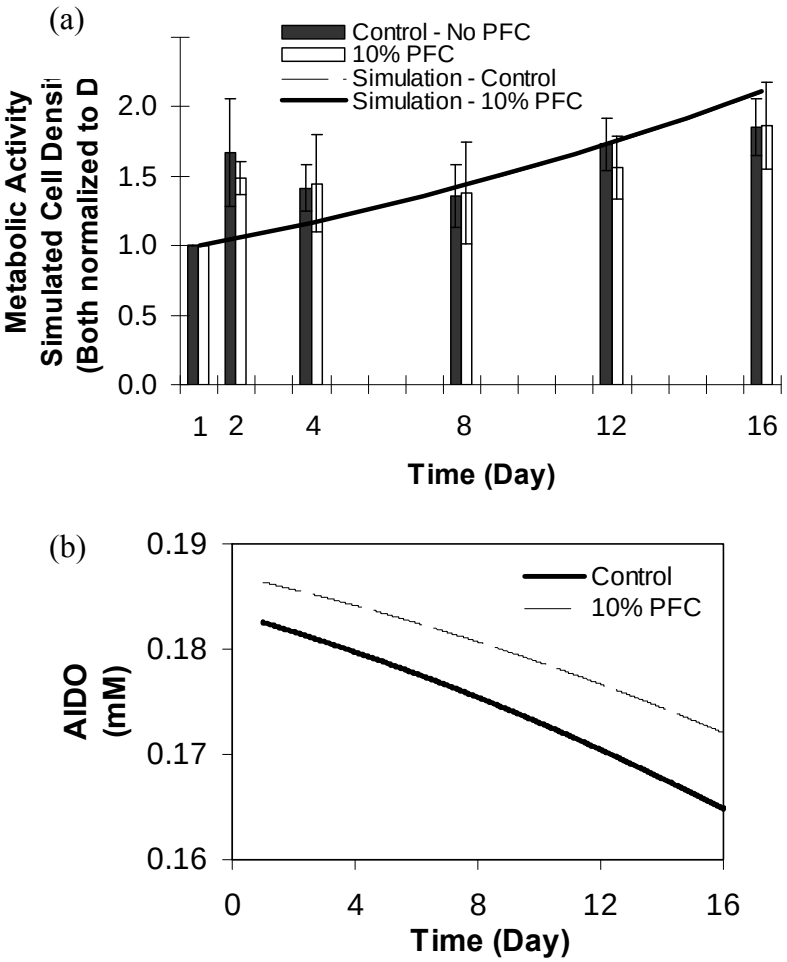

Figure 3.6 Simulated temporal profiles under normoxic conditions (0.2 mM). The model equations were solved for 1000 μm average diameter beads to calculate the cell density (a) and the average intrabead DO (AIDO) (b) in the aqueous phase in beads containing no PFC and 10% PFC. Simulated values are compared to the experimental data shown in Figure 3.2 obtained from APA beads under similar conditions. In (a), the scale of the graph makes the simulations for the 10% PFC and control beads essentially coincide.

The cell growth predicted by the model is in good agreement with the experimental results for the APA beads. Due to the increased effective diffusivity in the composite alginate/PFC phase, the AIDO for the PFC-containing beads started at a higher value of 0.186 mM, when compared to 0.182 mM for the control beads (Figure 3.6(b)). As the cell density, and hence the oxygen consumption, increased within the beads over time, the AIDO declined accordingly. The decrease in AIDO, however, was smaller in the PFC-containing beads relative to the control, and on Day 16 the AIDO were calculated to be 0.172 and 0.165 mM for the PFC and control beads, respectively. Although the presence of PFC improved the dissolved oxygen effective diffusivity and the AIDO in the beads, this supported only a slightly higher cell density relative to the PFC-free control. The maximum difference in simulated cell densities was on Day 16, where the control and PFC beads had cell densities of 7.75 and 7.79×10^7 cells/ml, respectively. This difference is small, making it essentially impossible to detect experimentally.

These findings are different from those reported by Khattak et al. [17] and by Chin et al. [94], who observed a statistical increase in the density of HepG2 cells encapsulated in calcium alginate containing 10% perfluorooctylbromide (PFOB) relative to PFC-free controls. The reason for this difference is not clear. The oxygen solubility is higher in PFOB relative to PFTBA, with the partition coefficients being 17.7 and 16 respectively. This, however, results only in a minimal difference in the effective diffusivities calculated by equations (4), (5) and (6), with values being the same within two significant figures, so the difference in solubility cannot explain the difference in results. A second possibility is the lower maximum oxygen consumption rate (v_{max}) of

βTC-tet relative to HepG2 cells. Indeed, reported v_{max} values for HepG2 cells of 5.44 [94] and 17 mmol/(10^9 cells·day) [151] are significantly higher than the 2.88 mmol/(10^9 cells·day) reported for βTC3 cells [152], resulting in a higher oxygen demand in the alginate matrix. A third possibility would be the higher growth rate of HepG2 cells both as monolayers and in beads, which may also result in a higher oxygen demand in the beads over time.

We therefore investigated the sensitivity of the model solutions to the values of v_{max} and $\mu_{g,max}$. Simulations were run with v_{max} equal to the value used in this study and the two values for HepG2 cells reported above; for $\mu_{g,max}$, model solutions were calculated with the value used in this study and with a higher value of 0.35 day^{-1}, which corresponds to a much faster growing cell type with a doubling time of 2 days [148]. The rest of the model parameters were kept as in Table 3.1, including the maximum cell density of 9×10^8 cells/ml in beads. Results are plotted as factor increase in cell density in the PFC-containing beads relative to PFC-free control vs. time and are shown in Figure 3.7.

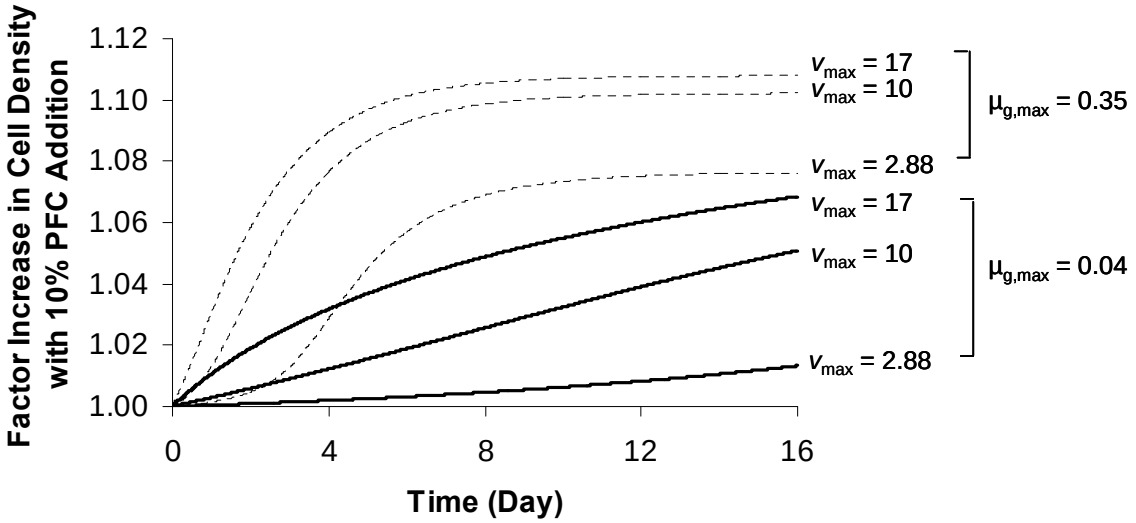

Figure 3.7 Simulated factor increase in cell density vs. time resulting from the incorporation of 10% PFC relative to PFC-free control for 3 different oxygen consumption rates, v_{max} (mmol/(10^9 cells·day)) and 2 different growth rates, $\mu_{g,max}$ (day^{-1}). Remaining model parameters are the same as those reported in Table 3.1.

As expected, cells with a higher $\mu_{g,max}$ arrive at their steady state cell density sooner, and the PFC effect increases with v_{max}, or as the oxygen demand within the alginate matrix increases. However, the cell density supported by the presence of PFC is predicted to be no more than 11% higher than the control, which may be detectable experimentally but does not improve the performance of the system in a substantive way.

3.4.4 Simulations under Hypoxic Conditions

Simulations on the effect of PFC on encapsulated cells under severely hypoxic conditions were also carried out for 500 μm beads. Figure 3.8(a) shows the time profiles of the cell density, normalized to Day 1, along with experimental data from Figure 3.4A on cell metabolic activity, under 0.004 mM external DO over 13 days in culture. Figure 3.8(b) shows the time profiles of the AIDO concentration in beads with no PFC (control)

and 10% PFC; the inset in this figure shows the same AIDO profiles under higher resolution for the initial 2 minutes.

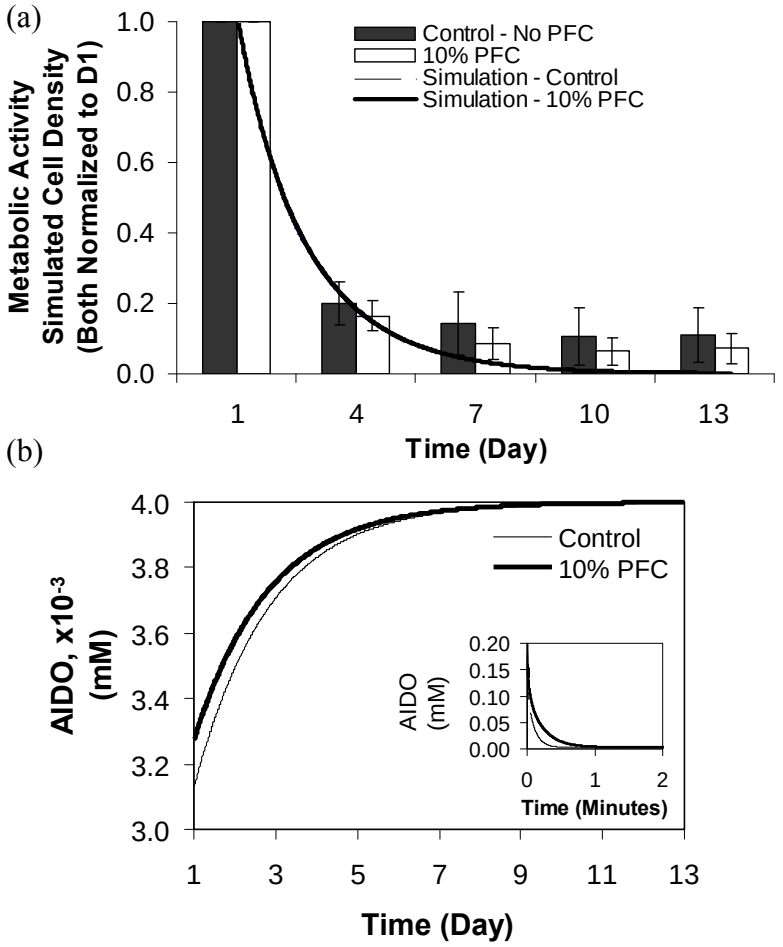

Figure 3.8 Simulated temporal profiles under hypoxic conditions (0.004 mM). Model solutions for cell density (a) and average intrabead DO (AIDO) (b) in the aqueous phase of 500 μm average diameter beads containing no PFC and 10% PFC. Simulated values are compared to the experimental data obtained from calcium alginate beads under similar conditions and reported in Figure 4. In (a), the scale of the graph makes the simulations for the 10% PFC and control beads essentially coincide. The inset in (b) shows the change in AIDO for the initial 2 min.

Model-predicted cell densities for both groups of beads decreased drastically within the first 4 days, which was also reflected in the increase AIDO towards the external DO due to cell death. The simulated cell density was generally in good

agreement with the experimental results. However, the model appears to underestimate the number of metabolically active cells on Days 7, 10, and 13. This could be due to the beads being temporarily removed from their hypoxic environment at every experimental time point from Day 4 onwards, which is not accounted for in the model.

As with the normoxia simulations, the AIDO in the PFC-containing beads started at a higher value of 0.033 mM, when compared to 0.031 mM in the control beads (Figure 3.8(b)). This difference was not significant enough to change the rate of cell death under hypoxia. At Day 4, simulations showed only a slightly higher cell density of 5.96×10^6 cells/ml in the PFC-containing relative to 5.77×10^6 cells/ml for the control. At steady state, the presence of PFC only sustained a cell density that is 3.7% higher than the control beads under these conditions. The model also shows that the capacity of PFC to provide oxygen to the aqueous phase is only minimal, as observed by the decrease in the AIDO within the first 2 minutes after exposure to the hypoxia (Figure 3.8(b) inset). This lack of significant difference in the calculated cell density between the two groups of beads demonstrates the limited capacity of PFC to provide long-term oxygen support to the construct under the conditions examined.

PFCs are effective as oxygen carriers when convectively transported from a domain of high oxygen, where they become oxygenated, to a domain of low oxygen, where they deliver the oxygen they contain. This is supported by the fact that oxygen is not chemically bound to the PFC carrier and that the thermodynamics of oxygen absorption by PFC follow a linear Henry law profile rather than a sigmoidal profile, as is the case for hemoglobin [153]. Our study shows, however, that in a stationary system, such as an encapsulated cell construct, the increase in construct oxygenation due to the

addition of 10% PFC had a minimal effect on the viable cell number and function when cultured in a high or low oxygen environment. A system in which the incorporation of PFC would potentially have an added benefit in maintaining viable cells is when the culture is surrounded with a large volume of PFC. This is, however, not feasible with encapsulated cells where the PFC emulsion is dispersed, as having a high concentration of PFC emulsion will compromise the integrity of the beads and possibly result in cytotoxic effects from the emulsifier. Furthermore, the cell density that can be accommodated in beads will be reduced due to the reduction of the volume of the aqueous phase.

3.5 Conclusions

In summary, the addition of PFTBA emulsion of 10 vol% to encapsulated systems of βTC-tet cells in calcium alginate beads did not have a statistically significant benefit to cell growth and metabolic activity, or to the induced insulin secretion from the cells. These results were obtained under normoxic conditions with APA and alginate-only beads, as well as under long- and short-term severely hypoxic conditions with alginate-only beads. This finding was consistent with the results of mathematical simulations that noted only a small, likely experimentally undetectable, increase in cell density in PFC-containing beads. Simulations also indicated an increased positive effect of PFC on cells with a higher oxygen consumption and growth rates, but this was also modest in magnitude.

CHAPTER 4

DUAL PERFLUOROCARBON METHOD TO NONINVASIVELY MONITOR DISSOLVED OXYGEN CONCENTRATION IN TISSUE ENGINEERED CONSTRUCTS *IN VITRO**

4.1 Abstract

Noninvasive monitoring of tissue implants provides important correlations between construct function and the observed physiologic effects. As oxygen is a key parameter affecting cell viability and function, we established a monitoring method that utilizes ^{19}F Nuclear Magnetic Resonance (NMR) spectroscopy, with perfluorocarbons (PFCs) as oxygen concentration markers, to noninvasively monitor dissolved oxygen concentration (DO) in tissue engineered constructs. Specifically, we developed a dual PFC method capable of simultaneously measuring DO within a tissue construct and its surrounding environment. *In vitro* studies using an NMR-compatible bioreactor demonstrated the feasibility of this method to monitor the DO within alginate beads containing metabolically active murine insulinoma βTC-tet cells, relative to the DO in the culture medium, under perfusion and static conditions. The DO profiles obtained under static conditions were supported by mathematical simulations of the system. The significance of the dual PFC system in providing critical DO measurements for encapsulated cells and other tissue constructs is discussed.

* Modification of a paper published in the **Biotechnology Progress** (in press)

4.2 Introduction

Tissue engineered constructs comprised of living cells entrapped in a biocompatible matrix or scaffold are promising in providing functional replacements of diseased tissues or organs. Such constructs are usually highly dynamic post-implantation, as the extent of cellular growth and remodeling, host reaction towards the implant, and oxygen availability at the implantation site all influence cell survival and the implant functional outcome. In this context, noninvasive methods of monitoring the physiological state of tissue implants would prove beneficial. Such methods would allow for important correlations to be drawn between construct function and the observed end physiologic effects, and thus provide a better understanding of the *in vivo* environment and possible mechanisms of construct failure [9, 125].

Nuclear magnetic resonance (NMR) is a useful modality, as it can provide information on both the structure and function of an implant via imaging and spectroscopy. Specifically, the use of the ^{19}F nucleus is appealing, as it has a 100% natural isotopic abundance and a sensitivity 0.83 times that of ^{1}H [13]. Furthermore, there is an absence of naturally occurring fluorine in most biological tissues, which eliminates the problem of interfering background signals [14]. We aim to establish a monitoring method that utilizes ^{19}F NMR spectroscopy, with perfluorocarbons (PFCs) as oxygen concentration markers, to evaluate dissolved oxygen concentration (DO) in a tissue engineered pancreatic construct. This method of monitoring works on the basis that the inverse spin lattice relaxation time, $1/T_1$, of ^{19}F resonances from PFCs varies linearly with oxygen tension [100, 102]. PFCs are nontoxic, highly fluorinated compounds with a high capacity for dissolving respiratory gases, including oxygen [14,

154]. While high concentrations of PFCs could potentially be incorporated to enhance construct oxygenation [17, 94, 155], a low concentration of PFC is generally sufficient to provide the needed ^{19}F NMR signal for monitoring.

The importance of DO assessment in tissue implants is evident as studies have demonstrated a high dependence of cell survival and function on oxygen. *In vitro* studies with beta cell lines have shown cell metabolic activity and insulin secretion being affected at low oxygen concentrations, although these cells appear more tolerant to hypoxia than intact islets [71, 156]. When islets were cultured under hypoxic conditions *in vitro*, their insulin secreting capacity was severely impaired and hypoxia-induced cell apoptosis or necrosis were observed [121, 157-159]. Similarly, post-transplantation, oxygen availability is an important determinant of graft survival and function, and substantial early cell death in implanted grafts due to hypoxic stress has been reported [7, 68, 160, 161]. The rate of cellular oxygen consumption also correlates with the number of metabolically active cells. Measurements with islets and cell lines demonstrated a proportional increase in oxygen consumption in culture with the viable cell number [9, 122, 162-164]. In fact, the oxygen consumption rate to DNA ratio has been used to evaluate islet quality and to predict the transplantation outcome in diabetic nude mice [165, 166].

The ^{19}F NMR noninvasive method of monitoring has been used to measure oxygenation of natural, pathological, and engineered tissues. Previous studies showed feasibility of this method to quantify oxygen levels in the liver, spleen, lung, and heart through the distribution of PFC compounds in these organs and tissues administered intraveneously or intraperitoneally [106, 167, 168]. The similar method of monitoring

has also been used extensively in the studies of *in vivo* tumor oxygenation, mainly to guide oxygen tension modulation in tumor tissue in order to improve radiotherapy treatment efficacy [111, 113]. Work in our laboratory proved this method successful in tracking the oxygenation state of βTC-tet cells encapsulated in an alginate/PFC matrix *in vitro*. Experimentally measured DO correlated well with cell metabolic activity and bioenergetics, and closely matched DO values predicted by a mathematical model [9]. *In vivo*, Noth et al. used this method to identify optimal implantation sites for cell survival in rats by performing quantitative DO measurements in PFC-containing alginate beads and reported very low average oxygen levels of approximately 3.4 % and 2.2 % (corresponding to 0.03 mM and 0.02 mM) in the peritoneal cavity and under the kidney capsule respectively. They also observed a large range of oxygen levels, which varied over time and among different rats [108].

As the *in vivo* DO can vary significantly from animal to animal but also for the same animal with physiologic conditions, we are pursuing the development of a dual PFC method for simultaneously monitoring DO in a tissue construct and its environment. In this method, two PFCs with proximal chemical shifts are incorporated, one in the construct containing cells, which is the experimental tissue implant, and the other in cell-free alginate beads. The latter is used to monitor the DO level in the medium or implantation milieu, as equilibration of the cell-free beads with the external DO is rapid. Initial *in vivo* studies in our lab demonstrated the capability of the dual PFC method to simultaneously monitor DO in cell-free alginate-only, and in cell-free, poly-L-lysine (PLL)-coated alginate beads. As PLL is highly inflammatory *in vivo*, PLL-coated beads implanted in the peritoneal cavity of mice became covered by host cells, whereas

alginate-only beads did not. The resulting lower intrabead DO in the PLL-coated vs. the alginate-only beads was detected and measured by the dual PFC method [9].

In this study, we further characterized and proved *in vitro* the feasibility of the dual PFC method in monitoring DO within cell-containing constructs relative to the surroundings. Our system consisted of murine βTC-tet insulinomas entrapped in an alginate matrix, which constitutes a commonly used architecture for a pancreatic tissue substitute. PFCs used were perfluorotributylamine (PFTBA) and perfluoro-15-crown-5-ether (PFCE), which differ in chemical shifts by only 9 ppm. Each type of PFC, prepared in the form of an emulsion, was incorporated at 5 vol%. Any transient partitioning of oxygen favoring the PFC phase does not considerably change the aqueous DO, as the total volume of PFC emulsion is insignificant compared to that of the aqueous phase. Furthermore, our previous experimental and modeling studies demonstrated that even at a 10 vol% concentration of the PFC emulsion, the presence of PFC had only a minimal effect on cell growth and intrabead DO [155] (CHAPTER 3). A similar situation exists with carbon dioxide, which also equilibrates between the PFC and aqueous phases, but with a partition coefficient lower than that of oxygen (2-4 vs. 10-20). Studies were performed in an NMR-compatible bioreactor loaded with cell-free and cell-containing beads cultured under perfused and static conditions. A mathematical model was also developed to best simulate the bioreactor culturing environment, to corroborate the acquired experimental data. The potential and limitations of the dual PFC method are discussed.

4.3 Materials and Methods

4.3.1 Cell Culture and Cell Encapsulation

Murine insulinoma βTC-tet cells [142] were obtained from the laboratory of Dr. Shimon Efrat, Albert Einstein College of Medicine, Bronx, NY. Cells were cultured as monolayers in T-175 flasks, in a 37°C, 5% CO_2 humidified incubator. Culture medium consisted of Dulbecco's Modified Eagle's Medium (DMEM, Sigma Chemical Co., St. Louis MO) with 25 mM glucose, supplemented with 10% fetal bovine serum, 1% penicillin-streptomycin, and 1% L-glutamine to a final concentration of 6 mM, and it was changed every 2-3 days. Cell monolayers that reached 80% to 90% confluency were split by treatment with 0.25% trypsin-EDTA (Sigma); passage number increased by one at each splitting. Cells of passage number 35-45 were used in this study.

Cells of 90% confluency were harvested by trypsin-EDTA and entrapped at a density of 1.0 to 7.0×10^7 cells/ml alginate in 2% w/v low viscosity, high mannuronic content alginate (LVM, NovaMatrix, Drammen, Norway) containing 50 mg/ml PFTBA or PFCE emulsion (see below) to produce calcium alginate beads. Using an electrostatic droplet generator (Nisco Engineering Inc., Zurich, Switzerland), cells were entrapped according to the procedure of Stabler et al., where the alginate/cell/PFC mixture was extruded into a 100 mM $CaCl_2$ solution [143]. Some of these beads were coated with poly-L-lysine (PLL), and a final layer of alginate to produce alginate-poly-L-lysine-alginate (APA) beads, used for *in vivo* studies. The coating protocol was as described by Papas et al. [144], which was based on a protocol by Lim and Sun [145]. Beads were prepared at 1000 ± 200 μm in diameter for *in vitro* studies to avoid an excessive pressure

drop across the packed bed bioreactor, and at 500 ± 150 μm in diameter for *in vivo* studies.

4.3.2 PFC Preparation and Incorporation in Beads

Liquid PFTBA and PFCE were sterile-filtered through a 0.2 μm polyethersulfone filter (Whatman, SpringHill, UK). Using egg yolk lecithin (Sigma) as the emulsifier, the PFC emulsion was prepared following a protocol adapted from Joseph et al. [146] and described by Gross et al. [9] (CHAPTER 3). The emulsion was sterile-filtered through a 0.8 μm cellulose membrane filter (Milipore, Billerica, MA), added to the sodium alginate solution at a concentration of 50 μg/ml and mixed thoroughly. The PFC droplets were homogeneously dispersed throughout the alginate beads and the droplet size was approximately 1-2 μm.

4.3.3 Perfusion System

For all *in vitro* experiments, beads were cultured in a 10 mm diameter × 9 in long NMR-compatible packed bed bioreactor (Wilmad Glass, Buena, NJ) connected to a computer-controlled, closed-loop perfusion circuit as described by Gross et al. [9] (Figure 4.1(a) and (b)). Culture medium was circulated between a medium reservoir and the bioreactor where the beads were held in place using a cotton plug upstream of the bed. The bioreactor could accommodate approximately 2 ml of beads and was positioned in the magnet so that the beads were within the radiofrequency coil region of the NMR probe. The temperature of the medium in the bioreactor was maintained at 37^{o}C through a computer-controlled air flow system and by heating the medium circulation lines. The

DO in the medium entering the bioreactor was pre-equilibrated by flowing 5% CO_2 balanced with air or N_2, and DO was measured using a fiber optic sensor (Ocean Optics, Dunedin, FL).

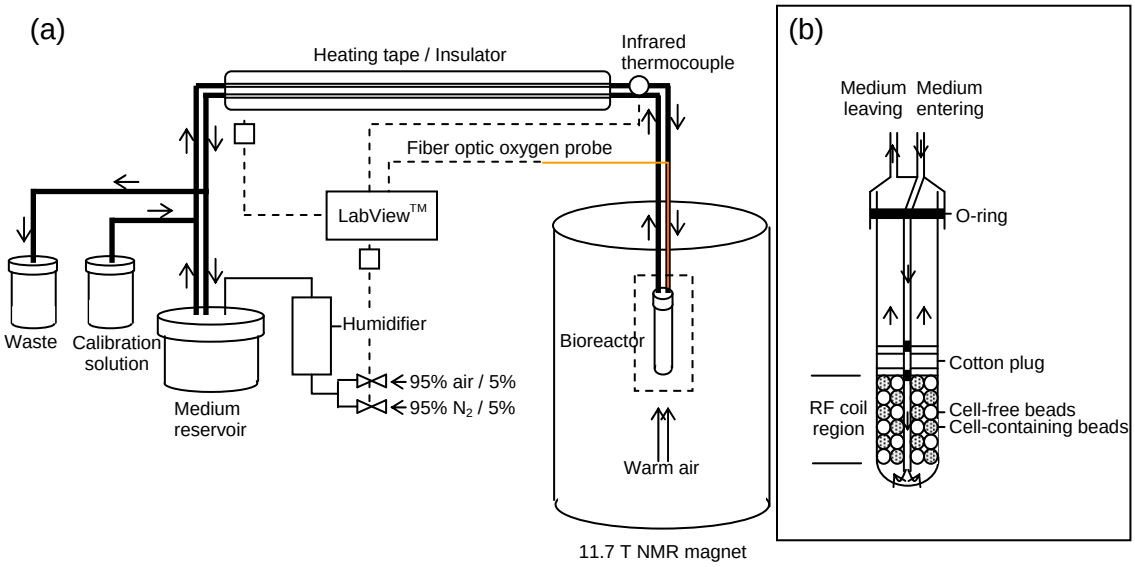

Figure 4.1. Schematic of (a) the perfusion circuit connected to (b) the NMR-compatible bioreactor used to circulate culture medium and control temperature and DO levels in the bioreactor. Figure adapted from Gross et al. [9].

4.3.4 11.7 T Magnet

^{19}F NMR spectra for *in vitro* studies were acquired using a 10 mm broadband probe on an 11.7 T vertical bore magnet equipped with a Bruker Avance console (Bruker, Billerica, MA) at the McKnight Brain Institute, University of Florida, Gainesville, FL. An inversion recovery pulse sequence was used to acquire T_1 relaxation measurements; there were 12 delay times ranging from 0.01 s to 1.6 s for each T_1 determination. Acquisition parameters for the experiments were: 5.6 kHz spectral width, 1 transient, 10 s relaxation delay. Peak intensity was extracted using the area under the peak, and all T_1

relaxation rates were determined through a 3-parameter exponential fit using Bruker Avance software.

4.3.5 Calibration of Inverse T_1 Relaxation versus DO

Cell-free alginate beads containing 50 mg/ml PFTBA or PFCE emulsion were loaded in the bioreactor. The DO in the medium entering the bioreactor was allowed to equilibrate at a particular level for at least 45 minutes before scanning. This inlet medium DO was set equal to the intrabead DO. T_1 is independent of pH changes [169] but is temperature sensitive [170]; temperature was therefore tightly controlled at 37°C during acquisitions. T_1 relaxation measurements were obtained at five or more DO levels and the two variables were correlated by the following equation:

$$\frac{1}{T_1} = M[DO] + I \qquad (4.1)$$

where M is the slope (s^{-1} mM^{-1}) and I is the anoxic y-intercept (s^{-1}). The calibration curves of the PFCs were generated under perfusion, at a flow rate of 6.5 ml/min, and under static conditions.

4.3.6 Measurements of Construct DO

βTC-tet cells were entrapped in calcium alginate at a density of 1, 3, and 7×10^7 cells/ml. Cell-free and cell-containing alginate beads, incorporating 50 mg/ml of either PFTBA or PFCE emulsion, were loaded in the bioreactor at a 1:1 ratio. Following experimentation, beads were removed from the bioreactor and cell viability was examined to ensure that cells were viable during measurements. DO values were

calculated using the appropriate calibration parameters established under perfusion and static conditions.

Flow System

For all experiments under perfused conditions, fully supplemented medium was circulated through the system at a flow rate of 6.5 ml/min. Medium temperature was allowed to equilibrate to 37^{o}C before any measurements were made, and the inlet DO in the medium was maintained at 0.18 ± 0.02 mM throughout the experiments. The sample was shimmed using the FID and T_1 relaxations measurements of PFCE and PFTBA were then obtained simultaneously.

Static System

Static experiments were conducted simply by stopping the flow of the medium in the system following the completion of a perfusion run. The air flow system of the magnet maintained the culture temperature at 37^{o}C. The sample was shimmed using the FID at the beginning of each run. T_1 relaxation measurements of PFCE and PFTBA were then obtained simultaneously and continuously until most of the oxygen in the medium was depleted. The flow of the system was then restarted to replace the medium in the bioreactor with nutrients and dissolved oxygen from the reservoir.

4.3.7 Mathematical Modeling

A mathematical model was developed as an extension of a previously published model [155] (CHAPTER 3) to simulate *in vitro* the difference in the average intrabead DO (AIDO) between the cell-free and cell-containing beads over time, under static

conditions. The model simulates the fixed bed bioreactor as a closed system, where there is a finite volume of medium containing the beads and no transport of oxygen across the boundaries of this volume. The model recognizes three compartments: the cell-containing beads, the cell-free beads, and the liquid medium. The cell-containing and cell-free beads are homogeneously distributed within the medium, which is well-mixed. Beads are assumed to be rigid spheres. Therefore contact points with neighboring beads do not affect the available area for mass transfer between the surrounding liquid and a bead. Radial DO gradients are present within the cell-containing and, transiently, the cell-free beads. The DO at the surface of the cell-free beads is assumed to be equal to that in the medium. A boundary layer exists around the cell-containing beads, with a DO gradient also present in this layer. The change in medium DO is dependent on the flux of oxygen across the surface of the cell-containing beads (Equation 4.2). All equations and parameter values used to simulate AIDO in the cell-containing beads are the same as those listed in Goh et al. [155] (CHAPTER 3), except for the boundary condition. The thickness of the boundary layer was an adjustable parameter evaluated by fitting simulations to experimental results. In cell-free beads, AIDO was calculated also from the same equations with $X = 0$. The transient model equations were solved numerically using finite difference equations programmed in MatLab software. Other model assumptions not explained above are listed below:

$$V_b \frac{dC_b}{dt} = k_L A\left(C_b - C_s\right) = D_{eff} A \frac{\partial C_{aq}}{\partial r}\left(r = R, t\right) \tag{4.2}$$

where V_b and C_b are the volume and oxygen concentration in the bulk medium, A is the surface area of the bead, and C_s is the oxygen concentration at the surface of the bead.

Model Assumptions

1. There is no cell growth during the time period in the simulations; i.e., the encapsulated cell density remains constant.
2. As cells cannot adhere to the alginate matrix, cells do not migrate within the matrix.
3. The PFC emulsion is homogeneously distributed throughout the contiguous alginate matrix.
4. Equilibration of DO between the aqueous and PFC phases at each locale in beads is instantaneous.
5. The values of the model parameters, including the effective diffusivity of DO through the encapsulated system, remain constant over the time period of the simulations.
6. The concentration gradient within the aqueous phase in beads is the only driving force for intra-bead oxygen diffusion.

4.3.8 Statistical Analysis

For each *in vitro* perfusion run, 6 or more T_1 relaxation measurements were obtained, converted to DO via the calibration curve, and standard deviations were determined from these DO measurements. The significance of DO differences between groups were evaluated using one way ANOVA with General Linear Model.

4.4 Results

4.4.1 Simultaneous T_1 Relaxation Measurements of the Dual PFC Bead Population

Figure 4.2 shows the ^{19}F resonance peaks obtained from PFTBA and PFCE-containing beads using an 11.7 T magnet.

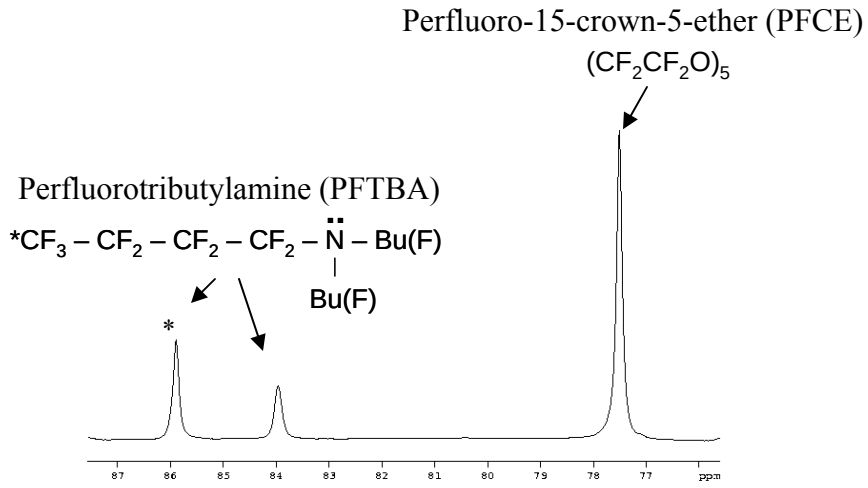

Figure 4.2 Representative image of ^{19}F resonance peaks obtained from PFTBA- and PFCE-containing alginate beads.

The spectrum was irradiated with a high-power short-duration pulse, with the transmitter offset set in the middle of the PFTBA and PFCE peaks of interest. The NMR spectrum of PFTBA exhibits 4 resonance peaks; only 2 are displayed in the figure. T_1 measurements were based on the CF_3 resonance, which is the predominant peak. PFCE, on the other hand, has a single resonance peak that is approximately 9 ppm away from the CF_3-PFTBA peak. An inversion recovery pulse sequence was carried out within this spectrum range for DO determinations within the two PFC bead populations.

4.4.2 Inverse T_1 Relaxation versus DO Calibration Curves

Figure 4.3(a) and (b) reports the calibration curves generated for PFCE and PFTBA under perfused and static conditions.

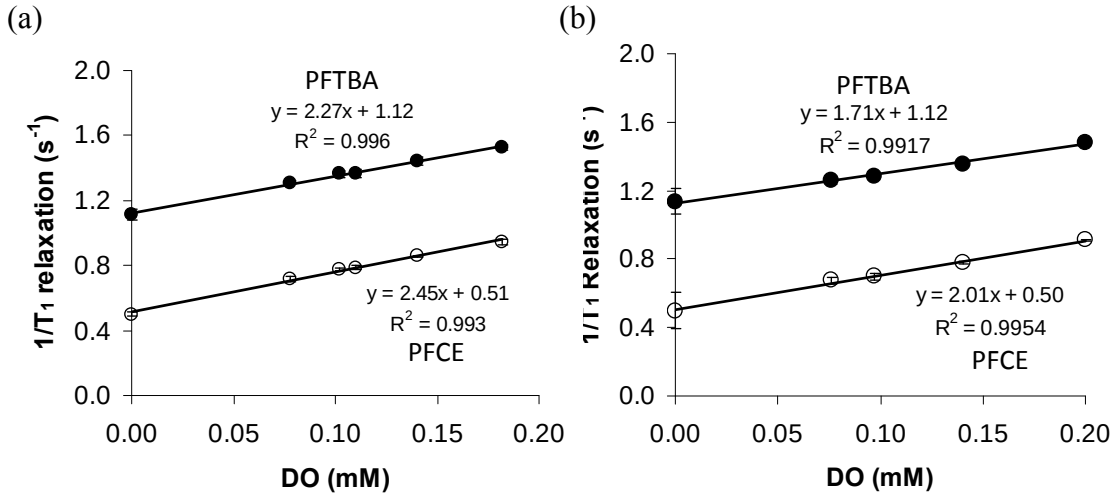

Figure 4.3 Calibration curves of PFTBA (CF_3) (●) and PFCE (○) generated from different medium DO conditions under (a) perfused and (b) static conditions using an 11.7 T magnet. Each data point is the average of 6 T_1 relaxation values with error bars representing their standard deviations.

For both PFCs, the inverse T_1 relaxation of the ^{19}F resonances increased linearly with an increase in DO. Under perfused conditions, T_1 relaxation values were found to be consistently and significantly lower ($p<0.05$) relative to values obtained at the same DO under static conditions, which resulted in higher slopes of the calibration lines. The reason for this difference is not clear; however, there is a possibility of a slight increase in pressure due to flow, therefore increasing the amount of DO, which would consequently cause a reduction in T_1. DO values under each condition were calculated from the respective calibration equations. Based on independent experiments under both conditions, a ± 0.005 mM DO error is estimated to exist from T_1 measurement and processing error.

4.4.3 Perfused Conditions: Monitoring Steady State Construct DO under Medium Flow

βTC-tet cells were encapsulated at a density of 1, 3, and 7×10^7 cells/ml in calcium alginate beads, and were co-cultured with cell-free calcium alginate beads in a bioreactor, each incorporating either PFTBA or PFCE. Table 4.1 shows the measured difference in DO between these two bead populations when cultured under perfused conditions.

Table 4.1 Measured ΔDO between cell-free (medium) and cell-containing calcium alginate beads cultured under perfused conditions. Standard deviations reported were determined from the measurement errors of 6 or more T_1 relaxation measurements for each n.

	ΔDO (mM)
1 x 10^7 cells/ml	
Cell-free PFCE beads / Cell-containing PFTBA (n = 4)	0.0007 ± 0.0112
Cell-free PFTBA beads / Cell-containing PFCE (n = 4)	-0.0014 ± 0.0084
3 x 10^7 cells/ml	
Cell-free PFCE beads / Cell-containing PFTBA (n = 2)	0.007 ± 0.0133
Cell-free PFTBA beads / Cell-containing PFCE (n = 2)	0.010 ± 0.0930
7 x 10^7 cells/ml	
Cell-free PFCE beads / Cell-containing PFTBA (n = 1)	0.011 ± 0.0098
Cell-free PFTBA beads / Cell-containing PFCE (n = 1)	0.012 ± 0.0051

Medium flow rate and external DO were maintained at 6.5 ml/min and 0.18 ± 0.02 mM respectively. As dissolved oxygen in the surrounding culture medium diffuses through the alginate beads very rapidly, the measured DO in the cell-free beads is assumed to be equal to that of the medium. DO in beads containing cells at 1 and 3×10^7 cells/ml were not significantly different than in the medium; ΔDO values were found to be small and within measurement error (± 0.005 mM). A measurable ΔDO was only obtained at a cell density of 7×10^7 cells/ml, where the DO in cell-containing beads was approximately 0.012 mM lower than in the medium.

4.4.4 Static Conditions: Monitoring Transient Construct DO in a Finite Medium Volume

Figures 4.4(a) and (b) show the DO time profiles measured by ^{19}F NMR in the cell-free and cell-containing beads when cultured under static conditions. βTC-tet cells were entrapped at a density of 3×10^7 cells/ml.

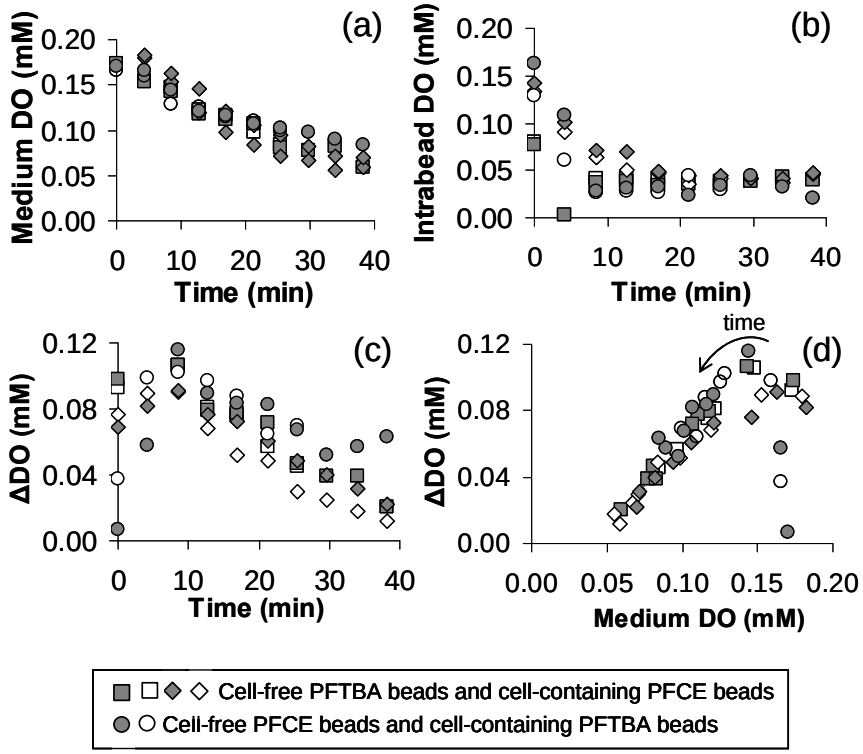

Figure 4.4 DO in the (a) medium, measured using cell-free calcium alginate beads, and (b) cell-containing calcium alginate beads at a density of 3×10^7 cells/ml, as a function of time, under static conditions. ΔDO measured within the two bead populations is reported as a function of time and medium DO in (c) and (d) respectively. Each symbol shape (□,◇,○) represents a different preparation (total n = 3); two runs were performed with each preparation, and the results from each run are distinguished by the shaded (run 1) and open (run 2) symbol of each preparation.

Total bead volume was approximately 2 ml, with a 1:1 ratio of cell-containing to cell-free beads. As cells consumed oxygen, the medium DO decreased from approximately 0.18 to 0.08 mM over 40 minutes. Similarly, the DO within the cell-

containing beads decreased over time but at a higher rate. The measured DO values were consistently lower in the cell-containing beads regardless of the PFC that was incorporated with the cells, indicating that the observed ΔDO was not due to any PFC effect but to the metabolizing cells. The ΔDO between these two bead populations was measurable, and ranged from 0.04 to 0.12 mM, with the difference being lower at low external DO (Figures 4.4(c) and (d)).

Static experiments were also conducted for beads prepared at a cell density of 1×10^7 cells/ml. Figures 4.5(a) and (b) show the DO time profiles in the cell-free and cell-containing beads.

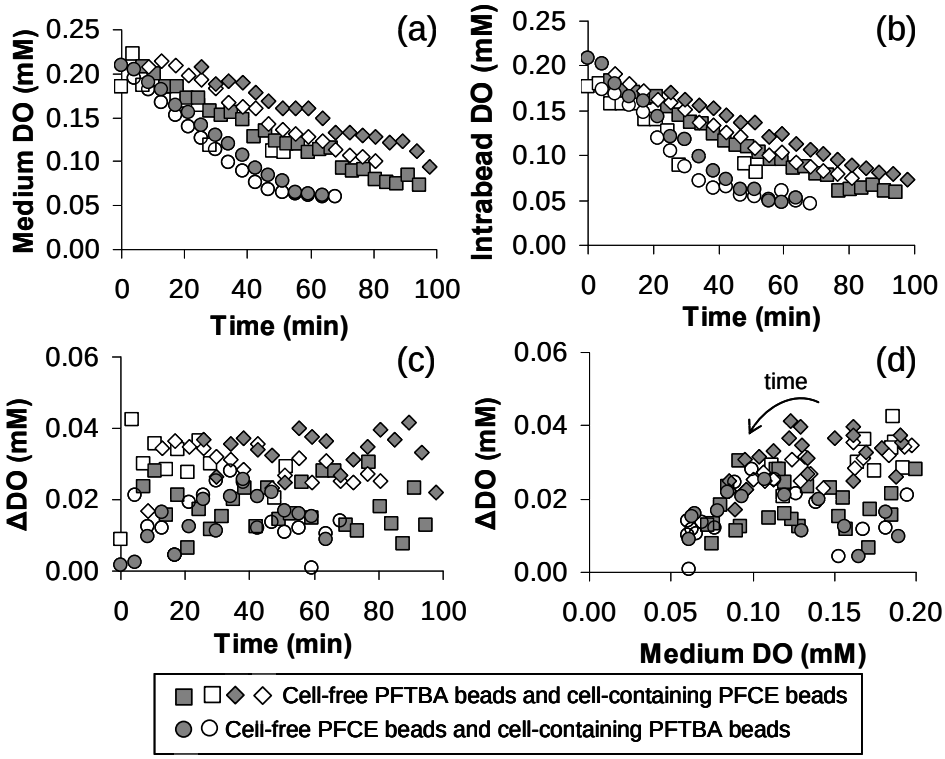

Figure 4.5 DO in the (a) medium, measured using cell-free calcium alginate beads, and (b) cell-containing calcium alginate beads at a density of 1×10^7 cells/ml, as a function of time, under static conditions. ΔDO measured within the two bead populations is reported as a function of time and medium DO in (c) and (d) respectively. Each symbol shape (□,◇,○) represents a different preparation (total n = 3); two runs were performed with each preparation, and the results from each run are distinguished by the shaded (run 1) and open (run 2) symbol of each preparation.

All other experimental parameters and procedures were similar to the previous experiment. As seen with the higher cell density, there was a decrease in DO in the medium and within the cell-containing beads over time. This decrease, however, happened at a lower rate and over a longer period of time. At this density, ΔDO ranged from 0 to 0.04 mM (Figures 4.5(c) and (d)). With these smaller ΔDO values, DO errors (± 0.005 mM) due to T_1 measurements are higher relative to the mean, resulting in a larger variability in the data.

4.4.5 Simulated DO Profiles Under Static Conditions

Mathematical simulations of the ΔDO profiles under static conditions were performed to corroborate the experimentally obtained ^{19}F NMR measurements. A sensitivity analysis was carried out to evaluate the effect of the oxygen mass transfer coefficient in the boundary layer, k_L, on ΔDO between the cell-free and cell-containing beads (data not shown). A k_L value of 20 cm/day was observed to be the best fit for the experimental data, and was used to simulate intrabead DO values. Figures 4.6(a) and (b) show the experimental and simulated ΔDO profiles as a function of external DO for cell densities 3×10^7 cells/ml and 1×10^7 cells/ml.

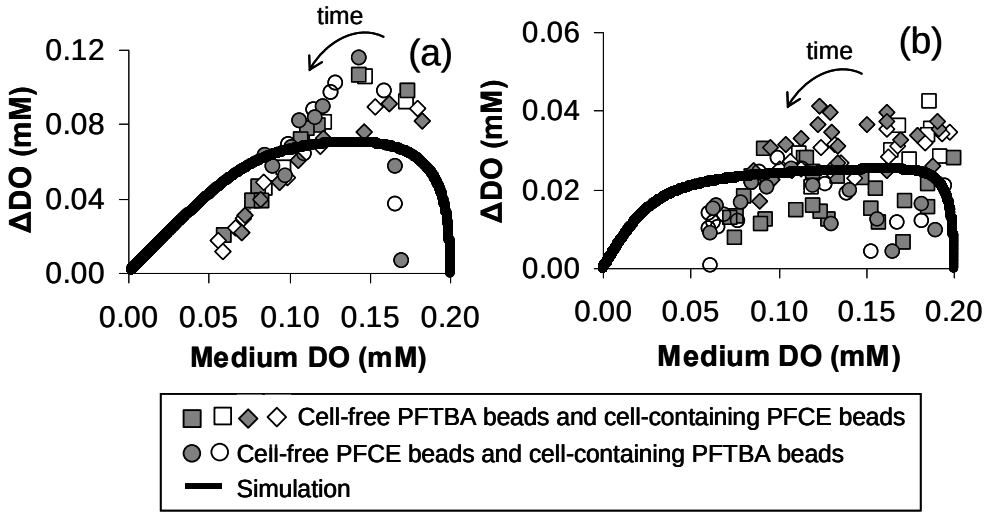

Figure 4.6 Mathematical simulation of the calculated ΔDO versus medium DO for beads cultured in a finite volume of medium. Simulated ΔDO profiles are compared to experimental measurements obtained for cells entrapped at a density of (a) 3×10^7 cells/ml and (b) 1×10^7 cells/ml.

The simulated ΔDO profiles resemble those obtained experimentally, where there was an initial rise in ΔDO, followed by a gradual decrease over time and as the external DO decreased. As expected, at 3×10^7 cells/ml, the simulated ΔDO achieved a higher maximum and had a higher rate of change relative to that at the lower cell density.

4.5 Discussion

An advantage of the dual PFC monitoring method is the chemical shift proximity of the fluorine resonances of PFTBA and PFCE which enables simultaneous T_1 relaxation acquisitions. The ability to obtain simultaneous T_1 measurements allows for the concurrent DO assessments in the construct of interest and the control. The inclusion of the control group of beads to measure the surrounding DO is important because the *in vivo* environment is different among animals and may also change in the same animal with conditions and over time.

In vitro studies using an NMR-compatible bioreactor demonstrated the initial feasibility of the dual PFC method. At a sufficiently short pulse length and high magnet strength, reliable simultaneous T_1 measurements in the dual PFC bead population were obtainable with negligible B_1 inhomogeneity. Under perfusion conditions, the DO in cell-containing beads was only minimally lower than in cell-free beads, which is indicative of convective transport of oxygen in beads as a result of the surrounding flow field. In fact, the difference in DO between the two bead populations was measurable only at the highest encapsulated cell density used of 7×10^7 cells/ml. On the other hand, under static conditions, significantly lower DO values were measured within beads containing metabolically active cells relative to that in the medium due to oxygen diffusion limitations that existed within and around these beads. The ΔDO profiles obtained experimentally were consistent with a mathematical simulation of the system. Because of the assumptions made, the ΔDO values calculated from the model did not closely match those obtained experimentally; however, the compatibility of the trend and the rough similarity of the values strongly indicate that the experimental DO data were not measurement artifacts. The static culturing conditions are more representative of the *in vivo* environment whereby cells within tissue constructs depend on passive diffusion of oxygen from the surroundings for survival. These *in vitro* studies also assisted in establishing the minimum cell density needed to achieve significant ΔDO values for the subsequent *in vivo* experiments.

4.5 Conclusions

We have developed a dual PFC method that utilizes ^{19}F NMR spectroscopy with PFCs as oxygen concentration markers to noninvasively monitor DO within a tissue construct relative to that in the culture medium. *In vitro* studies proved the feasibility of this method to simultaneously measure DO in two distinct bead populations under perfusion and static conditions. The established method was capable of distinguishing the oxygenation state of encapsulated cells from the DO in the surrounding medium. Transient changes in DO within beads cultured under static conditions were corroborated by mathematical simulations.

CHAPTER 5

DUAL PERFLUOROCARBON METHOD TO NONINVASIVELY MONITOR DISSOLVED OXYGEN CONCENTRATION IN TISSUE ENGINEERED CONSTRUCTS *IN VIVO**

5.1 Abstract

The function of an implanted tissue engineered pancreatic construct is influenced by many *in vivo* factors; however, its assessment is solely based on end physiologic effects. As oxygen significantly affects construct function, we established a dual perfluorocarbon (PFC) method that utilizes ^{19}F Nuclear Magnetic Resonance (NMR) spectroscopy, with PFCs as oxygen concentration markers, to noninvasively monitor dissolved oxygen concentration (DO) in βTC-tet cell-containing alginate constructs and in the implantation milieu. The constructs were implanted in the peritoneal cavity of normal and streptozotocin-induced diabetic mice. Using this method, the feasibility of acquiring real-time *in vivo* DO measurements was demonstrated. Results showed that the peritoneal environment is hypoxic and is significantly reduced when βTC-tet cell constructs were implanted. DO within cell-containing beads decreased considerably over time and can be correlated with relative changes in the number of viable encapsulated cells and/or the extent of host cell attachment. The reduction of construct DO due to the metabolic activity of the βTC-tet cells was also compatible with the implant therapeutic function, as observed in the reversal of hyperglycemia in diabetic mice.

* Modification of a paper published in **Biotechnology Progress** (in press)

5.2 Introduction

Insulin-dependent diabetes mellitus (IDDM) is an autoimmune disease resulting from the destruction of insulin-producing β cells of the pancreatic islets. Cell-based therapies are being explored as improved treatments relative to insulin injections, as they have the potential to provide tight regulation of blood glucose levels through physiologic secretion of insulin. Considerable research is being done in developing tissue engineered pancreatic constructs where islets or other insulin secreting cells are encapsulated in biocompatible materials for immune protection and improved *in vivo* survival post-implantation [46, 171]

Despite advances, the challenge of engineering a long-term functional pancreatic construct remains, as the causes and mechanisms of implant failure are numerous and poorly understood [7, 64, 68, 161]. Immune rejection is a main obstacle in successfully transplanting allogeneic or xenogeneic cells even with the current encapsulation systems available [7, 67, 172]. Several investigators have reported on the infiltration of large numbers of host immune cells in the peritoneal cavities of rats and mice during the rejection of encapsulated allografts and xenografts [63, 65, 67, 173]. Rejection due to an immune response can be related to direct cytokine-mediated damage, not prevented by the encapsulation material; it could also be related to a significant inflammatory or fibrotic reaction towards the implant which hampers the transport of nutrients, including oxygen, toward the implanted cells [7, 67, 174]. The problem of limited construct oxygenation may be exacerbated by the low oxygen at the implantation site and, in many cases, the absence of vascularization around these implants [7, 160, 175].

Currently, assessment of the *in vivo* function of a pancreatic construct relies on measurements of blood glucose and insulin or C-peptide levels during oral glucose challenges [126]. A direct evaluation of the physiological state of a construct can only be done at the experimental end-point; therefore, to obtain information on the dynamic changes occurring *in vivo,* animals need to be euthanized and constructs retrieved at various time points. Besides the large number of animals needed for such studies, the large inter-animal variability presents additional challenges. Thus, there are increasing efforts toward developing methods for evaluating *in vivo* construct function on the same animal in real-time, in a minimally or non-invasive way [125, 126, 176, 177]. As construct oxygenation significantly affects cell survival and function [7, 8, 121, 159] monitoring of oxygen levels in pancreatic implants could provide direct information on their functionality. However, most reports on the effect of hypoxia on construct function are limited to *in vitro* settings [9, 71, 121, 132, 158]; *in vivo* evaluation of hypoxia is currently performed through indirect methods post-explantation [160, 175, 178].

We are therefore pursuing the development of a noninvasive method of monitoring dissolved oxygen concentration (DO) in a tissue engineered pancreatic construct using ^{19}F Nuclear Magnetic Resonance (NMR) spectroscopy, with perfluorocarbons (PFCs) as oxygen concentration markers. The principle behind this method is the linear relationship between the inverse spin lattice relaxation time ($1/T_1$), of the fluorine resonances from PFCs and oxygen tension [102]. We developed a dual PFC method consisting of incorporating a different PFC in cell-containing experimental beads and cell-free control beads; the latter group of beads was used to monitor the DO at the implantation milieu, as instantaneous equilibration of intrabead and external DO could be

assumed. Measuring DO within the experimental implant offers an assessment of the metabolic activity of the cells within the construct [9].

In a previous study (CHAPTER 4), we demonstrated the feasibility of this method to acquire simultaneous DO measurements within cell-containing alginate beads and in the culture medium. In this study, we implemented the dual PFC method to acquire real-time DO measurements within βTC-tet cell-containing alginate beads implanted in the peritoneal cavity of normal and diabetic mice. Our goals were to obtain real-time measurements of construct DO, and to correlate these measurements to the physiological state and therapeutic function of the implant. Additionally, we investigated the effect of the implanted cell constructs on the peritoneal DO and compared the peritoneal DO of normal and diabetic mice. The usefulness of the information provided by these studies on the *in vivo* functionality of encapsulated cell implants, and on the effect of such implants on host animal physiology, is discussed.

5.3 Materials and Methods

5.3.1 Cell Culture, PFC Preparation, and Cell/PFC Encapsulation

Murine insulinoma βTC-tet cells [44] were obtained from the laboratory of Dr. Shimon Efrat, Albert Einstein College of Medicine, Bronx, NY. Cells were cultured as monolayers in T-175 flasks, in a 37^{o}C, 5% CO_2 humidified incubator. Culture medium consisted of Dulbecco's Modified Eagle's Medium (DMEM, Sigma Chemical Co., St. Louis, MO) with 25 mM glucose, supplemented with 10% fetal bovine serum, 1% penicillin-streptomycin, and 1% L-glutamine to a final concentration of 6 mM, and it was changed every 2-3 days. Cell monolayers that reached 80% to 90% confluency were split

by treatment with 0.25% trypsin-EDTA (Sigma); passage number increased by one at each splitting. Cells of passage number 37-42 were used in this study.

The PFCs used were perfluorotributylamine (PFTBA) and perfluoro-15-crown-5-ether (PFCE). The PFC emulsion was prepared following a protocol adapted from Joseph et al. [146] and described by Gross et al. [9] (CHAPTER 3). Cells of 90% confluency were harvested by trypsin-EDTA and entrapped at a density of 2.0×10^7 cells/ml alginate in 2% w/v low viscosity, high mannuronic content alginate (LVM, NovaMatrix, Drammen, Norway) containing 50 mg/ml PFTBA or PFCE emulsion (see below) to produce calcium alginate beads. Using an electrostatic droplet generator (Nisco Engineering Inc., Zurich, Switzerland), cells were entrapped according to the procedure of Stabler et al., where the alginate/cell/PFC mixture was extruded into a 100 mM $CaCl_2$ solution [143]. Calcium beads were coated with poly-L-lysine (PLL), and a final layer of alginate to produce alginate-poly-L-lysine-alginate (APA) beads, used for *in vivo* studies. The coating protocol was as described by Papas et al. [144], which was based on a protocol by Lim and Sun [51]. Cells were also entrapped at a density of 2×10^7 cells/ml alginate in 3% w/v LVM containing PFTBA or PFCE emulsion at 50 mg/ml to produce barium alginate beads. The entrapment procedure was similar to that for calcium alginate beads, except that the alginate/cell/PFC suspension was extruded into a 20 mM or 30 mM $BaCl_2$ solution and allowed to crosslink for 5 minutes; the beads were then washed 5 times with physiological saline and 3 times with unsupplemented DMEM. The average diameter of the resulting APA and barium beads after washing was 500 ± 100 μm and 700 ± 150 μm, respectively.

For one of the control groups (control 2, see below), encapsulated cells were killed through heating at 60^{o}C for half an hour. Cell death was confirmed through trypan blue (Sigma) exclusion method before implantation. The mechanical integrity of the beads was determined by measuring the Young's modulus via uniaxial compression using a Bose ElectroForce® 3100 apparatus (EnduraTec, Inc., Eden Prairie, MN) and was found not to be compromised by the heating process.[179]

5.3.2 7 T Magnet

For all *in vivo* measurements, ^{19}F NMR spectra were acquired using a 16 mm diameter surface coil (Doty Scientific, Columbia, SC) on a 7 T horizontal bore magnet equipped with a Bruker Avance console (Bruker, Billerica, MA) at the Nanomedicine Research Institute Magnetic Resonance Laboratory, Georgia Institute of Technology, Atlanta GA. An inversion recovery sequence with an 180^{o} adiabatic pulse (hyperbolic secant) was used to acquire T_1 relaxation measurements; there were 23 delay times ranging from 0.01 s to 7 s for each T_1 determination. Acquisition parameters for the experiments were: 2 transients, 4096 data points per free induction decay, 15 s relaxation delay. Peak intensity was extracted using the area under the peak, and all T_1 relaxation rates were determined through a 3-parameter exponential fit using Bruker Avance software.

5.3.3 Calibration of Inverse T_1 Relaxation versus DO

Cell-free alginate beads containing 50 mg/ml PFTBA or PFCE emulsion were loaded in a 50 ml centrifuge tube containing physiologic saline. The solution was

bubbled with nitrogen, air or oxygen at 37°C and atmospheric pressure for at least 45 minutes to allow for equilibration, then sealed and placed on the surface coil. Temperature was maintained with a water bath that pumped heated water through tubing wrapped around the centrifuge tube. T_1 relaxation measurements were obtained and correlated to DO by equation 5.1 below.

$$\frac{1}{T_1} = M[DO] + I \tag{5.1}$$

5.3.4 Animals and the Induction of Diabetes

All experiments were carried out in accordance with protocols approved by the Georgia Tech Animal Care and Use Committee. Balb/c mice were obtained from Jackson Labs (Bar Harbor, ME) and housed under specific pathogen-free conditions in the animal facility at Georgia Tech. Six-week old mice were used for subtherapeutic studies. Ten-week old mice were made diabetic through multiple i.p injections of 210 mg/kg of streptozotocin (Sigma), dissolved in sodium citrate buffer (pH 4.5) (Sigma). Mouse blood glucose levels and body weights were monitored daily. Blood glucose concentrations were measured in blood samples collected from mice tail veins by TRUEtrack glucose monitors (CVS, Woonsocket, RI). Mice were considered diabetic when their blood glucose levels were above 350 mg/dl for 2 consecutive days. Mice that had blood glucose levels above 250 mg/dl for 2 consecutive days after construct implantation were euthanized.

5.3.5 Construct Implantation and DO Measurements

This study is divided into two parts; subtherapeutic and therapeutic study where the constructs were implanted in normal mice and in STZ-induced diabetic mice, respectively. The alginate beads were implanted in the mouse peritoneal cavity through a simple injection. For all studies, the PFC emulsion was incorporated at a concentration of 50 mg/ml, and βTC-tet cells were entrapped at a density of 2×10^7 cells/ml. The groups of mice and types of implant are as listed in Table 5.1 below:

Table 5.1 Types and volumes of implanted beads in different groups of mice

Part I - Subtherapeutic Study	
Study 1	
Control Normal (n = 2)	0.4 ml of cell-free PFTBA calcium alginate beads and 0.4 ml of cell-free PFCE calcium alginate beads
Experimental Normal (n = 7)	0.6 ml of cell-free PFTBA calcium alginate beads and 0.2 ml of **cell-containing calcium APA beads**
Study 2	
Control Normal (n = 4)	0.4 ml of cell-free PFTBA barium alginate beads and 0.4 ml of cell-free PFCE barium alginate beads
Experimental Normal (n = 14)	0.6 ml of cell-free PFTBA barium alginate beads and 0.2 ml of **cell-containing barium alginate beads**
Part II: Therapeutic Study	
Control 1 - Normal (n = 4), Diabetic (n = 6)	0.7 ml of cell-free PFTBA barium alginate beads and 0.3 ml of cell-free PFCE barium alginate beads
Control 2 - Normal (n = 3), Diabetic (n = 4)	0.6 ml of cell-free PFTBA barium alginate beads and 0.2 ml of dead cell-containing PFCE barium alginate beads
Experimental Diabetic (n = 17)	0.6 ml of cell-free PFTBA barium alginate beads and 0.2 ml of **cell-containing PFCE barium alginate beads**

Two mice were also implanted with cell-free, PFC-free, alginate beads to ensure that there was no ^{19}F background signal and that the resonances observed were from the PFCs. PFC-containing beads were implanted at different volumes so that sufficient NMR signal can be obtained; this does not affect DO values.

Experimental normal mice that had blood glucose levels below 100 mg/dl were given drinking water containing 1 mg/ml tetracycline (Sigma) with 1.5% (w/v) sucrose (Sigma) to inhibit cell proliferation. Experimental diabetic mice were given drinking water containing 4 mg/ml tetracycline (Sigma) with 1.5% (w/v) sucrose (Sigma) starting from Days 1 to 4 until the end of the experiment. The tetracycline water was replaced every 2 days. βTC-tet undergoes growth arrest in the presence of tetracycline [44].

During NMR scans, mice were anesthesized in 1.5% isoflurane in oxygen flowing at 1.5 l/min, and kept at 37^{o}C with a warming pad.

5.3.6 Post-explantation Studies

Following NMR scans, experimental mice were euthanized on Days 4, 8 and 16, and control normal and diabetic mice were euthanized on Day 16 and Day 2 respectively. Beads were explanted via peritoneal lavage with Dulbecco's Phosphate-Buffered Saline (MediaTech, Manassas, VA). Bead integrity was visualized by light microscopy. Host cell attachment and cell growth were evaluated through histology, where beads were fixed in 2% glutaraldehyde (Sigma), embedded in paraffin, sectioned, and stained with hematoxylin/eosin (H/E). Cell viability was analyzed through a live/dead assay. Living and dead cells were stained with calcein-AM (excitation: 488 nm/emission: 500-530 nm) and ethidium homodimer (excitation: 543 nm / emission: 560 nm) (Invitrogen, Eugene, OR) and observed using a confocal microscope (LSM 510 META, Zeiss, Maple Grove, MI).

To evaluate β-cell function, retrieved beads were subjected to an insulin secretion test, where the cell-free and cell-containing bead mixture was cultured in basal medium (0 mM glucose, unsupplemented DMEM) for 1 hour and then transferred to stimulating medium (16 mM, fully supplemented DMEM) for 30 minutes. Medium samples withdrawn at the start and end of each basal and stimulation period were stored at -80^{o}C for later assays. Insulin concentration in collected samples was assayed using mouse insulin ELISA (Mercodia, Uppsala, Sweden) and absorbance was measured at 450 nm wavelength using a Spectra Max Plus Plate Reader (Molecular Devices, Sunnyvale, CA).

As the explanted bead samples used were random mixtures of cell-free and cell-containing beads, the number of βTC-tet cells could not be quantified; therefore, secretion results were reported only as positive when a stimulated insulin secretion response was detected.

5.3.7 Statistical Analysis

All data were analyzed using Minitab software (Minitab, Inc., State College, PA). A total of 3 T_1 relaxation measurements were obtained from a single mouse and DO was determined from the average of these values. DO data were reported as the mean of the average DO values from the mice scanned on a particular day ± standard deviation of the averages. The significance of DO differences between groups and days were evaluated using one-way analysis of variance (ANOVA) with General Linear Model.

Part I: Subtherapeutic Study

5.4 Results

5.4.1 Simultaneous T_1 Relaxation Measurements of the Dual PFC Bead Population

The inverse T_1 relaxation measurements of ^{19}F resonances increased linearly with DO. Table 5.2 summarizes the linear fit parameters for the two PFCs; these parameters were used for DO determinations from T_1 measurements of the implanted constructs.

Table 5.2 Slope (*M*) and y-intercept (*I*) of the linear calibration curves correlating the inverse T_1 relaxation to DO. Calibrations were performed for PFTBA and PFCE under static conditions on a 7 T horizontal bore magnet.

	M (s^{-1} mM^{-1})	I (s^{-1})	Correlation coefficient, R^2
PFTBA	2.04	0.44	1.000
PFCE	2.10	0.85	0.999

Figure 5.1 shows typical ^{19}F NMR spectra acquired from an anesthetized mouse implanted with (a) cell- and PFC-free barium alginate beads, and (2) cell-free, PFTBA and PFCE-containing barium alginate beads.

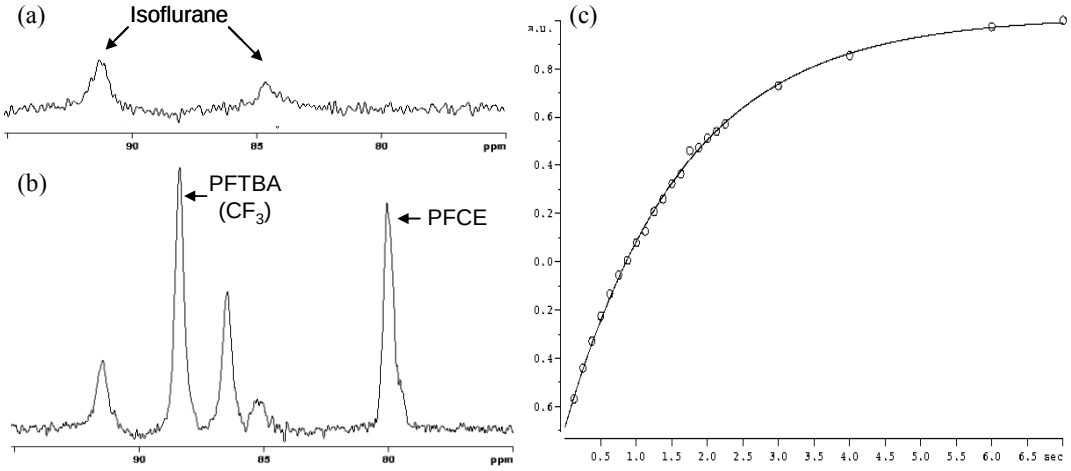

Figure 5.1 ^{19}F resonance peaks obtained from mice implanted with (a) cell- and PFC-free alginate beads and (b) cell-free, PFC-containing alginate beads. (c) Representative 3-parameter exponential fit of a typical inversion recovery experiment for T_1 determination. x-axis: relaxation delay time (s), y-axis: integrated peak area

When mice were placed under anesthesia, ^{19}F NMR measurements obtained yielded a flat baseline over the spectral region of interest, although 2 resonance peaks identified to be due to isoflurane were observed. The isoflurane peaks did not interfere with those of PFTBA or PFCE as seen in mice that were implanted with PFC-containing beads. Similar to *in vitro* observations, the PFTBA-CF_3 peak was approximately 9 ppm away from the single PFCE peak; the chemical shift proximity of these two peaks allowed for simultaneous T_1 acquisitions. All the exponential fits of the inversion recovery experiment for T_1 acquisitions were good, as seen in a representative fit shown in Figure 5.1(c). This indicates that there was a narrow distribution of DO values in the beads implanted in the peritoneal cavity.

5.4.2 Monitoring *in vivo* DO and Evaluation of Explanted Constructs

Study1: Calcium Alginate-PLL-Alginate (APA) Cell-containing Implant

APA beads containing βTC-tet cells/PFCE were implanted at subtherapeutic levels in the peritoneal cavity of experimental normal mice. Cell-free PFTBA calcium alginate beads were co-implanted to track the oxygen levels at the surrounding peritoneal environment. These DO values were also compared to those measured in the peritoneal cavity of control mice implanted with cell-free PFTBA and PFCE calcium alginate beads. Figure 5.2 shows the DO measurements obtained through ^{19}F NMR within these two bead populations in the experimental and control mice, along with images of explanted beads examined through light microscopy and histology.

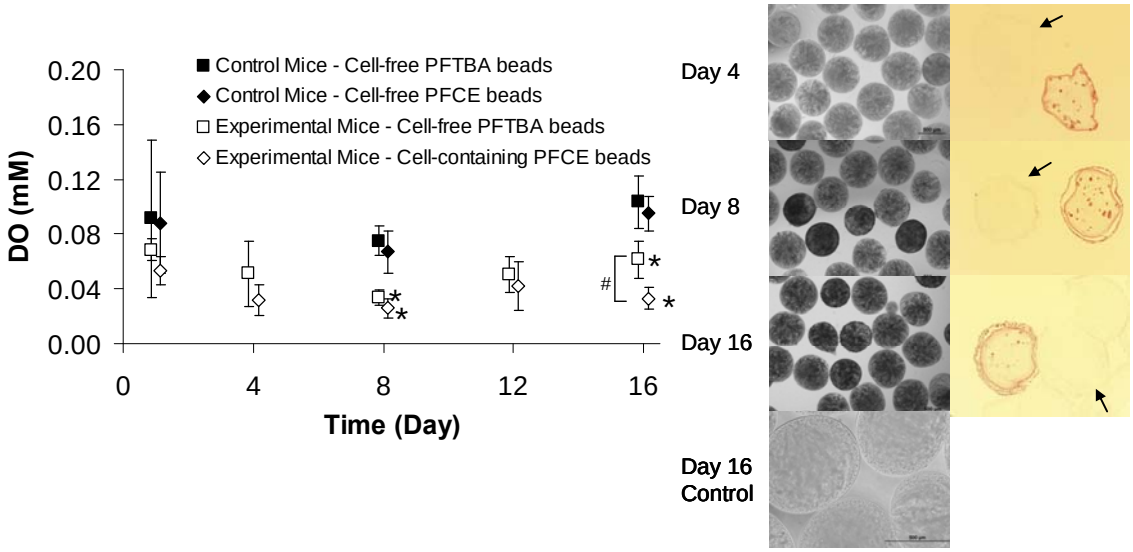

Figure 5.2 DO within cell-free calcium alginate beads implanted in the peritoneal cavity of control mice (n = 2 on all days); and DO within cell-free calcium alginate and cell-containing APA beads implanted in the peritoneal cavity of experimental mice (n = 4, 4, 5, 3, 3 for Days 1, 4, 8, 12, 16 respectively). Also shown are representative images of explanted cell-free and cell-containing beads, examined through light microscopy and histology. Histological image of the cell-free PFTBA bead is marked with an arrow. $^{\#}p<0.05$, compared between cell-free and cell-containing beads at a time point, $*p<0.05$, compared between experimental and control mice, the latter with nested PFC groups, both analyzed using one-way ANOVA with General Linear Model.

Measured DO within the implanted beads fluctuated considerably between acquisitions. DO in the peritoneal cavity of the control mice, measured using cell-free PFC beads, were found to be 0.09 ± 0.068, 0.07 ± 0.019 and 0.10 ± 0.023 mM on Days 1, 8 and 16 respectively. It is worthwhile to note that the actual peritoneal DO might be slightly lower than reported here due to the fact that mice were breathing isoflurane in 100% oxygen during NMR scans.

On Day 1, DO within cell-containing beads and the surrounding peritoneal cavity, measured using cell-free beads, were observed to be 0.053 ± 0.010 and 0.068 ± 0.008 mM respectively in experimental mice. These values were statistically similar to those obtained in control mice implanted with only cell-free beads. The DO in the cell-containing beads and the surrounding peritoneal cavity decreased over the first 8 days to significantly lower levels when compared to Day 1 ($p<0.05$). These DO values were also statistically lower than the peritoneal DO measured in control mice, and remained as such until the end of the experiment. On Day 16, the DO within the cell-containing beads was statistically lower than the surrounding peritoneal DO in experimental mice (0.033 ± 0.008 mM vs. 0.061 ± 0.014 mM, respectively).

All beads explanted from control and experimental mice were intact when visualized under light microscopy. Histological analysis and live/dead staining showed some initial cell growth the first 8 days, and that cell-containing APA beads exhibited host cell attachment which worsened over time. From Day 8 to Day 16, however, there were no further cell growth and the extent of host cell attachment remained the same. Co-implanted cell-free alginate beads were clear of overgrowth on Day 4. While a few adherent cells were detected around these beads on Days 8 and 16, generally less than

10% of the bead surface area was covered. All cell-free alginate beads implanted in the control mice were clear of host cell attachment. Insulin secretion was detected in explanted beads from experimental mice on all days, verifying the presence of viable βTC-tet cells (Results shown in Figure A4.1 in Appendix IV). .

Study 2: Barium Alginate Cell-containing Implant

Because PLL is known to induce *in vivo* host responses, as also observed in this study, we switched to using barium alginate beads, which have been found to be a more biocompatible material in comparison [62, 65]. Similar experiments were carried out with βTC-tet cells entrapped in barium alginate beads with PFCE, and co-implanted with cell-free PFTBA barium alginate beads. Control mice were implanted with cell-free PFTBA and PFCE barium alginate beads. Figure 5.3 shows the DO measurements obtained through ^{19}F NMR within these two bead populations in the two groups of mice, along with images of the explanted beads.

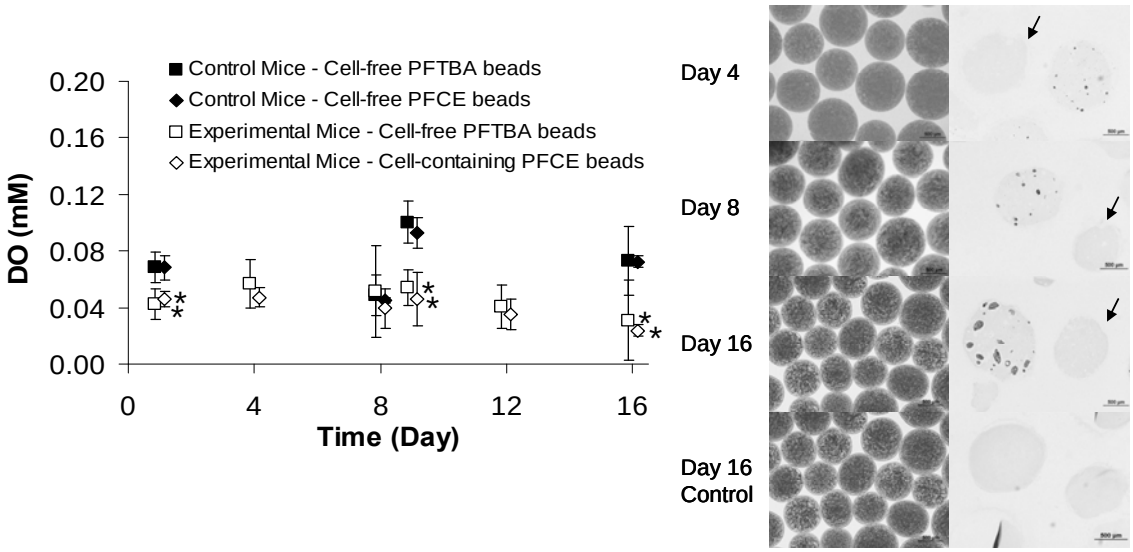

Figure 5.3 DO within cell-free barium alginate beads implanted in the peritoneal cavity of control mice (n = 4, 2, 2, 4 on Days 1, 8, 9, 16); and DO within cell-free and cell-containing barium alginate beads implanted in the peritoneal cavity of experimental mice (n = 7, 4, 5, 5, 6, 4 for Days 1, 4, 8, 9, 12, 16 respectively). Also shown are representative images of explanted cell-free and cell-containing beads, examined through light microscopy and histology. Histological image of the cell-free PFTBA bead is marked with an arrow. *$p<0.05$, compared between experimental and control mice, the latter with nested PFC groups, analyzed using one-way ANOVA with General Linear Model.

DO in the peritoneal cavity of control mice, measured using cell-free PFC beads, were found to be 0.068 ± 0.014, 0.047 ± 0.015, 0.096 ± 0.018 and 0.072 ± 0.025 mM on Days 1, 8, 9 and 16 respectively. In experimental mice, the DO within cell-containing beads and the surrounding peritoneal cavity were measured to be 0.046 ± 0.006 mM and 0.043 ± 0.011 mM respectively on Day 1, and were observed to gradually decrease over time. When compared to Day 1, this decrease was only significant on Day 16 ($p<0.05$), where DO values were 0.031 ± 0.029 mM and 0.024 ± 0.004 mM respectively. On Days 1, 9 and 16, the DO in the cell-containing beads and the surrounding peritoneal cavity in experimental mice were both significantly lower than the peritoneal DO in control mice.

There was no difference between the two bead populations implanted in the experimental mice on any of the days when measurements were performed.

The majority of the explanted beads from both control and experimental mice were intact when observed microscopically, although a few broken beads were found occasionally. Within the experimental time frame, all cell-free and cell-containing beads were clear of host cell attachment. Histological analysis and live/dead staining showed insignificant cell growth during the first 8 days, and the measured insulin secretion was low during this period of time. On Day 16, however, there was a marked increase in cell number and a significantly higher amount of insulin secreted during glucose stimulation (Results shown in Figure A4.2 in Appendix IV).

5.5 Discussion

Perfluorocarbons have been increasingly used as physiological markers of tissue oxygenation in ^{19}F NMR. The high fluorine content of these compounds make them good imaging contrast agents or concentration markers for dissolved oxygen, as a relatively low concentration of PFC is usually sufficient to achieve good signal intensities. Furthermore, most PFCs are safe and biocompatible, thus making them suitable for *in vivo* studies [13, 180, 181]. Zimmermann et al. evaluated the metabolic activity of mouse L-cells co-cultured with PFTBA up to 70%, and observed no apparent cytotoxicity when compared to a control group [109]. When entrapped in alginate beads, the PFC emulsion is stable, thereby preventing it from being eliminated from the body and allowing for long term monitoring studies [9]. In this study, the ^{19}F signal obtained from the PFCs on Day 16 was observed to be comparable to that obtained on Day 1,

indicating that the majority of the beads were still intact and that the PFC emulsion was stable. While this study was only 16 days long, other researchers have been able to detect ^{19}F signal of entrapped PFC over three months post-implantation [108, 109].

In this study, a single average T_1 value was obtained from the sum of the signal intensities from all volume elements across the sample in the peritoneal cavity. All the exponential fits for the T_1 values were good, indicating a narrow distribution of intrabead DO values for a particular animal at a time point. Although one could obtain the DO distribution within the peritoneal cavity by applying one or two-dimensional chemical shift imaging, construction of such oxygen profiles requires long acquisition times and high concentrations of PFC for sufficient signal. As we are ultimately concerned with evaluating the function of the entire implant over time, the average DO measurements used in this study were sufficient for this assessment.

The dual PFC method was proven capable of tracking both the DO in the cell-containing beads and the peritoneal DO over 16 days through ^{19}F NMR. The peritoneal cavity was found to be hypoxic, with oxygen levels varying significantly over time. This observation was consistent with other studies, including those of Noth et al. and Gross et al. who reported that peritoneal DO ranged from -0.007 to 0.24 mM in rats [108] and 0.02 to 0.27 mM in mice [9], respectively. Studies with APA beads indicated gradual cell growth and host cell attachment around the beads over the first 8 days; these observations were compatible with the decrease in DO within the cell-containing beads. The lack of further cell growth and host cell attachment could explain the DO stabilizing within these beads from Day 8 onwards. On the other hand, cell growth in barium alginate beads was slow the first 8 days; this delayed growth pattern being similar to that observed in βTC3

cells entrapped in high guluronic acid content alginate [182]. On Day 16, there was a marked increase in the viable cell number and amount of secreted insulin, which was also reflected in the significantly lower DO within the cell-containing beads when compared to Day 1. It should be noted that although the therapeutic function of the implanted constructs was not evaluated in this study, the measured DO and observed cell growth appeared consistent with the changes in the overall mouse blood glucose levels. Specifically, mice implanted with APA beads approached hypoglycemia within the first few days post-implantation, whereas mice implanted with barium alginate beads remained normal within the first 10 days, but started to approach hypoglycemia thereafter (data not shown).

For both studies with APA and barium alginate beads, a lower peritoneal DO was measured in the experimental mice implanted with βTC-tet cells when compared to the peritoneal DO of the control mice. This suggests that a considerable amount of oxygen was being consumed by the metabolically active βTC-tet cells, and possibly also by the peritoneal host cells surrounding the APA beads. Although inflammatory reaction towards the barium alginate beads was not observed, host cells could still be recruited to the implantation site as observed by Safley et al. who reported a significant increase in the number of host cells infiltrating the peritoneal cavity after one week following transplantation of xenogeneic adult porcine islets entrapped in barium alginate [65]. In this study, however, allogeneic cells were implanted in normal mice. The decrease in the peritoneal DO is also likely to be more pronounced in diabetic mice, as we would expect a higher metabolism and oxygen consumption by the implanted β cells to meet the demands for insulin secretion. Presumably then, through this dual PFC method of

monitoring, correlations between construct oxygenation and the achieved therapeutic effects can be established. It is also reasonably expected that this monitoring approach can be adapted for other implantation sites, or other tissue engineered constructs besides encapsulated cells.

Part II: Therapeutic Study

5.6 Results

5.6.1 Correction of Diabetes in STZ-Induced Diabetic Balb/c Mice

The construct therapeutic function was evaluated through daily determinations of random blood glucose levels in mice. Figure 5.4 shows blood glucose concentrations of diabetic mice implanted with encapsulated βTC-tet cells (experimental), cell-free beads (control 1D), and encapsulated dead βTC-tet cells (control 2D).

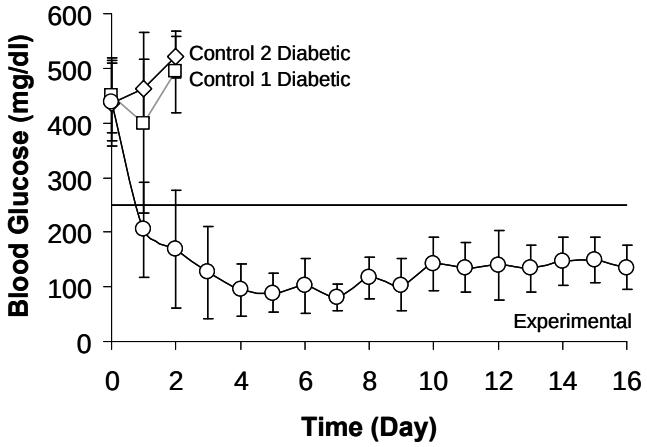

Figure 5.4 Blood glucose levels of control 1D and 2D mice receiving cell-free beads (n = 6) and dead cell-containing beads (n = 4), respectively, and of experimental mice receiving βTC-tet cell-containing beads (n = 9 to 17). On Day 4, 5 experimental mice were euthanized and on Day 8, 3 mice experimental were euthanized.

Implantation of βTC-tet cells corrected hyperglycemia within 3 days and maintained normoglycemia in the mice until euthanasia, indicating that the constructs were functional within the experimental time frame. As tetracycline regulated βTC-tet

cell proliferation, the mice did not become hypoglycemic at later time points but blood glucose levels stabilized within normal ranges. There was a 7% increase in the average body weight of these mice within 16 days. Control diabetic mice that received cell-free beads and dead cell-containing beads remained hyperglycemic and were euthanized two days post-implantation.

5.6.2 Monitoring DO in the Tissue Construct and the Peritoneal Cavity

STZ-induced diabetic mice (experimental) were implanted with βTC-tet cell-containing PFCE beads and cell-free PFTBA beads in the peritoneal cavity, and DO measurements within these two bead populations were obtained over time. These DO values were compared to those measured in cell-free PFCE and PFTBA beads, implanted in normal and diabetic mice (controls 1N and 1D, respectively), and in dead βTC-tet cell-containing PFCE beads and cell-free PFTBA beads, also implanted in normal and diabetic mice (controls 2N and 2D, respectively).

Figure 5.5 shows the ^{19}F NMR-acquired DO in beads from the experimental and control 1N and 2N mice over a 16 day period.

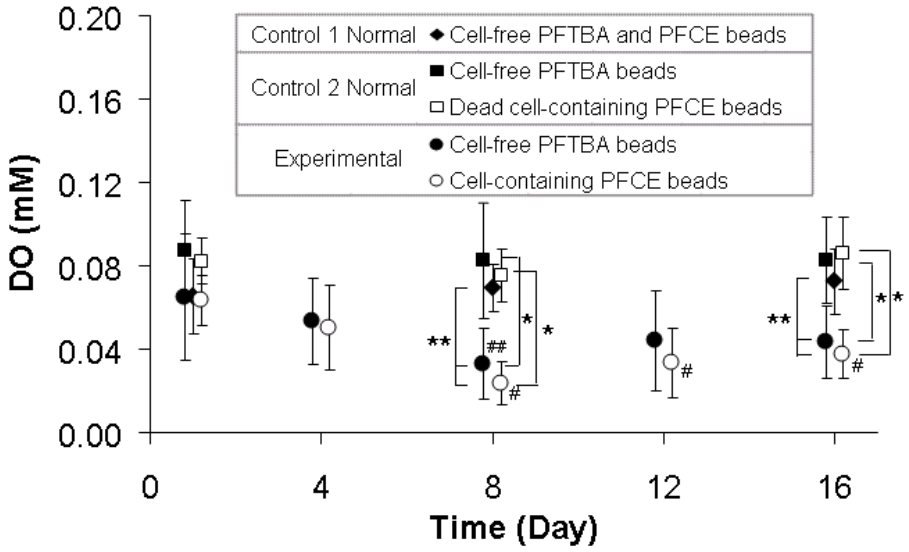

Figure 5.5 DO measurements in cell-containing PFCE beads and cell-free PFTBA beads implanted in experimental mice (n = 8 on Day 1, n = 9 on all other days), in cell-free PFCE and PFCE beads implanted in control 1N mice (n = 4), and in dead cell-containing PFCE beads and cell-free PFTBA beads implanted in control 2N mice (n = 3). **$p<0.05$, compared between experimental and control 1N mice, the latter with nested PFC groups; *$p<0.05$, compared between experimental and control 2N mice; $^{\#\#}p<0.05$, compared to Day 1 in cell-free beads in experimental mice; $^{\#}p<0.05$, compared to Day 1 in cell-containing beads in experimental mice. All comparisons analyzed using one-way ANOVA with General Linear Model.

The average DO in the peritoneal cavity of control 1N mice ranged from 0.065 to 0.073 mM during the Day 1 to 16 time period, with no statistical differences found between any of the days. The peritoneal DO of control 1D mice (n = 6) was also measured on Days 1 and 2 and found to be 0.088 ± 0.012 and 0.079 ± 0.016 mM, respectively; the DO on Day 1 was not different from that in control 1N mice.

One day post-implantation, the peritoneal DO in experimental mice was 0.065 ± 0.03 mM and in the βTC-tet cell-containing beads 0.063 ± 0.012 mM; these were not statistically different. The DO in the cell-containing beads decreased over time, and on Day 8 became and stayed significantly lower than the Day 1 value until the end of the

experiment. The peritoneal DO was also significantly lower on Day 8 than on Day 1. The DO in the cell-containing beads was comparable to the peritoneal DO on all days in the experimental mice. Notably, the DO within the cell-containing beads and the peritoneal cavity in experimental mice were both significantly lower than the peritoneal DO in control 1N mice on Days 8 and 16.

To assess whether the lowered DO observed in experimental mice was due to the metabolic activity of the implanted βTC-tet cells, or whether recruited host immune cells also played a role, measurements were obtained from control 2N mice implanted with cell-free and dead βTC-tet cell-containing beads. Average DO values in the dead cell-containing PFCE beads ranged from 0.075 to 0.086 from Day 1 to 16, with no statistical differences between any of the days. DO measurements were also obtained from the same type of beads implanted in control 2D mice (n = 4) on Days 1 and 2, and found to be 0.067 ± 0.014 and 0.072 ± 0.016 mM, respectively; the DO on Day 1 was not different than that in control 2N mice. DO measurements in the dead cell-containing beads were comparable to the surrounding peritoneal DO on all days for all mice. More importantly, these DO measurements were also comparable with the peritoneal DO in control 1N mice, but significantly higher than the DO measured in beads implanted in experimental mice.

5.6.3 Evaluation of the Physiological State of the Tissue Construct

Figure 5.6 shows representative images of beads explanted from control 1N and 2N mice on Day 16 and from experimental mice on Days 4, 8, and 16.

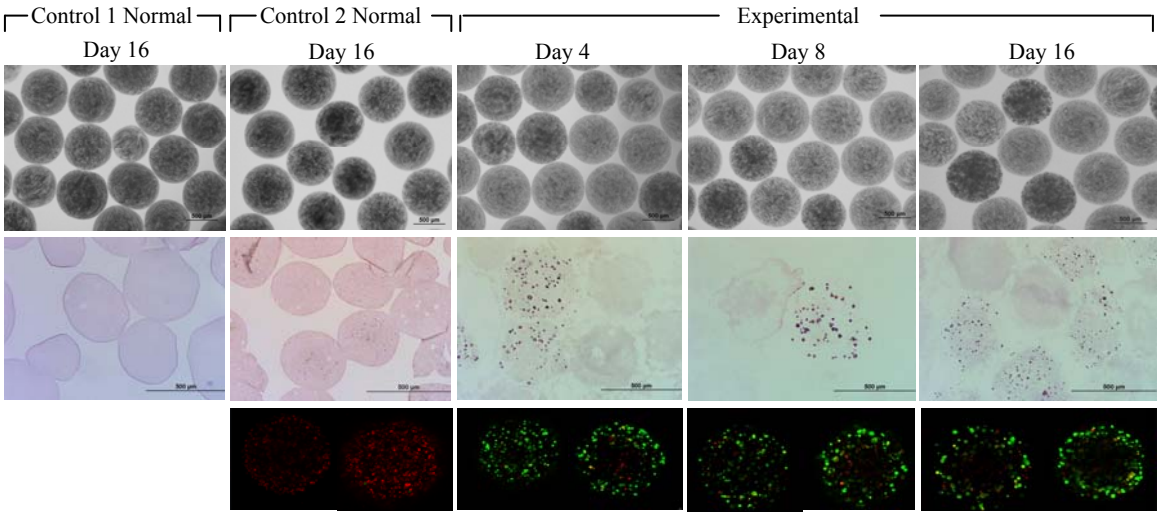

Figure 5.6 Light micrographs (4×), histological analysis (10×), and live/dead staining (10×) of representative beads explanted on Day 4 (n = 5), Day 8 (n = 3), and Day 16 (n = 9) from experimental mice and beads explanted on Day 16 from control 1N mice (n = 3) and control 2N mice (n = 4).

Explanted beads from all groups were intact when observed microscopically, although a few broken beads were found occasionally. Live/dead staining and histological examination showed that beads from experimental mice contained viable βTC-tet cells on all explantation days, and that both cell-free and cell-containing beads were clear of host cell attachment throughout the experimental time period. Some initial cell growth was observed the first week post-implantation; insignificant cell growth was observed thereafter. Encapsulated βTC-tet cells were also functional on all explantation days, as detected by an increase in insulin release to an *in vitro* glucose stimulation test (Results shown in Figure A4.3 in Appendix IV). With beads explanted from control mice 2N, no live βTC-tet cells were detected by live/dead staining and histology; also, when beads were subjected to an *in vitro* glucose stimulation test, no insulin was detected, confirming that the cells were indeed nonfunctional. Similar observations were made with beads explanted from the control mice 1D and 2D on Day 2 (images not shown).

5.7 Discussion

Tissue engineered pancreatic constructs have the potential to provide tight glycemic control in IDDM patients. The peritoneal cavity is a plausible implantation site as it can easily accommodate these constructs [183]. However, with beads implanted in the peritoneal cavity, the supply of oxygen to the cells occurs through passive diffusion only, and a host cellular response could further deplete oxygen within the encapsulation device [7]. As a multitude of studies have reported on compromised insulin secretory response of islets or transformed β cell lines under *in vitro* low oxygen conditions [8, 121, 132, 158] and on early post-implantation graft failure as a result of hypoxic stress [7, 68, 160] the ability to monitor construct oxygenation is evidently important.

While noninvasive evaluation of oxygen supply at different implantation sites has been performed using cell-free PFC constructs [109, 184], our work involves the investigation of oxygen levels within functional, cell-containing pancreatic implants. In this study, we demonstrated that *in vivo* real-time oxygen measurements within a tissue engineered pancreatic construct, implanted in a diabetic mouse model, can be obtained noninvasively through ^{19}F NMR. Furthermore, the design of the dual PFC method enabled simultaneous tracking of DO within the construct and at the implantation milieu. Measurements confirmed the peritoneal cavity of normal mice to be hypoxic, with DO values comparable to those obtained previously (Part I) and reported in literature [9, 184] Equivalent peritoneal DO values were also obtained in diabetic mice within two days post-implantation.

In experimental mice implanted with encapsulated βTC-tet cells, DO measurements in the cell-containing beads appeared to correlate with the relative change

in the number of viable cells examined post-explantation, as observed in the decrease in DO with cell growth over time. This reduced DO at later time points can be attributed to a higher oxygen consumption by βTC-tet cells, as there was no host cell attachment to any of the beads. Notably, the implantation of viable encapsulated cells resulted in a significant reduction of the peritoneal DO relative to mice that did not receive viable cell implants. However, even though there was no inflammatory reaction to the beads, a cellular immune response could still be elicited due to antigens secreted by the βTC-tet cells. Shed antigens can combine with antibodies to form complexes which bind to the receptors on peritoneal macrophages [63, 67]. If the antigen load is sufficiently high, the recruitment of host peritoneal cells could be significant, possibly contributing to the observed reduction in peritoneal DO.

To assess this possibility, an antigenic load from a similar encapsulation system was introduced by implanting beads containing dead βTC-tet cells in control 2N and 2D mice; dead cells would eventually lyse and hence release antigens. Inevitably, control 2D mice which received such nonfunctional cell implants remained hyperglycemic and were euthanized two days post-implantation. In control 2N, the DO within dead cell-containing beads and the peritoneal DO did not decrease over time, but remained comparable to the peritoneal DO of control 1N mice at all measured time points. Therefore, these results indicate that the observed reduction in construct and peritoneal DO in experimental mice was caused by the metabolic needs imposed by the viable implant. Although unlikely, the possibility of a higher recruitment of host cells by the viable βTC-tet cells relative the dead cells cannot be excluded. Nevertheless, regardless of its precise cause, the lowered DO has significant implications with respect to implant

survival and function. This is especially critical in situations in which a higher number of implanted cells may be needed, such as with xenografts or with larger animal models.[64]

Contrary to our *in vitro* observations [185], *in vivo* measurements showed the DO within beads containing metabolically active cells to be equivalent to the surrounding peritoneal DO at all measured time points. This might be due to the lower magnet strength (7 T versus 11.7 T) and smaller sample volume used for the *in vivo* studies

The analysis of construct DO in relation to implant function is important, as the presence of viable islets or transformed β cells does not ascertain insulin secretory capacity [71, 121, 186]. In this study, the encapsulated βTC-tet cells survived well in the peritoneal cavity and the number of implanted cells was sufficient to restore normoglycemia in diabetic mice. Despite the reduced DO in the cell-containing beads in experimental animals, sufficient insulin secretory capacity was apparently maintained, as normoglycemia was maintained in these mice. This can be attributed to the high tolerance of transformed β cell lines to hypoxia; for instance, Papas et al. reported insulin secretion of βTC3 being compromised only at an oxygen levels below 0.009 mM [71]. The observed implant therapeutic function was compatible with the overall reduction in DO within constructs containing metabolically active βTC-tet cells.

^{19}F NMR is a useful modality that can be utilized to obtain *in vivo* quantitative DO measurements within implants without relying on indirect measurement methods. Correlations established between construct DO and the observed end physiologic effects may provide a better insight into the *in vivo* factors that affect implant function and assist in the development of a long-term functional tissue engineered pancreatic construct for diabetes treatment.

5.0 Conclusions

Using ^{19}F NMR, the dual PFC method of monitoring allows for real-time, noninvasive *in vivo* tracking of DO within a tissue engineered pancreatic construct and at the implantation milieu. Measurements showed that the peritoneal oxygen environment is variable and hypoxic in normal and diabetic mice. In APA beads, construct DO was reduced over time and correlated with cell growth and host cell-attachment examined post-explantation. Barium alginate beads did not elicit inflammatory responses within the experimental time period; the obtained construct DO measurements can be used for the detection of the relative changes in the number of viable cells within the construct. In all studies, the implantation of metabolically active βTC-tet cells significantly reduced the surrounding peritoneal DO. The overall reduction in construct DO due to the metabolic activity of βTC-tet cells was compatible with implant function as observed in the reversal of hyperglycemia in diabetic mice.

CHAPTER 6

CONCLUSIONS AND FUTURE DIRECTIONS

6.1 Conclusions

A major issue in tissue engineering a pancreatic construct is ensuring sufficient oxygenation of the cells within the construct to maintain cell viability and function. As oxygen is always the limiting nutrient, the rate or extent of oxygen consumption is a good indicator of the number of metabolically active cells. Using alginate-encapsulated βTC-tet cells as our model system, we explored the use of PFCs to (1) improve cell viability and function by increasing construct oxygenation and (2) develop a method of monitoring oxygen levels within the construct and its surroundings through ^{19}F NMR.

In CHAPTER 3 of this thesis, the effects of PFTBA on βTC-tet cells encapsulated within calcium alginate beads were investigated through experimental studies and mathematical simulations. The addition of 10 vol% PFTBA emulsion into the construct did not significantly increase cell growth and metabolic activity, or the induced insulin secretion from the cells under both normoxic and short- and long-term hypoxic conditions. Mathematical simulations showed that although the presence of PFC improved the DO effective diffusivity and the overall construct oxygenation, there was only a slight, likely experimentally undetectable, increase in the cell density supported by the presence of PFC. Furthermore, the capacity of PFC to provide oxygen to the aqueous phase of the construct when exposed to hypoxic conditions was also minimal. Therefore, the incorporation of PFC appeared to have limited beneficial effects on the encapsulated cells.

The incorporation of PFC also enabled construct DO measurements through T_1 relaxation acquisition of the fluorine resonances. We established a dual PFC method that utilizes ^{19}F NMR spectroscopy, with PFCs as oxygen concentration markers, to noninvasively monitor DO within a tissue implant relative to that in the surrounding environment. The dual PFC method consisted of the incorporation of each of the PFCE and PFTBA emulsion, either with cells encapsulated in alginate beads or in cell-free alginate beads. The latter group of beads was used to monitor the DO in the culture medium or at the implantation milieu. PFCE and PFTBA have chemical shifts that are 9 ppm apart from each other, which enabled simultaneous T_1 acquisitions for DO determination within the beads. As reported in CHAPTER 4 of this thesis, *in vitro* studies using an NMR-compatible bioreactor demonstrated the feasibility of this method to simultaneously obtain DO measurements within alginate beads containing βTC-tet cells and in the culture medium. Under perfusion conditions, the steady state DO within the cell-containing beads was only minimally different from the surrounding medium except at a high encapsulation density of 7×10^7 cells/ml. This is indicative of the convective transport of oxygen due to the surrounding flow field. Under static conditions, however, significantly lower DO levels were measured within the cell-containing beads when compared to the surrounding medium; this demonstrates the capability of the method to track the oxygenation state of constructs containing metabolically active cells. Apart from proof-of-concept, the *in vitro* studies assisted in the optimization of the experimental parameters of the method, which was subsequently used for *in vivo* studies.

In CHAPTER 5 of this thesis, we reported on the monitoring of DO levels within the dual PFC bead population implanted in the peritoneal cavity of both normal and streptozotocin-induced diabetic mice. Two types of implants were examined; calcium alginate-poly-L-lysine-alginate (APA) beads and barium alginate beads, both containing βTC-tet cells. Using ^{19}F NMR, the dual PFC method allowed for real-time, noninvasive *in vivo* tracking of DO within the cell-containing beads and the peritoneal surroundings for 16 days. In both normal and diabetic mice, measurements from the cell-free beads showed that the peritoneal oxygen environment is variable and hypoxic, and is significantly lower in the presence of viable βTC-tet cells. DO within the cell-containing APA beads decreased with the extent of cell growth and host cell attachment examined post-explantation. When host cell attachment was absent, as seen with barium alginate beads, the obtained DO measurements correlated with the relative changes in the number of viable cells within a construct. The reduction of construct DO due to the metabolic activity of the βTC-tet cells was also compatible with the implant therapeutic function, as observed in the maintenance of normoglycemia in mice.

The established correlations between *in vivo* DO measurements and the observed end physiologic effects demonstrated the reliability and applicability of the developed ^{19}F NMR method to noninvasively monitor implant function. Using this method, the effects of the βTC-tet cell implant on host animal physiology were observed. Of particular importance is the significantly reduced peritoneal DO in the presence of a viable implant. This indicates a possibility of hypoxic stress under implantation conditions such as when using cells with a high oxygen demand or when a high number of implanted cells is needed. Ultimately, this method can be used to provide a better insight into the *in vivo*

factors that affect implant function and assist in the development of an optimal, long-term functional tissue engineered pancreatic construct.

6.2 Future Directions

PFC Effect on Encapsulated Cell Systems

The work in this thesis demonstrated the limited benefits of PFC incorporation in an encapsulated cell system. As discussed in CHAPTER 3, there are instances at which changes to the construct could potentially improve the effects of PFC on cell viability and function. One scenario is when PFCs are incorporated at a higher volume concentration. However, in our experience, it is not feasible to fabricate stable beads at a PFC concentration over 10 vol%. Furthermore, the reduction of aqueous volume available to accommodate the cells is nonideal *in vivo* as larger implantation volumes will be required. Since the observed results are specific to βTC-tet cells, another instance at which PFCs could possibly have a significant effect is when constructs contain cell types with a high oxygen consumption rate. Nevertheless, our modeling studies have shown that even with a 6-fold increase in the consumption rate, the steady-state increase in cell density is only approximately 10% higher. As we have fully addressed through experimental and modeling studies the limited usefulness of PFC as an oxygen carrier or reservoir, and discussed the limitations of constructing potentially beneficial PFC-alginate-cell constructs, no future work can be suggested to improving PFC effects as it relates to encapsulated cell systems.

The Dual PFC Method of Monitoring

The primary goals of establishing a noninvasive method of construct monitoring are to (1) understand the *in vivo* factors that affect construct function and elucidate the mechanisms of implant failure and (2) detect implant failure ahead of end physiological effects. The work in this thesis proves the capability of a developed ^{19}F NMR method to noninvasively measure DO within a tissue engineered pancreatic construct. Here, we have taken an important step to thoroughly demonstrate that with this method, important correlations can be established between DO measurements and the construct's (1) physiological state and (2) functionality, as reflected through insulin secretion by metabolically active βTC-tet cells.

In order to arrive at the long-term goals of this method, its applicability after a longer period *in vivo* needs to be examined. While researchers have observed intact PFC-containing barium alginate beads for up to 18 months post-implantation [109], this has yet to be tested in our system. Two issues that could potentially cause a decrease in NMR signal over time are the gradual loss of PFC emulsion stability and the breakage of the beads; both will cause the emulsion to be released from the beads and be eliminated by the macrophage system. One could evaluate these potential issues through a few methods such as determining the changes in *in vivo* NMR signal intensities, characterizing the bead retrieval rate and the degree of bead breakage, and studying the progression of emulsion droplet size and size distribution over time. Based on the observations made in this study, slight modifications to the developed construct may be necessary. The mechanical stability of the beads can be increased by increasing the concentration of alginate used, reducing the emulsion concentration, or changing the

formulation of the cross-linking solution to form inhomogeneous beads. Studies have shown that inhomogeneous alginate beads have higher long-term stability, as measured by a significantly lower release of encapsulated blue dextran when compared to homogeneous beads [48]. Also, the emulsion stability can possibly be increased by changing the type or concentration of surfactant used.

In this work, barium alginate beads containing βTC-tet cells remained functional throughout the 16 day experimental period. The long-term functional survival of this tissue implant has not been studied, although Black et al. have reported on the normalization of blood glucose levels in NOD mice implanted with PLL-coated calcium alginate beads containing βTC-tet cells for up to 8 weeks post-implantation [46]. Once the long-term stability of the PFC constructs is characterized, the dual PFC method can be used to track construct DO for a longer period of time. Both construct DO and the glycemic state of initially diabetic mice should be monitored continuously until implant failure. Using the established method, observations of DO measurements occurring around the time of implant failure, as measured by the return to hyperglycemia, might provide valuable information on the *in vivo* physiological state of the construct and assist in discerning between the two widely conjectured reasons for construct failure – immune rejection and hypoxia. Each mechanism leading to compromised construct function is expected to differently affect the measured DO. An increase in construct DO can be associated to a direct immunological attack causing cell death and therefore a reduction in the oxygen consumption. On the other hand, a decrease in DO will most likely indicate a decrease in oxygen available to the cells, either due to the hypoxic implantation site or host cell attachment to the constructs, both of which could lead to a suppression of

cell functionality or even cell death. While the *in vivo* environment is complex and the correlations might not be as straightforward, these initial speculations are based on the *in vitro* observations of construct DO profiles acquired through ^{19}F NMR by Gross [187]. In his study, the *in vitro* culturing conditions were designed to mimic an *in vivo* inflammatory response and immune rejection by changing the medium dissolved oxygen and inducing toxicity through the addition of puromycin, respectively. Nevertheless, the validity of these speculations should be verified by checking the consistencies of the measured DO with the observations of the explants immediately after implant failure. While simultaneously studying the mechanisms of construct failure, the ability of the dual PFC method to detect this failure ahead of end physiological effects can also be tested. The implanted cells are expected to maintain normoglycemia in the animals even with an increase in cell death, as the remaining fraction of viable cells is able to compensate for this loss by secreting more insulin. Therefore, changes in DO are expected to occur before blood glucose regulation is lost.

A drawback of the dual PFC method is its incapability to distinguish between oxygen consumption by the implanted βTC-tet cells and the host immune peritoneal cells. In our short-term study, there was no host cell attachment around the barium alginate beads. However, the observed reduction in construct and peritoneal DO when compared to control groups could also be due to the oxygen consumption by the host peritoneal cells, whose number might increase after implantation over time. Even though a peritoneal fluid cell count can be carried out to determine this increase, the oxygen consumption rate/capacity of these peritoneal cells in comparison to βTC-tet cells would still be uncertain. A more robust way of clarifying this issue is to implant the constructs

into immunocompromised mice, such as scid or nude mice, to minimize the numbers of immune cells present around the constructs. Through the use of these mice, the consumption of oxygen by the implanted cells and host cells could be better distinguished.

Apart from alginate-encapsulated βTC-tet cells, a variety of TEPCs using other cell types, construct materials, or configurations are being studied and developed. It would be beneficial to examine the use of the dual PFC method in these different systems. Since the PFC emulsion is not chemically bound to the matrix, this method can be easily adapted in other materials as long as construct stability is maintained. An important next step is to monitor DO in constructs containing allogeneic or xenogenic islets, which are currently the most clinically relevant systems. This is crucial as researchers are constantly trying to understand reasons behind the failure of encapsulated islet grafts so as to find ways to improve upon encapsulation techniques and methods that could prolong graft survival. Making a transition to tracking DO within islet constructs would require that the preliminary characterization of the system be re-tested; this includes the effects of PFC on the encapsulated islets, the stability of the islet-containing beads when PFC is incorporated, and the sufficiency of the NMR signal if there is a reduction in implantation volumes.

It is also worthwhile to investigate the survival and function of these TEPCs at different implantation sites and different animal models using the dual PFC method. This will enable the assessment of oxygen levels within the implant and its surroundings to determine whether a location is suitable for such implantation as it relates to construct oxygenation. Researchers have implanted pancreatic constructs into sites such as below

the kidney capsule and in the muscle, and in other animal models, particularly rats and, in certain cases, non-human primates [188, 189]. It will be beneficial to examine, in the case of a larger implant or animal model, if there will be a significant reduction in the DO at the implantation site. In these instances, T_1 measurements to determine DO are possible provided that the surface coil used is large enough to cover the area of where the constructs are located.

APPENDIX A

PERFLUOROCARBON EMULSION CHARACTERIZATION

A.1 Distribution of PFC Emulsion within the Beads

The PFC emulsion has to be homogeneously distributed throughout the beads in order to accurately measure the average DO within the beads. To determine the distribution of PFC, lecithin, the surfactant used to make the emulsion, was tagged with a fluorescently labeled fatty acid phospholipid membrane. The lecithin tag used was 1-Caproyl-2-[6-[(7-nitro-2-1,3-benzoxadiazol-4-yl)amino]caproyl]-sn-glycerol-3-phosphorac-(1-glycerol) (466 excitation/536 emission). 1.0 mg of this tagged lecithin was added to 95 mg of the untagged lecithin and PFCE emulsion was prepared (as described in Section 5.4). The alginate beads were then imaged using a fluorescent microscope, as shown in Figure A.1.1.

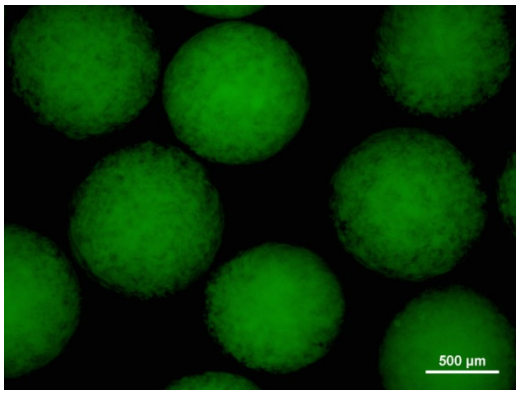

Figure A.1 Distribution of PFCE emulsion throughout calcium alginate beads

The green fluorescence is seen throughout the beads and is not concentrated at any specific region, indicating that the PFC emulsion is homogeneously distributed throughout the beads.

A.2 PFC Emulsion Stability

The formulation of stable PFC emulsion is important for them to be used as oxygen carriers or markers for monitoring, especially for long-term analyses. Currently, two proposed mechanisms responsible for their aging are coalescence and molecular diffusion. As both mechanisms leads to the formation of larger droplets of the emulsion, one of the ways to study emulsion stability is simply through droplet size measurements. Figure A1.2 (a) and (b) show PFC emulsion droplets before implantation and after 16 days *in vivo* observed through light microscopy. Freshly made emulsion size is approximately 2 µm. The emulsion remained stable throughout the 16 days, as seen in the maintenance of emulsion droplet size.

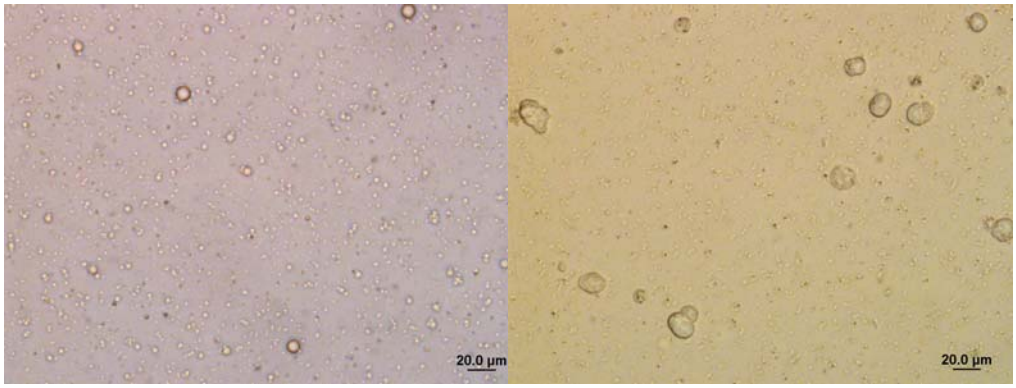

Figure A.2 PFC emulsion droplets (a) before implantation and (b) after 16 days *in vivo*

APPENDIX B

CHAPTER 3 ADDITIONAL FIGURES

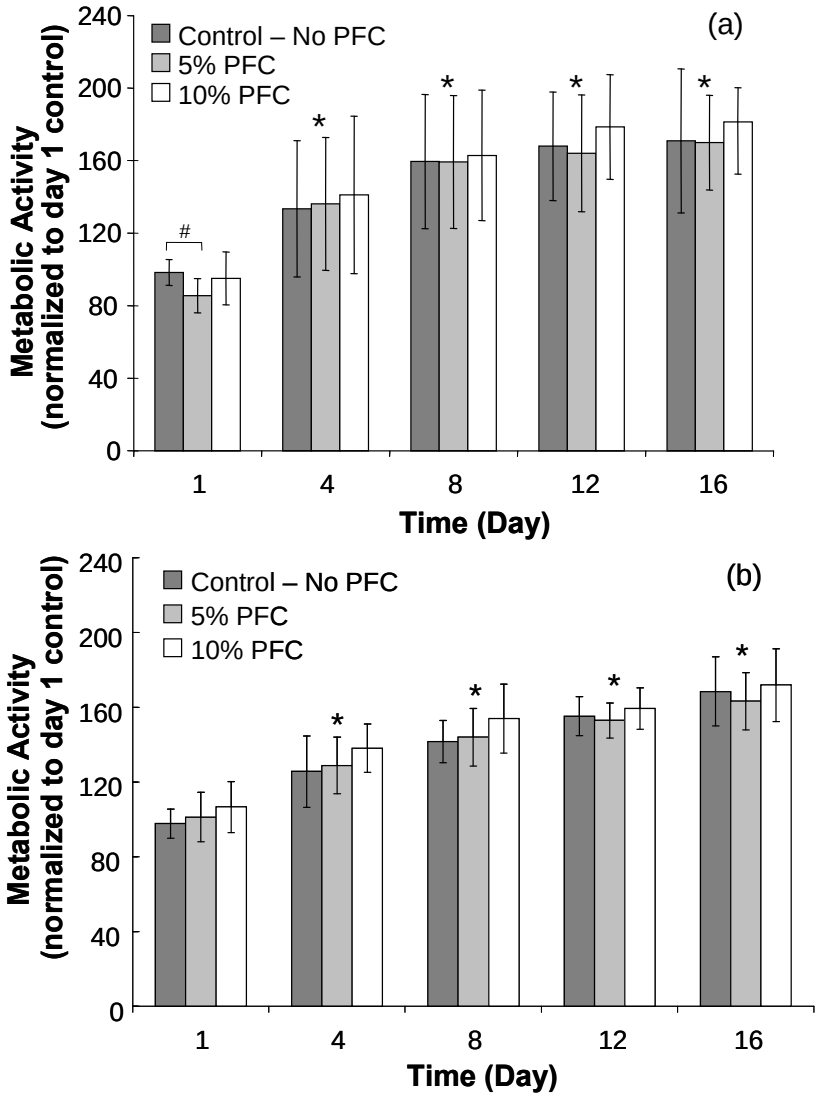

Figure B.1 Metabolic activity of encapsulated βTC-tet cells under normoxic conditions. The number of metabolically active cells was measured as a function of time by alamarBlue™ and normalized to Day 1. Measurements were performed with calcium alginate beads of (a) 500 μm and (b) 1000 μm average diameter with no PFTBA, 5 vol% PFTBA, and 10 vol% PFTBA (n = 4 each). The initial density of the encapsulated cells was 3.5×10^7 cells/ml. * $p<0.05$ when compared to Day 1.

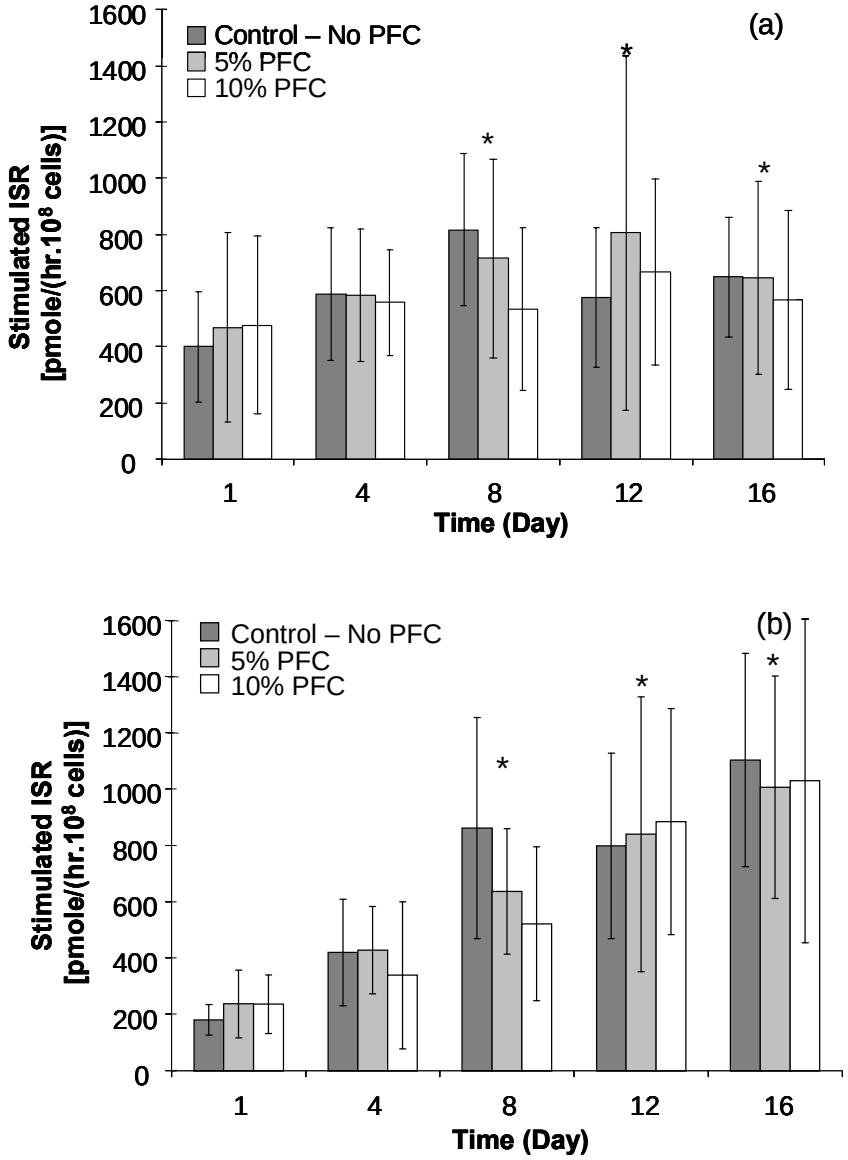

Figure B.2 Stimulated insulin secretion rate (ISR) of βTC-tet cells under normoxic conditions. ISR was measured over 30 min of stimulation by 16 mM glucose, normalized to the initial number of encapsulated βTC-tet cells, and expressed on a per unit time basis. Measurements were carried out with (a) 500 μm and (b) 1000 μm average diameter calcium alginate beads with no PFTBA, 5 vol% PFTBA, and 10 vol% PFTBA (n = 4 each). Each glucose stimulation episode followed 1 hour of exposure to basal, 0 mM glucose, medium. * $p<0.05$ when compared to Day 1.

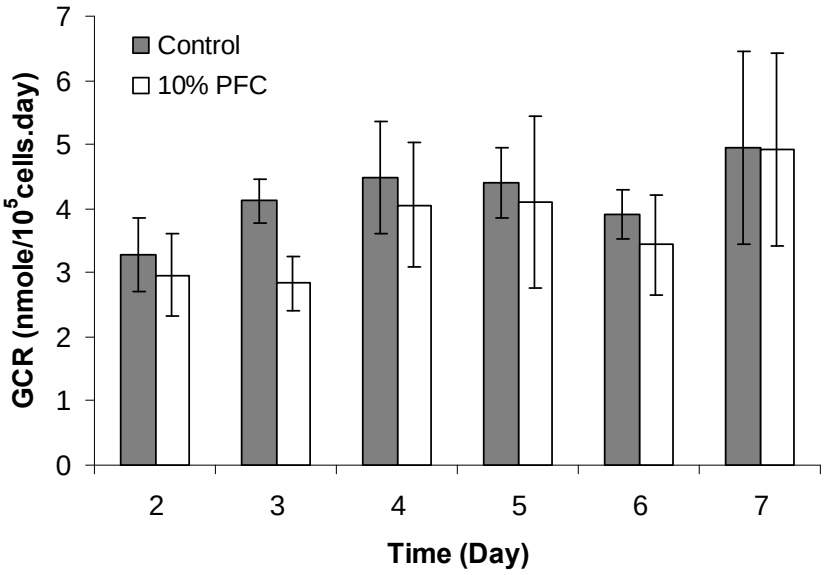

Figure B.3 Glucose consumption rate (GCR) of βTC-tet cells under normoxic conditions. Measurements were performed with 1000 μm average diameter calcium alginate beads with no PFTBA and 10 vol% PFTBA (n = 4 each).

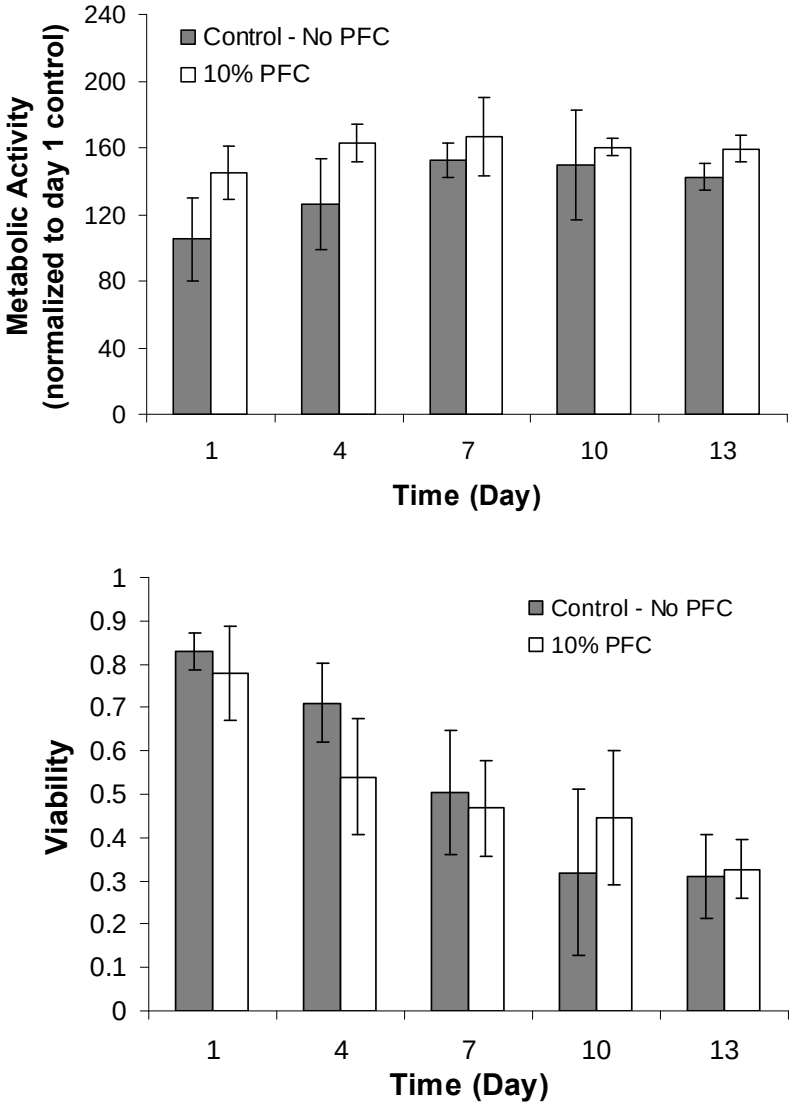

Figure B.4 (a) Metabolic activity and (b) viability of encapsulated HepG2 cells under normoxic conditions. The number of metabolically active cells was measured as a function of time by alamarBlue™ and normalized to Day 1 control group. Cell viability was measured with trypan blue exclusion assay. Measurements were performed with calcium alginate beads of 1000 μm average diameter with no PFTBA (control) and 10 vol% PFTBA, using lecithin as the surfactant (n = 4 each). The initial density of the encapsulated cells was 3.5×10^7 cells/ml.

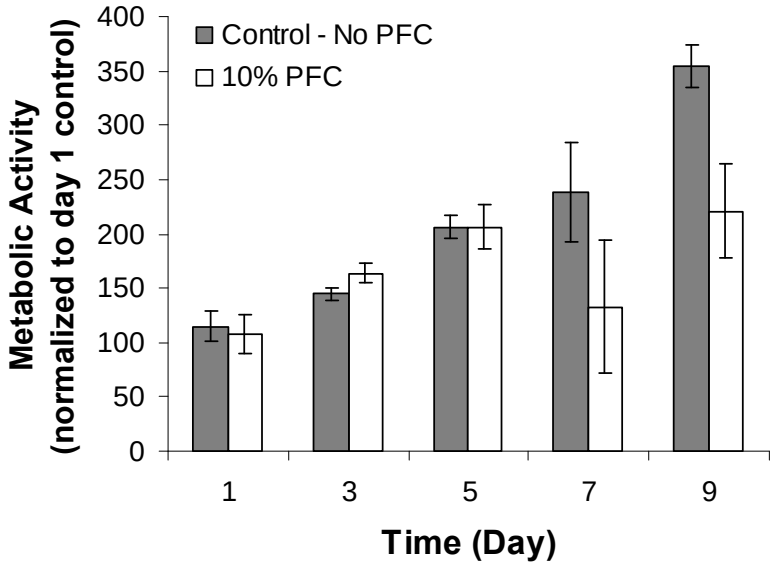

Figure B.5 (a) Metabolic activity of encapsulated HepG2 cells under normoxic conditions. The number of metabolically active cells was measured as a function of time by alamarBlue™ and normalized to Day 1 control group. Measurements were performed with calcium alginate beads of 1000 μm average diameter with no PFTBA (control) and 10 vol% PFTBA, using pluronic F-68 as the surfactant (n = 4 each). The initial density of the encapsulated cells was 2×10^6 cells/ml.

APPENDIX C

PERFUSION SYSTEM

Bench top experiments (without the NMR system) were carried out to test the capability of this system to provide a well controlled environment. This is important to ensure that the cells are being cultured under well optimized conditions during which measurements are being made.

βTC-tet cells encapsulated at a density of 7×10^7 cells/ml alginate in 1000μm calcium alginate beads were placed in the bioreactor. The DO of medium entering the bioreactor at 6.5 ml/min was kept at approximately 0.18 mM. Figure A3.1 shows the temperature profile and oxygen consumption rate (OCR) of the encapsulated cells, measured using the fiber optic sensors at the inlet and outlet of the bioreactor.

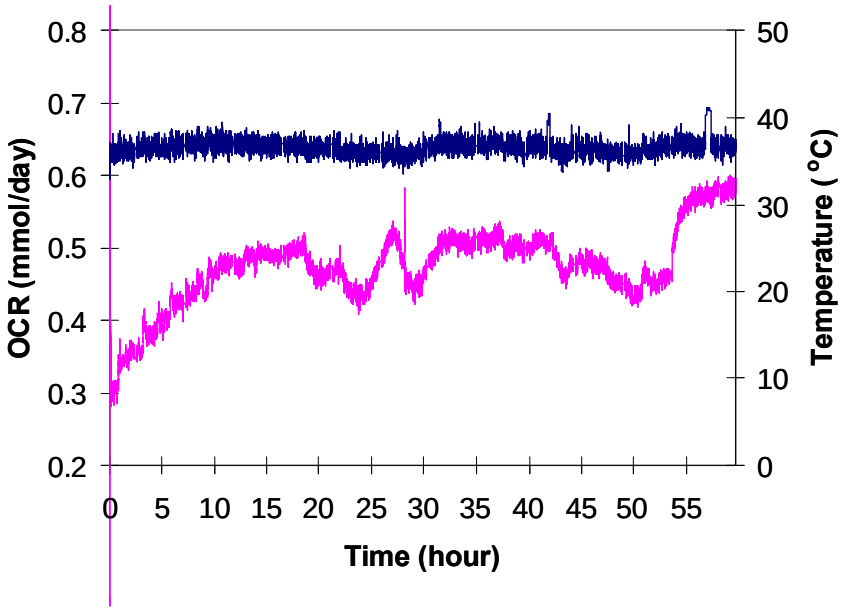

Figure C.1 Time profile of temperature (right) and oxygen consumption rate (OCR) of encapsulated βTC-tet cells (left) maintained in the perfusion system.

Temperature was maintained at 37^{o}C and the oxygen sensors were capable of tracking medium dissolved oxygen throughout the experimental period. The initial OCR of the cells was 2.0mmol/day.10^{9}cells. At the end of 60 hours, the cell population doubled, as observed in the increase in OCR. The total viable cell number, measured at the beginning and end of this run using typan blue exclusion method, was also observed to double over this time period. Cell survival and proliferation indicates that the perfusion system is able to provide a well controlled culturing environment, where cell metabolic activity will not be compromised during T_1 relaxation acquisitions.

APPENDIX D

CHAPTER 4 ADDITIONAL FIGURES

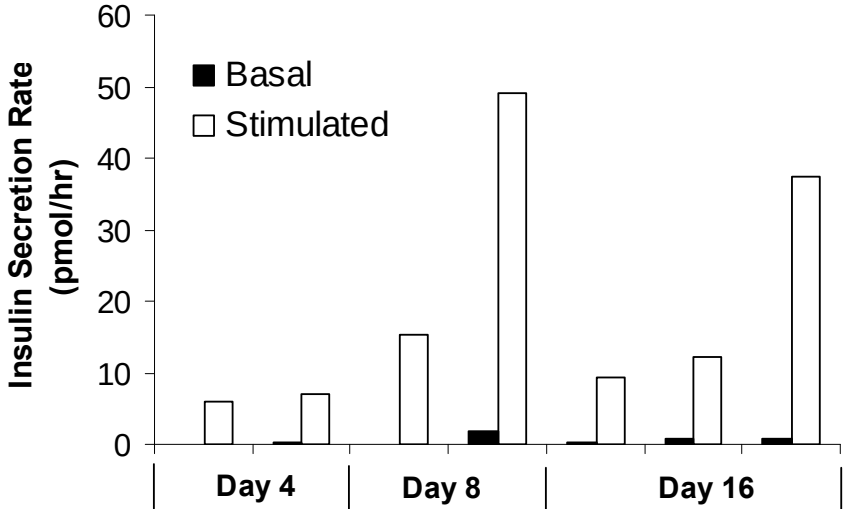

Figure D.1 Insulin secretion rate of βTC-tet cells encapsulated in APA beads, measured over 1 hour in basal medium (0 mM glucose, unsupplemented) and 30 minutes in stimulated medium (16 mM glucose, supplemented). Explants consist of a mixture of cell-free and cell-containing beads; therefore data are reported from each experimental mouse. No insulin was detected in control mice.

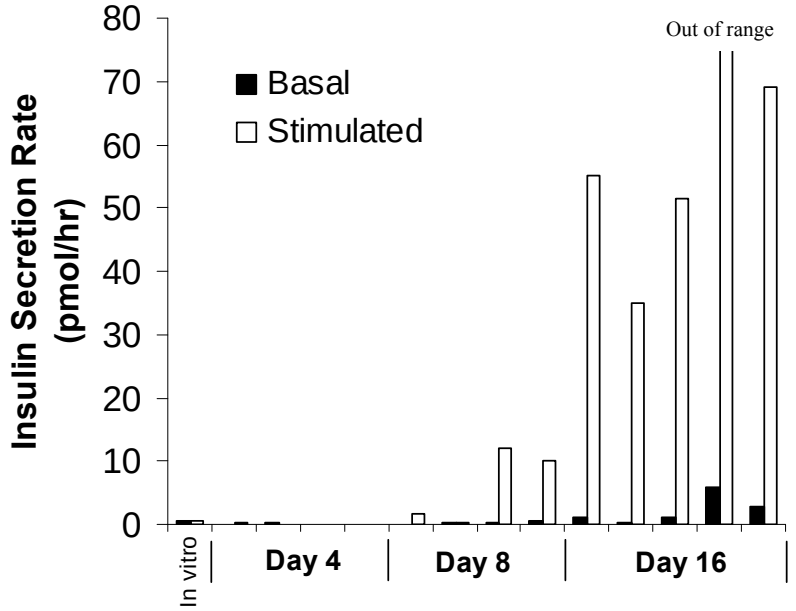

Figure D.2 Insulin secretion rate of βTC-tet cells encapsulated in barium beads, measured over 1 hour in basal medium (0 mM glucose, unsupplemented) and 30 minutes in stimulated medium (16 mM glucose, supplemented). Explants consist of a mixture of cell-free and cell-containing beads; therefore data are reported from each experimental mouse. No insulin was detected in control mice.

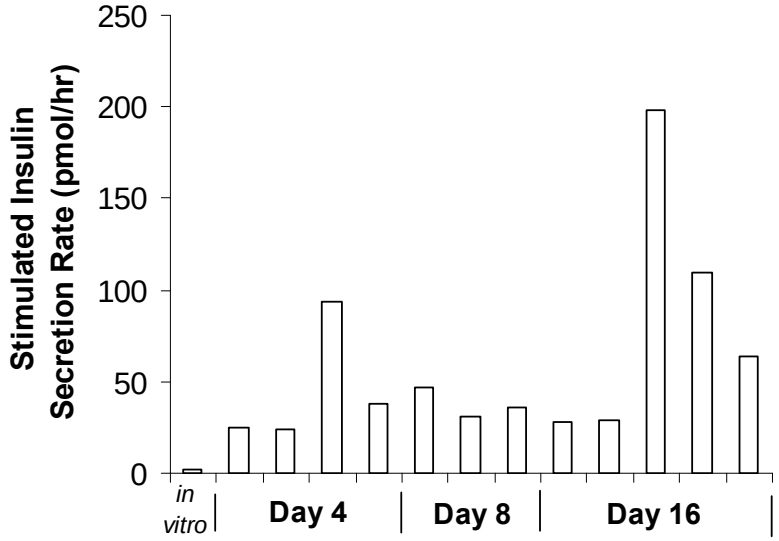

Figure D.3 Stimulated insulin secretion rate of βTC-tet cells encapsulated in barium beads, measured over 30 minutes in stimulated medium (16 mM glucose, supplemented) after exposure to 1 hour basal medium (0 mM glucose, unsupplemented). Explants consist of a mixture of cell-free and cell-containing beads; therefore data are reported from each experimental mouse.

REFERENCES

1. National Center for Chronic Disease Prevention and Health Promotion and D.o.D. Translation. *2007 National Diabetes Fact Sheet*. 2007 [cited 3rd Dec 2010].

2. Mehta, S.N. and J.I. Wolfsdorf, *Contemporary management of patients with type 1 diabetes.* Endocrinol Metab Clin North Am, 2010. **39**(3): p. 573-93.

3. Silva, A.I., de Matos, A.N, Brons, I.G., Mateus, M., *An overview on the development of a bio-artificial pancreas as a treatment of insulin-dependent diabetes mellitus.* Medicinal Research Reviews, 2005. **26**(2): p. 181-222.

4. Mullen, Y., M. Maruyama, and C.V. Smith, *Current progress and perspectives in immunoisolated islet transplantation.* J Hepatobiliary Pancreat Surg, 2000. **7**(4): p. 347-57.

5. Efrat, S., *Genetically engineered pancreatic beta-cell lines for cell therapy of diabetes.* Ann N Y Acad Sci, 1999. **875**: p. 286-93.

6. Kizilel, S., M. Garfinkel, and E. Opara, *The bioartificial pancreas: progress and challenges.* Diabetes Technol Ther, 2005. **7**(6): p. 968-85.

7. de Groot, M., T.A. Schuurs, and R. van Schilfgaarde, *Causes of limited survival of microencapsulated pancreatic islet grafts.* J Surg Res, 2004. **121**(1): p. 141-50.

8. Papas, K.K., et al., *Development of a bioartificial pancreas: II. Effects of oxygen on long-term entrapped betaTC3 cell cultures.* Biotechnol Bioeng, 1999. **66**(4): p. 231-7.

9. Gross, J.D., et al., *Monitoring of dissolved oxygen and cellular bioenergetics within a pancreatic substitute.* Biotechnol Bioeng, 2007. **98**(1): p. 261-70.

10. Lowe, K.C., M.R. Davey, and J.B. Power, *Perfluorochemicals: their applications and benefits to cell culture.* Trends in Biotechnology, 1998. **16**(6): p. 272-277.

11. Castro, C.I. and J.C. Briceno, *Perfluorocarbon-based oxygen carriers: review of products and trials.* Artif Organs, 2010. **34**(8): p. 622-34.

12. Matsumoto, S. and Y. Kuroda, *Perfluorocarbon for organ preservation before transplantation.* Transplantation, 2002. **74**(12): p. 1804-9.

13. Mason, R.P., *Non-invasive physiology: 19F NMR of perfluorocarbons.* Artif Cells Blood Substit Immobil Biotechnol, 1994. **22**(4): p. 1141-53.

14. Diaz-Lopez, R., N. Tsapis, and E. Fattal, *Liquid Perfluorocarbons as Contrast Agents for Ultrasonography and F-19-MRI.* Pharmaceutical Research, 2010. **27**(1): p. 1-16.

15. Kinasiewicz, A., et al., *Impact of oxygenation of bioartificial liver using perfluorocarbon emulsion perftoran on metabolism of human hepatoma C3A cells.* Artif Cells Blood Substit Immobil Biotechnol, 2008. **36**(6): p. 525-34.

16. Tan, Q., et al., *The effect of perfluorocarbon-based artificial oxygen carriers on tissue-engineered trachea.* Tissue Eng Part A, 2009. **15**(9): p. 2471-80.

17. Khattak, S.F., et al., *Enhancing oxygen tension and cellular function in alginate cell encapsulation devices through the use of perfluorocarbons.* Biotechnol Bioeng, 2007. **96**(1): p. 156-66.

18. Kin, T., et al., *Islet isolation and transplantation outcomes of pancreas preserved with University of Wisconsin solution versus two-layer method using preoxygenated perfluorocarbon.* Transplantation, 2006. **82**(10): p. 1286-90.

19. Caballero-Corbalan, J., et al., *No beneficial effect of two-layer storage compared with UW-storage on human islet isolation and transplantation.* Transplantation, 2007. **84**(7): p. 864-869.

20. Bergert, H., et al., *Effect of oxygenated perfluorocarbons on isolated rat pancreatic islets in culture.* Cell Transplant, 2005. **14**(7): p. 441-8.

21. Sambanis, A., *Bioartificial Pancreas*, in *Principles of Tissue Engineering, 3rd edition*, L. Lanza, Vacanti, Editor. 2007, Elsevier, Boston.

22. Cohen, N.D. and J.E. Shaw, *Diabetes: advances in treatment.* Intern Med J, 2007. **37**(6): p. 383-8.

23. Goh, S.Y. and M.E. Cooper, *The role of advanced glycation end products in progression and complications of diabetes.* Journal of Clinical Endocrinology & Metabolism, 2008. **93**(4): p. 1143-1152.

24. Crowley, L.V., *An introduction to human disease*. 8th edition ed. 2010, Jones and Barlett, Massachussets

25. Alsaleh, F.M., et al., *Insulin pumps: from inception to the present and toward the future.* J Clin Pharm Ther. **35**(2): p. 127-38.

26. George, C.M., *Future trends in diabetes management.* Nephrol Nurs J, 2009. **36**(5): p. 477-83.

27. Piper, M., J. Seidenfeld, and N. Aronson, *Islet transplantation in patients with type 1 diabetes mellitus.* Evid Rep Technol Assess (Summ), 2004(98): p. 1-6.

28. Mineo, D., et al., *Point: steady progress and current challenges in clinical islet transplantation.* Diabetes Care, 2009. **32**(8): p. 1563-9.

29. Gremizzi, C., et al., *Impact of pancreas transplantation on type 1 diabetes-related complications.* Curr Opin Organ Transplant, 2010. **15**(1): p. 119-23.

30. Kelly, W.D., et al., *Allotransplantation of the pancreas and duodenum along with the kidney in diabetic nephropathy.* Surgery, 1967. **61**(6): p. 827-37.

31. Lam, V.W., et al., *Evolution of pancreas transplant surgery.* ANZ J Surg, 2010. **80**(6): p. 411-8.

32. Allen, R.D., et al., *Pancreas and islet transplantation: an unfinished journey.* Transplant Proc, 2001. **33**(7-8): p. 3485-8.

33. Shapiro, A.M., et al., *Islet transplantation in seven patients with type 1 diabetes mellitus using a glucocorticoid-free immunosuppressive regimen.* N Engl J Med, 2000. **343**(4): p. 230-8.

34. Azzi, J., et al., *Immunological aspects of pancreatic islet cell transplantation.* Expert Rev Clin Immunol, 2010. **6**(1): p. 111-24.

35. Fiorina, P., et al., *The clinical impact of islet transplantation.* Am J Transplant, 2008. **8**(10): p. 1990-7.

36. Tharavanij, T., et al., *Improved long-term health-related quality of life after islet transplantation.* Transplantation, 2008. **86**(9): p. 1161-7.

37. Leitao, C.B., et al., *Restoration of hypoglycemia awareness after islet transplantation.* Diabetes Care, 2008. **31**(11): p. 2113-5.

38. Bertuzzi, F., S. Marzorati, and A. Secchi, *Islet cell transplantation.* Curr Mol Med, 2006. **6**(4): p. 369-74.

39. Harlan, D.M., et al., *Current advances and travails in islet transplantation.* Diabetes, 2009. **58**(10): p. 2175-84.

40. Efrat, S., *Cell-based therapy for insulin-dependent diabetes mellitus.* Eur J Endocrinol, 1998. **138**(2): p. 129-33.

41. Efrat, S., *Development of engineered pancreatic beta-cell lines for cell therapy of diabetes.* Adv Drug Deliv Rev, 1998. **33**(1-2): p. 45-52.

42. McClenaghan, N.H. and P.R. Flatt, *Engineering cultured insulin-secreting pancreatic B-cell lines.* J Mol Med, 1999. **77**(1): p. 235-43.

43. Fleischer, N., et al., *Functional analysis of a conditionally transformed pancreatic beta-cell line.* Diabetes, 1998. **47**(9): p. 1419-25.

44. Efrat, S., et al., *Conditional transformation of a pancreatic beta-cell line derived from transgenic mice expressing a tetracycline-regulated oncogene.* Proc Natl Acad Sci U S A, 1995. **92**(8): p. 3576-80.

45. Efrat, S., *Regulation of insulin secretion: insights from engineered beta-cell lines.* Ann N Y Acad Sci, 2004. **1014**: p. 88-96.

46. Black, S.P., et al., *Immune responses to an encapsulated allogeneic islet beta-cell line in diabetic NOD mice.* Biochem Biophys Res Commun, 2006. **340**(1): p. 236-43.

47. Sambanis, A., Tang, S.C., Cheng, S.Y., Stabler, S.L., Long, Jr, R.C., Constantinidis, I, *Core technologies in tissue engineering and their application to the bioartificial pancreas*, in *Tissue Engineering for Therapeutic Use 6*, Y. Ikada, Umakoshi, Y., Hotta, T., Editor. 2002, Elsevier Science B.V., The Netherlands. p. 5 - 18.

48. Thu, B., et al., *Alginate polycation microcapsules. II. Some functional properties.* Biomaterials, 1996. **17**(11): p. 1069-79.

49. Smidsrod, O. and G. Skjakbraek, *Alginate as Immobilization Matrix for Cells.* Trends in Biotechnology, 1990. **8**(3): p. 71-78.

50. Simpson, N.E., et al., *NMR properties of alginate microbeads.* Biomaterials, 2003. **24**(27): p. 4941-8.

51. Lim, F. and A.M. Sun, *Microencapsulated islets as bioartificial endocrine pancreas.* Science, 1980. **210**(4472): p. 908-10.

52. Sambanis, A., *Engineering challenges in the development of an encapsulated cell system for treatment of type 1 diabetes.* Diabetes Technol Ther, 2000. **2**(1): p. 81-9.

53. Lum, Z.P., et al., *Xenografts of Rat Islets into Diabetic Mice - an Evaluation of New Smaller Capsules.* Transplantation, 1992. **53**(6): p. 1180-1183.

54. Krestow, M., et al., *Xenotransplantation of microencapsulated fetal rat islets.* Transplantation, 1991. **51**(3): p. 651-5.

55. Omer, A., et al., *Survival and maturation of microencapsulated porcine neonatal pancreatic cell clusters transplanted into immunocompetent diabetic mice.* Diabetes, 2003. **52**(1): p. 69-75.

56. Sun, Y., et al., *Normalization of diabetes in spontaneously diabetic cynomologus monkeys by xenografts of microencapsulated porcine islets without immunosuppression.* J Clin Invest, 1996. **98**(6): p. 1417-22.

57. Soon-Shiong, P., et al., *Successful reversal of spontaneous diabetes in dogs by intraperitoneal microencapsulated islets.* Transplantation, 1992. **54**(5): p. 769-74.

58. Fritschy, W.M., et al., *Glucose tolerance and plasma insulin response to intravenous glucose infusion and test meal in rats with microencapsulated islet allografts.* Diabetologia, 1991. **34**(8): p. 542-7.

59. Orive, G., Hernandez, R.M., Gascon, A.R., Pedraz, J.L, *Challenges in cell encapsulation*, in *Applications of cell immobilisation technology*, R.W. Viktor Nedovic, Editor. 2005, Springer, The Netherlands. p. 185-96.

60. Zekorn, T., Bretzel, R, *Immunoprotection of islets of langerhans by microencapsulation in barium alginate beads*, in *Cell encapsulation technology and therapeutics*, W.M. Kuhtreiber, Lanza, R.P, Editor. 1999, Birkhauser, Ann Arbor.

61. de Vos, P., et al., *Alginate-based microcapsules for immunoisolation of pancreatic islets.* Biomaterials, 2006. **27**(32): p. 5603-17.

62. Duvivier-Kali, V.F., et al., *Complete protection of islets against allorejection and autoimmunity by a simple barium-alginate membrane.* Diabetes, 2001. **50**(8): p. 1698-705.

63. Cui, H., et al., *Long-term metabolic control of autoimmune diabetes in spontaneously diabetic nonobese diabetic mice by nonvascularized microencapsulated adult porcine islets.* Transplantation, 2009. **88**(2): p. 160-9.

64. Duvivier-Kali, V.F., et al., *Survival of microencapsulated adult pig islets in mice in spite of an antibody response.* Am J Transplant, 2004. **4**(12): p. 1991-2000.

65. Safley, S.A., et al., *Biocompatibility and immune acceptance of adult porcine islets transplanted intraperitoneally in diabetic NOD mice in calcium alginate poly-L-lysine microcapsules versus barium alginate microcapsules without poly-L-lysine.* J Diabetes Sci Technol, 2008. **2**(5): p. 760-7.

66. Zekorn, T.D., et al., *Biocompatibility and immunology in the encapsulation of islets of Langerhans (bioartificial pancreas).* Int J Artif Organs, 1996. **19**(4): p. 251-7.

67. Weber, C.J., et al., *Evaluation of graft-host response for various tissue sources and animal models.* Ann N Y Acad Sci, 1999. **875**: p. 233-54.

68. Emamaullee, J.A. and A.M. Shapiro, *Factors influencing the loss of beta-cell mass in islet transplantation.* Cell Transplant, 2007. **16**(1): p. 1-8.

69. Fritschy, W.M., et al., *The efficacy of intraperitoneal pancreatic islet isografts in the reversal of diabetes in rats.* Transplantation, 1991. **52**(5): p. 777-83.

70. De Vos, P., et al., *Kinetics of intraperitoneally infused insulin in rats. Functional implications for the bioartificial pancreas.* Diabetes, 1996. **45**(8): p. 1102-7.

71. Papas, K.K., et al., *Effects of short-term hypoxia on a transformed cell-based bioartificial pancreatic construct.* Cell Transplant, 2000. **9**(3): p. 415-22.

72. Riess, J.G., *Understanding the fundamentals of perfluorocarbons and perfluorocarbon emulsions relevant to in vivo oxygen delivery.* Artif Cells Blood Substit Immobil Biotechnol, 2005. **33**(1): p. 47-63.

73. Freire, M.G., et al., *Aging mechanisms of perfluorocarbon emulsions using image analysis.* J Colloid Interface Sci, 2005. **286**(1): p. 224-32.

74. Cohn, C.S. and M.M. Cushing, *Oxygen therapeutics: perfluorocarbons and blood substitute safety.* Crit Care Clin, 2009. **25**(2): p. 399-414, Table of Contents.

75. Kim, H.W. and A.G. Greenburg, *Artificial oxygen carriers as red blood cell substitutes: A selected review and current status.* Artificial Organs, 2004. **28**(9): p. 813-828.

76. Spahn, D.R. and R. Kocian, *Artificial O2 carriers: status in 2005.* Curr Pharm Des, 2005. **11**(31): p. 4099-114.

77. Habler, O.P., et al., *Hemodilution and intravenous perflubron emulsion as an alternative to blood transfusion: effects on tissue oxygenation during profound hemodilution in anesthetized dogs.* Transfusion, 1998. **38**(2): p. 145-155.

78. Keipert, P.E., et al., *Enhanced oxygen delivery by perflubron emulsion during acute hemodilution.* Artif Cells Blood Substit Immobil Biotechnol, 1994. **22**(4): p. 1161-7.

79. Habler, O., et al., *IV Perflubron emulsion versus autologous transfusion in severe normovolemic anemia: effects on left ventricular perfusion and function.* Research in Experimental Medicine, 1998. **197**(6): p. 301-318.

80. Spahn, D.R., et al., *Use of perflubron emulsion to decrease allogeneic blood transfusion in high-blood-loss non-cardiac surgery - Results of a European phase 3 study.* Anesthesiology, 2002. **97**(6): p. 1338-1349.

81. Spahn, D.R., et al., *Perflubron emulsion delays blood transfusions in orthopedic surgery.* Anesthesiology, 1999. **91**(5): p. 1195-1208.

82. Frumento, R.J., et al., *Preserved gastric tonometric variables in cardiac surgical patients administered intravenous perflubron emulsion.* Anesth Analg, 2002. **94**(4): p. 809-14, table of contents.

83. Kuroda, Y., et al., *A new, simple method for cold storage of the pancreas using perfluorochemical.* Transplantation, 1988. **46**(3): p. 457-60.

84. Matsumoto, S., *Clinical application of perfluorocarbons for organ preservation.* Artif Cells Blood Substit Immobil Biotechnol, 2005. **33**(1): p. 75-82.

85. Matsumoto, S., et al., *Effect of the two-layer (University of Wisconsin solution-perfluorochemical plus O2) method of pancreas preservation on human islet isolation, as assessed by the Edmonton Isolation Protocol.* Transplantation, 2002. **74**(10): p. 1414-9.

86. Tsujimura, T., et al., *Influence of pancreas preservation on human islet isolation outcomes: impact of the two-layer method.* Transplantation, 2004. **78**(1): p. 96-100.

87. Ricordi, C., et al., *Improved human islet isolation outcome from marginal donors following addition of oxygenated perfluorocarbon to the cold-storage solution.* Transplantation, 2003. **75**(9): p. 1524-7.

88. Lakey, J.R., et al., *Preservation of the human pancreas before islet isolation using a two-layer (UW solution-perfluorochemical) cold storage method.* Transplantation, 2002. **74**(12): p. 1809-11.

89. Atias, S., et al., *Preservation of pancreatic tissue morphology, viability and energy metabolism during extended cold storage in two-layer oxygenated University of Wisconsin/perfluorocarbon solution.* Isr Med Assoc J, 2008. **10**(4): p. 273-6.

90. Kuroda, Y., et al., *Role of adenosine in preservation by the two-layer method of ischemically damaged canine pancreas.* Transplantation, 1994. **57**(7): p. 1017-20.

91. Zekorn, T., et al., *Impact of the perfluorochemical FC43 on function of isolated islets: a preliminary report.* Horm Metab Res, 1991. **23**(6): p. 302-3.

92. Takahashi, T., et al., *Impact of the two-layer method on the quality of isolated pancreatic islets.* Hepatogastroenterology, 2006. **53**(68): p. 179-82.

93. Terai, S., et al., *Effect of oxygenated perfluorocarbon on isolated islets during transportation.* J Surg Res, 2010. **162**(2): p. 284-9.

94. Chin, K., et al., *Hydrogel-perfluorocarbon composite scaffold promotes oxygen transport to immobilized cells.* Biotechnol Prog, 2008. **24**(2): p. 358-66.

95. Laukemper-Ostendorf, S., et al., *19F-MRI of perflubron for measurement of oxygen partial pressure in porcine lungs during partial liquid ventilation.* Magn Reson Med, 2002. **47**(1): p. 82-9.

96. Eidelberg, D., et al., *F-19 Nmr Imaging of Blood Oxygenation in the Brain.* Magnetic Resonance in Medicine, 1988. **6**(3): p. 344-352.

97. Shukla, H.P., et al., *Regional myocardial oxygen tension: F-19 MRI of sequestered perfluorocarbon.* Magnetic Resonance in Medicine, 1996. **35**(6): p. 827-833.

98. Fan, X.B., et al., *Effect of carbogen on tumor oxygenation: Combined fluorine-19 and proton MRI measurements.* International Journal of Radiation Oncology Biology Physics, 2002. **54**(4): p. 1202-1209.

99. McNab, J.A., A.C. Yung, and P. Kozlowski, *Tissue oxygen tension measurements in the Shionogi model of prostate cancer using F-19 MRS and MRI.* Magnetic Resonance Materials in Physics Biology and Medicine, 2004. **17**(3-6): p. 288-295.

100. Reid, R.S., et al., *The influence of oxygenation on the 19F spin-lattice relaxation rates of fluosol-DA.* Phys Med Biol, 1985. **30**(7): p. 677-86.

101. Parhami, P.F., B.M, *Fluorine-19 Relaxation Study of Perfluoro Chemicals as Oxygen Carriers.* The Journal of Physical Chemistry, 1983. **87**(11): p. 1928-1931.

102. Parhami, P. and B.M. Fung, *F-19 Relaxation Study of Perfluoro Chemicals as Oxygen Carriers.* Journal of Physical Chemistry, 1983. **87**(11): p. 1928-1931.

103. Kodibagkar, V.D., X. Wang, and R.P. Mason, *Physical principles of quantitative nuclear magnetic resonance oximetry.* Front Biosci, 2008. **13**: p. 1371-84.

104. Thomas, S.R., Pratt, R.G., Millard, R.W., Samaratunga, R.C., Shiferaw, Y., McGoron, A.J., Tan, K.K., *In vivo pO2 imaging in the porcine model with perfluorocarbon F-19 NMR at low field.* Magnetic Resonance Imaging, 1996. **14**(1): p. 103-14.

105. Thomas, S.R., Millard, R.W., Pratt, R.G., Shiferaw, Y. Samaratunga, R.C., *Quantitative pO2 imaging in vivo with perfluorocarbon F-19 NMR: tracking oxygen from the airway through the blood to organ tissues.* Artif Cells Blood Substit Immobil Biotechnol, 1994. **22**(4): p. 1029-42.

106. Shukla, H.P., et al., *Regional myocardial oxygen tension: 19F MRI of sequestered perfluorocarbon.* Magn Reson Med, 1996. **35**(6): p. 827-33.

107. Mason, R.P., H. Shukla, and P.P. Antich, *Oxygent: a novel probe of tissue oxygen tension.* Biomater Artif Cells Immobilization Biotechnol, 1992. **20**(2-4): p. 929-32.

108. Noth, U., et al., *F-19-MRI in vivo determination of the partial oxygen pressure in perfluorocarbon-loaded alginate capsules implanted into the peritoneal cavity and different tissues.* Magnetic Resonance in Medicine, 1999. **42**(6): p. 1039-1047.

109. Zimmermann, U., et al., *Non-invasive evaluation of the location, the functional integrity and the oxygen supply of implants: 19F nuclear magnetic resonance imaging of perfluorocarbon-loaded Ba2+-alginate beads.* Artif Cells Blood Substit Immobil Biotechnol, 2000. **28**(2): p. 129-46.

110. Robinson, S.P. and J.R. Griffiths, *Current issues in the utility of 19F nuclear magnetic resonance methodologies for the assessment of tumour hypoxia.* Philos Trans R Soc Lond B Biol Sci, 2004. **359**(1446): p. 987-96.

111. Noth, U., et al., *In vivo determination of tumor oxygenation during growth and in response to carbogen breathing using 15C5-loaded alginate capsules as fluorine-19 magnetic resonance imaging oxygen sensors.* Int J Radiat Oncol Biol Phys, 2004. **60**(3): p. 909-19.

112. van der Sanden, B.P., et al., *Characterization and validation of noninvasive oxygen tension measurements in human glioma xenografts by 19F-MR relaxometry.* Int J Radiat Oncol Biol Phys, 1999. **44**(3): p. 649-58.

113. McNab, J.A., A.C. Yung, and P. Kozlowski, *Tissue oxygen tension measurements in the Shionogi model of prostate cancer using 19F MRS and MRI.* Magma, 2004. **17**(3-6): p. 288-95.

114. Vaupel, P., S. Briest, and M. Hockel, *Hypoxia in breast cancer: pathogenesis, characterization and biological/therapeutic implications.* Wien Med Wochenschr, 2002. **152**(13-14): p. 334-42.

115. Vaupel, P., et al., *Oxygenation of human tumors: evaluation of tissue oxygen distribution in breast cancers by computerized O2 tension measurements.* Cancer Res, 1991. **51**(12): p. 3316-22.

116. Hunjan, S., et al., *Regional tumor oximetry: 19F NMR spectroscopy of hexafluorobenzene.* Int J Radiat Oncol Biol Phys, 1998. **41**(1): p. 161-71.

117. Zhao, D., Constantinescu, A., Jiang, L., Hahn, E.W., Mason, R.P, *Prognostic radiology: Quantitative assessment of tumor oxygen dynamics by MRI.* Am J Clin Oncol, 2001. **24**(5).

118. Fan, X., et al., *Effect of carbogen on tumor oxygenation: combined fluorine-19 and proton MRI measurements.* Int J Radiat Oncol Biol Phys, 2002. **54**(4): p. 1202-9.

119. Scholz, A.W., et al., *Ventilation-perfusion ratio in perflubron during partial liquid ventilation.* Anesth Analg. **110**(6): p. 1661-8.

120. Heussel, C.P., Scholz, a., Schmittner, M., Laukemper-Ostendorf, S., Schreiber, W.G., Ley, S., Quintel, M., Weiler, N., Thelen, M., Kauczor, H.U, *Measurements of alveolar pO2 using 19F-MRI in partial liquid ventilation.* Invest Radiol, 2003. **38**(10): p. 635-41.

121. Dionne, K.E., C.K. Colton, and M.L. Yarmush, *Effect of hypoxia on insulin secretion by isolated rat and canine islets of Langerhans.* Diabetes, 1993. **42**(1): p. 12-21.

122. Papas, K.K., et al., *A stirred microchamber for oxygen consumption rate measurements with pancreatic islets.* Biotechnol Bioeng, 2007. **98**(5): p. 1071-82.

123. Jorjani, P. and S.S. Ozturk, *Effects of cell density and temperature on oxygen consumption rate for different mammalian cell lines.* Biotechnol Bioeng, 1999. **64**(3): p. 349-56.

124. Gross, J.D., I. Constantinidis, and A. Sambanis, *Modeling of encapsulated cell systems.* Journal of Theoretical Biology, 2007. **244**(3): p. 500-510.

125. Stabler, C.L., et al., *In vivo noninvasive monitoring of a tissue engineered construct using 1H NMR spectroscopy.* Cell Transplant, 2005. **14**(2-3): p. 139-49.

126. Leoni, L. and B.B. Roman, *MR imaging of pancreatic islets: tracking isolation, transplantation and function.* Curr Pharm Des, 2010. **16**(14): p. 1582-94.

127. Sambanis, A., et al., *Towards the development of a bioartificial pancreas: immunoisolation and NMR monitoring of mouse insulinomas.* Cytotechnology, 1994. **15**(1-3): p. 351-63.

128. Constantinidis, I., et al., *Noninvasive monitoring of a retrievable bioartificial pancreas in vivo.* Ann N Y Acad Sci, 2002. **961**: p. 298-301.

129. Constantinidis, I. and A. Sambanis, *Noninvasive monitoring of tissue-engineered constructs by nuclear magnetic resonance methodologies.* Tissue Engineering, 1998. **4**(1): p. 9-17.

130. Papas, K.K., et al., *Role of ATP and Pi in the mechanism of insulin secretion in the mouse insulinoma betaTC3 cell line.* Biochem J, 1997. **326** (Pt 3): p. 807-14.

131. Constantinidis, I. and A. Sambanis, *Towards the development of artificial endocrine tissues: (31)P NMR spectroscopic studies of immunoisolated, insulin-secreting AtT-20 cells.* Biotechnol Bioeng, 1995. **47**(4): p. 431-43.

132. Papas, K.K., et al., *Development of a bioartificial pancreas: I. long-term propagation and basal and induced secretion from entrapped betaTC3 cell cultures.* Biotechnol Bioeng, 1999. **66**(4): p. 219-30.

133. Long, R.C., Jr., et al., *In vitro monitoring of total choline levels in a bioartificial pancreas: (1)H NMR spectroscopic studies of the effects of oxygen level.* J Magn Reson, 2000. **146**(1): p. 49-57.

134. Stabler, C.L., et al., *Noninvasive measurement of viable cell number in tissue-engineered constructs in vitro, using 1H nuclear magnetic resonance spectroscopy.* Tissue Eng, 2005. **11**(3-4): p. 404-14.

135. Barnett, B.P., et al., *Fluorocapsules for Improved Function, Immunoprotection, and Visualization of Cellular Therapeutics with MR, US, and CT Imaging.* Radiology, 2011. **258**(1): p. 182-191.

136. Volland, N.A., et al., *Development of an inductively coupled MR coil system for imaging and spectroscopic analysis of an implantable bioartificial construct at 11.1 T.* Magn Reson Med, 2010. **63**(4): p. 998-1006.

137. Radisic, M., et al., *Mathematical model of oxygen distribution in engineered cardiac tissue with parallel channel array perfused with culture medium containing oxygen carriers.* Am J Physiol Heart Circ Physiol, 2005. **288**(3): p. H1278-89.

138. Radisic, M., et al., *Biomimetic approach to cardiac tissue engineering: oxygen carriers and channeled scaffolds.* Tissue Eng, 2006. **12**(8): p. 2077-91.

139. Caballero-Corbalan, J., et al., *No beneficial effect of two-layer storage compared with UW-storage on human islet isolation and transplantation.* Transplantation, 2007. **84**(7): p. 864-9.

140. Papas, K.K., et al., *Pancreas oxygenation is limited during preservation with the two-layer method.* Transplant Proc, 2005. **37**(8): p. 3501-4.

141. Johnson, A.S., et al., *Oxygen consumption and diffusion in assemblages of respiring spheres: Performance enhancement of a bioartificial pancreas.* Chemical Engineering Science, 2009. **64**(22): p. 4470-4487.

142. Efrat, S., et al., *Conditional transformation of a pancreatic beta-cell line derived from transgenic mice expressing a tetracycline-regulated oncogene.* Proc Natl Acad Sci U S A, 1995. **92**(8): p. 3576-80.

143. Stabler, C., et al., *The effects of alginate composition on encapsulated betaTC3 cells.* Biomaterials, 2001. **22**(11): p. 1301-10.

144. Papas, K.K., I. Constantinidis, and A. Sambanis, *Cultivation of recombinant, insulin-secreting AtT-20 cells as free and entrapped spheroids.* Cytotechnology, 1993. **13**(1): p. 1-12.

145. Lim, F. and A.M. Sun, *Microencapsulated Islets as Bioartificial Endocrine Pancreas.* Science, 1980. **210**(4472): p. 908-910.

146. Joseph, P.M., et al., *In vivo 19F NMR imaging of the cardiovascular system.* J Comput Assist Tomogr, 1985. **9**(6): p. 1012-9.

147. Cheng, S.Y., I. Constantinidis, and A. Sambanis, *Insulin secretion dynamics of free and alginate-encapsulated insulinoma cells.* Cytotechnology, 2006. **51**(3): p. 159-70.

148. Gross, J.D., I. Constantinidis, and A. Sambanis, *Modeling of encapsulated cell systems.* J Theor Biol, 2007. **244**(3): p. 500-10.

149. Benson, J.P., et al., *Towards the development of a bioartificial pancreas: effects of poly-L-lysine on alginate beads with BTC3 cells.* Cell Transplant, 1997. **6**(4): p. 395-402.

150. Simpson, N.E., et al., *Effects of pH on murine insulinoma betaTC3 cells.* Biochem Biophys Res Commun, 2000. **273**(3): p. 937-41.

151. Mishra, A. and B. Starly, *Real time in vitro measurement of oxygen uptake rates for HEPG2 liver cells encapsulated in alginate matrices.* Microfluidics and Nanofluidics, 2009. **6**(3): p. 373-381.

152. Tziampazis, E. and A. Sambanis, *Tissue engineering of a bioartificial pancreas: modeling the cell environment and device function.* Biotechnol Prog, 1995. **11**(2): p. 115-26.

153. Lowe, K.C., M.R. Davey, and J.B. Power, *Perfluorochemicals: their applications and benefits to cell culture.* Trends Biotechnol, 1998. **16**(6): p. 272-7.

154. Riess, J.G., *Understanding the fundamentals of perfluorocarbons and perfluorocarbon emulsions relevant to in vivo oxygen delivery.* Artificial Cells Blood Substitutes and Biotechnology, 2005. **33**(1): p. 47-63.

155. Goh, F., et al., *Limited beneficial effects of perfluorocarbon emulsions on encapsulated cells in culture: experimental and modeling studies.* J Biotechnol, 2010. **150**(2): p. 232-9.

156. Papas, K.K., et al., *Effects of oxygen on metabolic and secretory activities of beta TC3 cells.* Biochim Biophys Acta, 1996. **1291**(2): p. 163-6.

157. Ryu, G.R., et al., *Activation of AMP-activated protein kinase mediates acute and severe hypoxic injury to pancreatic beta cells.* Biochem Biophys Res Commun, 2009. **386**(2): p. 356-62.

158. de Groot, M., et al., *Response of encapsulated rat pancreatic islets to hypoxia.* Cell Transplant, 2003. **12**(8): p. 867-75.

159. Giuliani, M., et al., *Central necrosis in isolated hypoxic human pancreatic islets: evidence for postisolation ischemia.* Cell Transplant, 2005. **14**(1): p. 67-76.

160. Lau, J., et al., *Oxygenation of islets and its role in transplantation.* Curr Opin Organ Transplant, 2009. **14**(6): p. 688-93.

161. Biarnes, M., et al., *Beta-cell death and mass in syngeneically transplanted islets exposed to short- and long-term hyperglycemia.* Diabetes, 2002. **51**(1): p. 66-72.

162. Zacharovova, K., et al., *In vitro assessment of pancreatic islet vitality by oxymetry.* Transplant Proc, 2005. **37**(8): p. 3454-6.

163. Papas, K.K., et al., *Development of a bioartificial pancreas: II. Effects of oxygen on long-term entrapped beta TC3 cell cultures.* Biotechnology and Bioengineering, 1999. **66**(4): p. 231-237.

164. Jorjani, P. and S.S. Ozturk, *Effects of cell density and temperature on oxygen consumption rate for different mammalian cell lines.* Biotechnology and Bioengineering, 1999. **64**(3): p. 349-356.

165. Papas, K.K., et al., *Human islet oxygen consumption rate and DNA measurements predict diabetes reversal in nude mice.* Am J Transplant, 2007. **7**(3): p. 707-13.

166. Sweet, I.R., et al., *Glucose stimulation of cytochrome c reduction and oxygen consumption as assessment of human islet quality.* Transplantation, 2005. **80**(8): p. 1003-1011.

167. Scholz, A.W., et al., *Ventilation-perfusion ratio in perflubron during partial liquid ventilation.* Anesth Analg, 2010. **110**(6): p. 1661-8.

168. Thomas, S.R., et al., *In vivo PO2 imaging in the porcine model with perfluorocarbon F-19 NMR at low field.* Magn Reson Imaging, 1996. **14**(1): p. 103-14.

169. Thomas, S.R., et al., *Evaluation of the influence of the aqueous phase bioconstituent environment on the F-19 T1 of perfluorocarbon blood substitute emulsions.* J Magn Reson Imaging, 1994. **4**(4): p. 631-5.

170. Berkowitz, B.A., J.T. Handa, and C.A. Wilson, *Perfluorocarbon Temperature-Measurements Using F-19 Nmr.* Nmr in Biomedicine, 1992. **5**(2): p. 65-68.

171. Nerem, R.M. and A. Sambanis, *Tissue engineering: from biology to biological substitutes.* Tissue Eng, 1995. **1**(1): p. 3-13.

172. De Vos, P., de Haan, B.J., de Haan, A., van Zanten, J., Faas, M.M, *Factors influencing functional survival of microencapsulated islet grafts.* Cell Transplantation, 2004. **13**: p. 515-24.

173. Safley, S.A., et al., *Inhibition of cellular immune responses to encapsulated porcine islet xenografts by simultaneous blockade of two different costimulatory pathways.* Transplantation, 2005. **79**(4): p. 409-18.

174. Newgard, C.B., et al., *Understanding of basic mechanisms of beta-cell function and survival: prelude to new diabetes therapies.* Cell Biochem Biophys, 2004. **40**(3 Suppl): p. 159-68.

175. De Vos, P., et al., *Why do microencapsulated islet grafts fail in the absence of fibrotic overgrowth?* Diabetes, 1999. **48**(7): p. 1381-1388.

176. Constantinidis, I., et al., *Non-Invasive monitoring of a bioartificial pancreas in vitro and in vivo.* Ann N Y Acad Sci, 2001. **944**: p. 83-95.

177. Witkowski, P., et al., *Islet grafting and imaging in a bioengineered intramuscular space.* Transplantation, 2009. **88**(9): p. 1065-74.

178. Miao, G., et al., *Dynamic production of hypoxia-inducible factor-1alpha in early transplanted islets.* Am J Transplant, 2006. **6**(11): p. 2636-43.

179. Mukherjee, I.N., *A rational design approach for the cryopreservation of natural and engineered tissues* in *Department of Chemical and Biomolecular Engineering*. 2008, Georgia Institute of Technology, Atlanta, GA.

180. Raquel Diaz-Lopez, N.T., Elias Fattal, *Liquid Perfluorocarbons as Contrast Agents for Ultrasonography and 19F-MRI.* Pharmaceutical Research, 2010. **27**(1).

181. Kim, H.W. and A.G. Greenburg, *Artificial oxygen carriers as red blood cell substitutes: a selected review and current status.* Artif Organs, 2004. **28**(9): p. 813-28.

182. Stabler, C., et al., *The effects of alginate composition on encapsulated beta TC3 cells.* Biomaterials, 2001. **22**(11): p. 1301-1310.

183. Merani, S., et al., *Optimal implantation site for pancreatic islet transplantation.* Br J Surg, 2008. **95**(12): p. 1449-61.

184. Noth, U., et al., *19F-MRI in vivo determination of the partial oxygen pressure in perfluorocarbon-loaded alginate capsules implanted into the peritoneal cavity and different tissues.* Magn Reson Med, 1999. **42**(6): p. 1039-47.

185. Goh, F., Long, Jr, R,Simpson, N, Sambanis, A. *Dual Perfluorocarbon Method to Noninvasively Monitor Dissolved Oxygen Concentration in Tissue Engineered Constructs in vitro and in vivo*. Biotechnol Prog. (in press)

186. Carlsson, P.O., et al., *Markedly decreased oxygen tension in transplanted rat pancreatic islets irrespective of the implantation site.* Diabetes, 2001. **50**(3): p. 489-95.

187. Gross, J., *Noninvasive monitoring of oxygen concentrations and metabolic functions in pancreatic substitutes* in *Department of Biomedical Engineering*. 2007, Georgia Institute of Technology, Atlanta, GA

188. Dufrane, D., et al., *Six-month survival of microencapsulated pig islets and alginate biocompatibility in primates: proof of concept.* Transplantation, 2006. **81**(9): p. 1345-53.

189. Dufrane, D., R.M. Goebbels, and P. Gianello, *Alginate Macroencapsulation of Pig Islets Allows Correction of Streptozotocin-Induced Diabetes in Primates up to 6 Months Without Immunosuppression.* Transplantation, 2010. **90**(10): p. 1054-1062.

190. Tham, M.K., R.D. Walker, Jr, and J.H., Modell, *Diffusion Coefficients of O2, N2, and CO2 in Fluorinated Ethers*. J Chem Eng Data, 1973. **18**(2): p.411-412

200. Graeber, T.G., et al., *Hypoxia-mediated Selection of Cells with Diminished Apoptotic Potential in Solid Tumors*. Nature, 1996. 379 (6560): p. 88-91